Coffea canephora Pierre ex A. Froehner GROWN UNDER RECURRENT WATER DEFICIT CONDITIONS: ECOPHYSIOLOGICAL ACCLIMATION AT LEAF AND WHOLE-CANOPY LEVELS

GUILHERME AUGUSTO RODRIGUES DE SOUZA

STATE UNIVERSITY OF THE NORTH FLUMINENSE DARCY RIBEIRO

CAMPOS DOS GOYTACAZES – RJ
MARCH – 2025

Coffea canephora Pierre ex A. Froehner GROWN UNDER RECURRENT WATER DEFICIT CONDITIONS: ECOPHYSIOLOGICAL ACCLIMATION AT LEAF AND WHOLE-CANOPY LEVELS

GUILHERME AUGUSTO RODRIGUES DE SOUZA

"Thesis presented to Centro de Ciências e Tecnologias Agropecuárias da Universidade Estadual do Norte Fluminense Darcy Ribeiro, as part of the requirements for obtaining a PhD degree in Plant Production"

Advisor: D.Sc. Eliemar Campostrini

CAMPOS DOS GOYTACAZES – RJ
MARCH – 2025

FICHA CATALOGRÁFICA
UENF - Bibliotecas
Elaborada com os dados fornecidos pelo autor.

S729 Souza, Guilherme Augusto Rodrigues de.

Coffea Canephora Pierre ex A. Froehner grown under recurrent water deficit conditions : ecophysiological aspects at leaf and whole-canopy level / Guilherme Augusto Rodrigues de Souza. - Campos dos Goytacazes, RJ, 2025.

152 f. : il.
Inclui bibliografia.

Tese (Doutorado em Produção Vegetal) - Universidade Estadual do Norte Fluminense Darcy Ribeiro, Centro de Ciências e Tecnologias Agropecuárias, 2025.
Orientador: Eliemar Campostrini.

1. conilon coffee. 2. heat stress. 3. photosynthesis. 4. stress memory. 5. water stress. I. Universidade Estadual do Norte Fluminense Darcy Ribeiro. II. Título.

CDD - 630

Coffea canephora Pierre ex A. Froehner GROWN UNDER RECURRENT WATER DEFICIT CONDITIONS: ECOPHYSIOLOGICAL ACCLIMATION AT LEAF AND WHOLE-CANOPY LEVELS

GUILHERME AUGUSTO RODRIGUES DE SOUZA

"Thesis presented to Centro de Ciências e Tecnologias Agropecuárias da Universidade Estadual do Norte Fluminense Darcy Ribeiro, as part of the requirements for obtaining a PhD degree in Plant Production"

Approved: March 27, 2025

Judgment committee

Documento assinado digitalmente
gov.br
ELIAS FERNANDES DE SOUSA
Data: 01/09/2026 15:32:40-0300
Verifique em https://validar.iti.gov.br

Prof. Elias Fernandes de Sousa (PhD., Plant Production) - UENF

Documento assinado digitalmente
gov.br
MIROSLAVA RAKOCEVIC
Data: 31/08/2026 15:18:55-0300
Verifique em https://validar.iti.gov.br

Miroslava Rakocevic (PhD, Plant Ecophysiology) – Visitant researcher, UENF

Documento assinado digitalmente
gov.br
WEVERTON PEREIRA RODRIGUES
Data: 01/09/2026 06:41:35-0300
Verifique em https://validar.iti.gov.br

Prof. Weverton Pereira Rodrigues (PhD, Plant Production) - UEMASUL

Documento assinado digitalmente
gov.br
ELIEMAR CAMPOSTRINI
Data: 05/09/2026 16:07:18-0300
Verifique em https://validar.iti.gov.br

Prof. Eliemar Campostrini (PhD, Plant Production) – UENF
(Advisor)

I dedicate this thesis to my parents, for their unconditional love and support, and for being the first to make me believe in education as an agent of social transformation. You have always been my greatest teachers.

“Jurei amor aos meus sonhos”

ACKNOWLEDGMENTS

To my parents, Orotides and Augusta, for the unconditionality of your love, and for being the driving force behind my dreams and achievements. You are the reason I am who I am today and why I strive to be a little better every day.

To my brother, José Geraldo, for being an inspiration and a constant source of support.

To the Universidade Estadual do Norte Fluminense Darcy Ribeiro (UENF) and the Graduate Program in Plant Production, to make this course possible. I extend my gratitude to UENF and Coordenação de Aperfeiçoamento de Pessoal de Nível Superior – Brasil (CAPES) for the scholarships granted (SEI-260009/001953/2021 and 88887.968322/2024-00, respectively); and to Fundação Carlos Chagas Filho de Amparo à Pesquisa do Estado do Rio de Janeiro (FAPERJ) and Conselho Nacional de Desenvolvimento Científico e Tecnológico (CNPq) for the funding and resources that made this research possible. This study was financed in part by the CAPES - Finance Code 001.

To the Laboratory of Ecophysiology of Tropical and Subtropical Plants at UENF and its team, who have been with me since the beginning of my master's degree. It has been a pleasure sharing this path with you.

To the researchers and friends who opened doors for me and allowed me to follow my path to this point. Especially to Wellington Almeida, for introducing me to the world of plant ecophysiology and making me fall in love with it. To José Altino, for giving me an opportunity and broadening my horizons; you will always be a reference for me. To Sara Dousseau, for showing me that science requires passion, dedication, and commitment. To Weverton Rodrigues, for being an inspiration and a reference as a researcher. And to Misroslava Rakocevic, for being such a meticulous friend and teacher, and for your teachings and patience.

To my advisor, Dr. Eliemar Campostrini, for being more than an advisor, but an admirable human being. You saw in me things I couldn’t see in myself and gave me all the tools and opportunities to become an excellent professional. I hope that one day I can be, for my students, at least 1% of what you have been to me and my colleagues.

To my main team and friends, who made every page of this work possible. Especially to Danilo Baroni, for allowing me to reap the fruits of his work, and to Laisa Zanelato, for being more than a friend, but emotional and professional support throughout these four years. And to the dear Ellen Vale, Diesily Andrade, Anne Reis, Larissa Barcelos, and Caroline Souza, for making my evaluations lighter and more fun, even when everything seemed to hang by a thread.

To my lifelong friends and beyond: you have always been an inspiration to me.

To the examining board, for your valuable contributions to my work and for being admirable professionals.

To all the divine forces, my other family members, colleagues, and friends...

...Thank you so much for making this dream come true!

SUMARY

ABSTRACT

SOUZA, Guilherme Augusto Rodrigues de; D.Sc.; Universidade Estadual do Norte Fluminense Darcy Ribeiro; March 2025; *Coffea canephora* Pierre ex A. Froehner grown under recurrent water deficit conditions: ecophysiological acclimation at leaf and whole-canopy levels; Advisor: Dr. Eliemar Campostrini.

Coffea canephora is typically cultivated at low altitudes and consequently under higher temperature conditions. Due to the intensification of climate change, particularly the increase in average air temperature and changes in rainfall distribution patterns, many areas dedicated to the cultivation of *C. canephora* have been impacted by the recurrence of drought events combined with supra-optimal temperatures. In non-irrigated cultivation areas, these conditions induce a series of stress responses that affect the physiology, morphology, and productivity of this important commodity. To investigate the effects of recurrent drought cycles on the ecophysiological aspects of *C. canephora*, two experiments were conducted. In the first experiment, two clones of *C. canephora* were cultivated in a greenhouse: the '3V' clone, characterized by deeper root growth, and the 'A1' clone, with shallower root growth. These plants were cultivated for 60 days under full irrigation. Subsequently, one plant group was maintained under irrigation, and the other group was subjected to two recurrent cycles of soil drying and rehydration. After full recovery, leaf discs from both '3V' and 'A1' clones, grown under well-watered (WW) and water-stressed (WS) conditions, were collected and exposed to thermal stress in a water bath at different temperatures (35°C, 40°C, 45°C, 50°C, and 55°C). Chlorophyll *a* fluorescence emission measurements were then performed, followed by OJIP transient and JIP_{Test} analyses. In this experiment, results indicated that increasing temperature in coffee leaves triggered conformational changes in the OJIP transient curves, resulting in alterations in the JIP_{Test} parameters. These changes are related to the leaf photochemical apparatus damage. Additionally, under both WW and WS conditions, the '3V' and 'A1' clones responded differentially to temperature increases. Under WS, the '3V' clone showed greater sensitivity to thermal stress, while the 'A1' clone exhibited greater tolerance, indicating that recurrent drought cycles induced priming responses in 'A1', possibly associated to "stress memory" in this clone. In the second experiment, 'LB1' clone was cultivated

for 10 months under full irrigation, following a period where one group had been kept under irrigation (WW), and the other had been subjected to three cycles of soil dehydration and rehydration (WS). Through cycles 1 and 3, leaf and whole-canopy gas exchange were monitored in both treatments. In this study, both leaf and whole-canopy gas exchange were strongly impacted by drought, though recovery occurred after rehydration. However, the full recovery of whole-canopy gas exchange was significantly compromised due to intense leaf shedding triggered by the drought events. Nevertheless, a few weeks after soil rehydration, even with reduced leaf area, the plants that underwent drought events were able to achieve photosynthesis and canopy transpiration rates comparable to continuously irrigated plants.

Keywords: conilon coffee, heat stress, photosynthesis, stress memory, transpiration, water stress.

RESUMO

SOUZA, Guilherme Augusto Rodrigues de; D.Sc.; Universidade Estadual do Norte Fluminense Darcy Ribeiro; março 2025; *Coffea canephora* Pierre ex A. Froehner cultivado sob condições de déficit hídrico recorrente: aclimatação ecofisiológica aos níveis de folha e de planta inteira; Orientador: Dr. Eliemar Campostrini.

O cultivo de *Coffea canephora* é comumente realizado em baixas altitudes e, portanto, em condições de temperaturas mais altas. Devido à intensificação das mudanças climáticas, em especial o aumento da temperatura média do ar e a alteração do padrão distribuição de chuvas, muitas áreas destinadas ao cultivo de *C. canephora* têm sido impactadas pela recorrência de eventos de seca em associação com temperaturas supra ótimas. Em áreas onde o cultivo não é irrigado, a ocorrência destas condições induz uma série de respostas de estresse que impactam a fisiologia, morfologia e produtividade desta importante commodity agrícola. Para estudar os efeitos dos ciclos recorrentes de seca sobre os aspectos ecofisiológicos de plantas de *C. canephora* realizaram-se dois experimentos. No primeiro experimento, cultivado em casa de vegetação dois clones de *C. canephora*; o clone '3V', com crescimento radicular mais profundo, e o clone 'A1', com crescimento radicular mais superficial. Estas plantas foram cultivadas durante 60 dias sob irrigação plena, posteriormente um grupo de plantas foi mantido sob irrigação e outro grupo foi submetido a dois ciclos recorrentes de secagem e reidratação do solo. Após a completa recuperação das plantas, discos foliares de ambos os clones '3V' e 'A1', cultivados em condições bem-irrigadas (WW) e sob estresse hídrico (WS) foram coletadas e submetidos ao estresse térmico em banho-maria em diferentes temperaturas (35ºC, 40ºC, 45ºC, 50ºC e 50ºC). Depois de submetidos ao estresse térmico, mediu-se a emissão de fluorescência da clorofila *a* e realizou-se a análise do transiente OJIP e JIP_{Test}. Neste experimento, descobriu-se que o aumento da temperatura em folhas de café desencadeia mudanças conformacionais nas curvas do transiente OJIP, resultando alterações nos parâmetros do JIP_{Test}. Estas alterações estão relacionadas a danos ao aparato fotoquímico das folhas. Além disso, em WW e WS, os clones '3V' e 'A1', responderam diferencialmente ao aumento de temperatura. Em WS, o clone '3V' apresentou maior sensibilidade ao estresse térmico e o clone 'A1' em WS

apresentou maior tolerância, indicando que os ciclos recorrentes de seca induziram respostas de *priming* em ‘A1’, possivelmente relacionadas à “memória de estresse” neste clone. No segundo experimento, foi cultivado o clone ‘LB1’ durante 10 meses sob irrigação plena, e após este período um grupo de plantas foi mantido sob irrigação (WW) e outro grupo foi submetido a três ciclos de secagem e reidratação do solo (WS). Ao longo dos ciclos 1 e 3, foram monitoradas as trocas gasosas foliares e de planta inteira em ambos os tratamentos. Neste trabalho, foi observado que tanto as trocas gasosas foliares quanto de planta inteira foram fortemente impactadas pela seca, mas após a reidratação do solo, as plantas conseguem se recuperar. Entretanto, a recuperação plena das trocas gasosas de planta inteira é fortemente comprometida devido à intensa queda de folhas, desencadeada pelos eventos de seca. Mas algumas semanas após a reidratação do solo, mesmo com uma área foliar menor, as plantas que passaram pelos eventos de seca, conseguem atingir valores de fotossíntese e transpiração da copa similares aos observados em plantas irrigadas continuamente.

Palavras-chave: café conilon, estresse hídrico, estresse térmico, fotossíntese, memória de estresse, transpiração.

1. INTRODUCTION

Coffea *canephora* Pierre ex A. Froehner, commonly known as Conilon or Robusta coffee, originates from the Congo Basin in Guinea and currently accounts for approximately 40% of global coffee production (ICO, 2025). Compared to *C. arabica* (the most widely cultivated species), *C. canephora* tends to exhibit greater hardiness and tolerance to pests and diseases, as well as enhanced adaptability to tropical edaphoclimatic conditions at low altitudes and elevated temperatures, a trait linked to its biogeographical origin. Furthermore, unlike *C. arabica*, the Conilon coffee is characterized by cross-fertilization and genetic self-incompatibility, resulting in high genetic variability (Ferrão et al., 2017; Campuzano-Duque et al., 2021).

In the context of climate change, projected global temperature increases exceeding 1.5°C (IPCC, 2022; Calvin et al., 2023) suggest differential responses between *C. canephora* and *C. arabica* (Rodrigues et al., 2016; Rodrigues et al., 2018). This is because *C. arabica* demonstrates greater sensitivity to high temperatures, whereas *C. canephora* exhibits superior resilience to such conditions (Ferrão et al., 2017). Therefore, considering current genotypes and cultivation practices, *C. arabica* is likely to experience greater adverse impacts, with cultivation areas progressively shifting toward *C. canephora* (Ferrão et al., 2017).

Although new agricultural areas may become suitable for Conilon coffee, up to 55% of current production zones are projected to become unsuitable (Magrach and Ghazoul, 2015; Lorençone et al., 2023). This is because the temperature rise associated with climate change is accompanied by shifts in rainfall patterns, leading to prolonged dry spells in these regions (Magrach and Ghazoul, 2015). These water deficits directly reduce the species' productive potential by diminishing photosynthetic capacity, an effect exacerbated when combined with elevated temperatures (DaMatta and Ramalho, 2006; Gichimu and Cheserek, 2012; DaMatta, 2018; Semedo et al., 2018).

In Brazilian Conilon coffee-growing regions, particularly Espírito Santo state, drought periods primarily occur during the winter (April to September), characterized by low precipitation and extended intervals between rainfall events (Venancio et al., 2020). Throughout this season, rainfed *C. canephora* crops experience recurrent soil water deficit cycles, which induce stomatal and diffusive limitations, in addition to

photochemical, hydraulic, biochemical, and molecular constraints. These factors adversely affect the photosynthetic process and, consequently, the productivity of the plants (Menezes-Silva et al., 2017; Guedes et al., 2018; Almeida et al., 2021).

Under field conditions, soil water deficit is often accompanied by high air temperatures, particularly in *C. canephora* growing regions (Venancio et al., 2020). This rising air temperature has a significant impact on coffee yield (Bunn et al., 2015; Mbwambo et al., 2022). In general, elevated temperatures diminish plant growth through photosynthetic suppression (Zahra et al., 2023) and increase respiration rates, leading to greater carbon loss and a reduction in the availability of non-structural carbohydrates (Sharma et al., 2022). Moreover, high temperatures can disrupt flowering and fruit sets, ultimately affecting fruit yield and quality (Chacón-Villalobos et al., 2021).

Several studies have demonstrated that plant stress responses may be either exacerbated (Pandey et al., 2015; Pascual et al., 2022; Jing et al., 2024) or mitigated (Rejeb et al., 2014; Pandey et al., 2015) depending on simultaneous biotic and/or abiotic stressor interactions. In coffee plants, concurrent water deficit and supra-optimal temperatures intensify stress responses (Semedo et al., 2018). This combination reduces carbon assimilation through enhanced stomatal and non-stomatal limitations (Rodrigues et al., 2018; Dubberstein et al., 2020), increases cellular damage, and accelerates reactive oxygen species (ROS) accumulation (Dubberstein et al., 2020; Rodrigues et al., 2024).

Recent research on *Coffea* spp. under water-limiting conditions reveals that plants respond differentially to single or recurrent water deficit events (Menezes-Silva et al., 2017). Plants experiencing single drought events exhibit acute stress responses, such as a reduction in photosynthetic rate, decreased leaf water potential, wilting, leaf senescence, and severe oxidative damage (Seleiman et al., 2021). In contrast, plants exposed to recurrent water stress events demonstrate stress acclimation through "stress memory" mechanisms. This priming enables faster activation of protective strategies, including spanning physiological, biochemical, and molecular adaptations, to mitigate stress-induced impairment (Menezes-Silva et al., 2017; Guedes et al., 2018).

The understanding of the ecophysiological responses of *C. canephora* cultivated under water-limiting conditions has contributed to the development of strategies aimed at enhancing the species' productive potential, particularly in the

context of current climate change. These strategies are based on both the selection of genetic materials exhibiting drought resistance (long-term) and cultural management practices (short-term) capable of mitigating the effects of stress on the plants (Zia et al., 2021). In this regard, numerous studies have established efficient water-scarcity management techniques, including deficit irrigation priming (Sseremba et al., 2023), CO_2 enrichment (Avila et al., 2020), calcium (Ramírez-Builes et al., 2020) and selenium plant biofortification (Mateus et al., 2021), the use of exogenous melatonin (Campos et al., 2019), among others (Seleiman et al., 2021).

Despite substantial research on C. *canephora* ecophysiology under water deficit, most gas exchange (photosynthesis and transpiration) studies under stress conditions focus on leaf-level measurements, with whole-canopy scale analysis remaining exceptionally rare. To date, only limited whole-canopy gas exchange studies exist for *Coffea* spp. (Marur e de Faria, 2007; Rodrigues et al., 2016), while other approaches extrapolate single-leaf data to model canopy photosynthesis (Rakocevic et al., 2023; 2024). Consequently, there is a gap in scientific knowledge regarding the effect of different stress conditions, particularly water stress, on the gas exchange capacity at the whole-canopy scale in coffee trees.

Studies on gas exchange in single leaves using commercial equipment provide significant insights into the physiological state of plants and their interaction with the environment (Long, 2003; Haworth et al., 2018). However, these responses can often be under- or overestimated, as the measurements do not account for light variability or the developmental stage of leaves across different plant strata (Delrot et al., 2010; Medrano et al., 2012; 2015; Ferraz et al., 2016).

Single-leaf measurements typically target photosynthetically optimal young, fully expanded leaves. Additionally, monitoring gas exchange over a full day or an extended period is often challenging due to equipment and labor limitations. In contrast, a multi-chamber system for monitoring whole-canopy gas exchange (Rodrigues et al., 2016) can provide more realistic data on water demand and photosynthetic assimilation capacity of plants over a day or analysis period, as well as the balance of carbon fixation relative to nocturnal respiration (Pérez-Priego et al., 2015; Salazar-Tortosa et al., 2018). Furthermore, this system enables a deeper understanding of the dynamic responses of plants under stress conditions, potentially enhancing crop management decision-making.

From this perspective, this study aims to investigate the ecophysiological responses at both the leaf and whole-canopy levels in *C. canephora* plants cultivated under recurrent water stress conditions. The first chapter examines how recurrent cycles of soil water deficit, followed by rehydration, can impact the leaf-level photosynthetic apparatus and whether these stress cycles induce thermotolerance in *C. canephora* genotypes with differential drought tolerance. The second chapter correlates gas exchange at the leaf and whole-canopy levels in *C. canephora* plants subjected to recurrent water stress cycles. To achieve this, a single-leaf gas exchange measurement system and a multi-chamber system for whole-canopy gas exchange measurements were employed.

2. LITERATURE REVIEW

2.1 *Coffea* spp. general aspects

The coffee plant (*Coffea* spp.) is a perennial shrub belonging to the Rubiaceae family (Ferrão et al., 2017). Its center of origin and diversity lies in the African (primary) and Asian continents, where approximately 130 species of the genus have been cataloged, with a few also found in Asia (Davis and Rakotonasolo, 2021). Despite this diversity, global production focuses predominantly on *C. arabica*, *C. canephora* Pierre ex A. Froehner, and a small portion on *C. liberica* (Ferreira et al., 2019). *C. arabica* is the most widely produced species, accounting for about 60% of global production, followed by *C. canephora* (35% to 40%) (Ferrão et al., 2017; Campuzano-Duque et al., 2021). In general terms, Brazil is the world's largest coffee producer and the second-largest producer of *C. canephora*, surpassed only by Vietnam (ICO, 2025).

The species *C. arabica* originates from the highlands of southwestern Ethiopia, at altitudes ranging between 1000 and 2000 meters. It is a tetraploid and self-compatible species that reproduces through self-fertilization (Ferreira et al., 2019). Consequently, *C. arabica* exhibits greater cold tolerance, adaptation to high altitudes, reduced genetic variability, and lower resistance despite its superior cup quality and beverage characteristics (Ferreira et al., 2019). In contrast, the species *C. canephora* originates from central and western sub-Saharan Africa and is native to tropical forests in Guinea and Uganda (0 to 1000 meters in altitude). As a result, it demonstrates greater adaptability to tropical edaphoclimatic conditions at low altitudes and higher temperatures (Ferrão et al., 2017; Campuzano-Duque et al., 2021). As a diploid species with gametophytic self-incompatibility, *C. canephora* relies on cross-fertilization, which grants its greater genetic variability, hardiness, and tolerance to pests, diseases, and less favorable abiotic conditions (Bragança et al., 2001; Ferrão et al., 2017).

2.2 Effects of climate change on *Coffea* spp. production

According to the Intergovernmental Panel on Climate Change projections (Calvin et al., 2023), intensified greenhouse gas emissions have accelerated global warming, with the average air temperature expected to exceed 1.5°C above pre-industrial levels by 2030 (IPCC, 2022). This temperature increase, directly and indirectly, impacts agriculture, as it alters precipitation patterns, leads to prolonged drought periods, increases crop exposure to supra-optimal temperatures, and compromises the suitability of areas for agricultural development (Koutouleas et al., 2022).

Like other crops, coffee faces significant threats from climate change (Koutouleas et al., 2022). Rising temperatures will have more pronounced effects on the productivity of *C. arabica* productivity, given its adaptation to cooler climates (DaMatta, 2018). However, recent studies have indicated that the increase in temperatures is occurring at such a critical rate that it has also led to productivity losses in *C. canephora* (Kath et al., 2020).

Productivity losses in *Coffea* spp. primarily occur due to the high sensitivity of the photosynthetic process to increases in vapor pressure deficit (VPD), which is directly related to rising temperatures and reduced air relative humidity (Kath et al., 2020). This elevation in VPD impairs the stomatal regulation of *Coffea* spp., limiting the entry of CO_2 into the carboxylation sites within the leaf mesophyll (Rodrigues et al., 2018).

Furthermore, supra-optimal temperatures for each species lead to pigment degradation and photochemical limitations, impairing electron transport and, consequently, decreasing the generation of reducing power [adenosine triphosphate (ATP) and nicotinamide adenine dinucleotide phosphate hydrogen (NADPH)] required for CO_2 fixation in the Calvin-Benson cycle (Rodrigues et al., 2018; Dubberstein et al., 2020). Additionally, elevated temperatures trigger biochemical constraints due to the thermal sensitivity of many enzymes involved in the photosynthetic process, such as ribulose-1,5-bisphosphate carboxylase/oxygenase (RUBISCO) (Rodrigues et al., 2016).

Beyond direct temperature impacts on photosynthesis and productivity, another climate change-related limitation that reduces productive potential is water deficit during drought periods (DaMatta, 2018). As previously mentioned, increasing

temperatures alter precipitation regimes, increasing the frequency of extreme water scarcity events. Primary coffee-growing regions in the intertropical zones are frequently affected by rainfall shortages, resulting in extended and more severe drought periods (DaMatta, 2018). The effects of water deficit on the productivity of *Coffea* spp. are discussed in the following section.

Current and future climatic changes, particularly in temperature and precipitation, challenge the sustainability of the high coffee yields observed today. Evidence indicates that the impacts of climate change on the photosynthetic process of *Coffea* spp. may be mitigated by rising atmospheric CO_2 concentrations (Rodrigues et al., 2016; Avila et al., 2020; Dubberstein et al., 2020). Nevertheless, approximately 50% of the areas currently dedicated to coffee production are projected to be lost due to rising temperatures and the increased incidence of severe droughts (Magrach and Ghazoul, 2015; Lorençone et al., 2023).

2.3 Effects of water deficit and supra-optimal temperatures on the *Coffea* spp. photosynthesis

Future coffee productivity is directly correlated with climate changes, particularly shifts in precipitation patterns and rising temperatures, which will lead to reduced water availability and increased drought frequency in coffee-growing regions (DaMatta and Ramalho, 2006; Richardson et al., 2023). These water scarcity events, combined with high temperatures, trigger a series of stress responses that, in most cases, result in decreased productivity due to reductions in photosynthetic capacity, growth, and reproduction of coffee plants.

In coffee plants, as in most plant species, the primary response to soil water limitation is reduced cell expansion (Borgo et al., 2024). This occurs because tissue water content is crucial for maintaining cellular turgor, which enables cell expansion (Yang et al., 2021). Reduced water availability compromises hydration, diminishing cellular expansion capacity and ultimately impairing growth and biomass accumulation (Dias et al., 2007).

Additionally, water-stressed plants may alter the partitioning of assimilations to compensate for water limitation, which can be observed, for instance, by an increase in the root/shoot ratio (Avila et al., 2020). In this way, the plant limits the

growth of the transpiring area (shoots) and invests in its ability to explore the soil for water through root growth (Pinheiro et al., 2005; De Souza et al., 2025). Photosynthetic limitations arising from both water and thermal stress also compromise the photoassimilate production and export for biomass accumulation (DaMatta, 2018; Dubberstein et al., 2020).

The reduction in the photosynthetic capacity of coffee plants involves both stomatal and non-stomatal limitations (Rodrigues et al., 2018; Dubberstein et al., 2020). Stomatal limitations in the photosynthesis of *Coffea* spp. are associated with stomatal closure, which results from the synthesis of abscisic acid in the roots and leaves, and its signaling role in guard cells (Silva et al., 2018; Bharath et al., 2021; Semedo et al., 2021). This stomatal closure increases the resistance to CO_2 entry into the leaf mesophyll, reducing the carbon assimilation rate. Moreover, in many cases, due to low mesophyll conductance (co-regulated with stomatal conductance), a significant diffusional limitation is observed, which reduces the ability of CO_2 to reach the carboxylation sites in the chloroplasts, resulting in low photosynthetic rates (Barros et al., 1997; Niinemets et al., 2009; Martins et al., 2014; Semedo et al., 2021).

Under severe water deficit and thermal stress, coffee plants exhibit accelerated degradation of photosynthetic pigments and oxidative stress (Fahad et al., 2017; Dubberstein et al., 2020; Semedo et al., 2021; Rodrigues et al., 2024), resulting from imbalances between the photochemical and biochemical stages of photosynthesis. Either individually or in combination, water and thermal stresses lead to reduced stomatal conductance (g_s) and the subsequent decrease in CO_2 entry into the mesophyll (C_i). However, the electron flow is maintained, causing this energy to bind with oxygen radicals, forming reactive oxygen species (ROS) that degrade pigment-protein components (Dubberstein et al., 2020; Rodrigues et al., 2024).

Furthermore, these stressors can reduce photochemical efficiency (Rodrigues et al., 2018; Dubberstein et al., 2020), electron transport rate, and the ability to generate reducing power (ATP and NADPH) (Semedo et al., 2021). Besides, exposure to these stressors also induces the denaturation of crucial proteins in the photosynthetic process, in addition to reducing the activity of RUBISCO and RUBISCO activase (Fahad et al., 2017; Dubberstein et al., 2020a). All these responses involved in the absorption and transfer of light energy for the

formation of reducing power are related to the non-stomatal limitations of *Coffea* spp. photosynthesis.

2.4 “Stress memory” in plants

Research on the photosynthetic responses of coffee plants to water deficit has predominantly focused on single drought events (Menezes-Silva et al., 2017). From this perspective, many experimental findings may either underestimate or overestimate the responses of plants growing in natural environments, where they are subjected to recurrent cycles of environmental stress.

Upon stress exposure, plants remodel their signaling networks to initiate molecular reprogramming, which involves transcription factors, stress-related proteins, and secondary messengers (Tani et al., 2019). This reprogramming encompasses epigenetic, biochemical, physiological, and morphological adjustments (Liu et al., 2022; Sharma et al., 2022; Kambona et al., 2023), enabling stress memory retention and facilitating a faster activation of stress responses in subsequent stress cycles (Fleta-Soriano and Munné-Bosch, 2016; Sharma et al., 2022).

In plants that have undergone priming, the increased accumulation of chlorophyll and RUBISCO, as well as the accumulation of osmotically active solutes and the synthesis of antioxidants and protective compounds (e.g., chaperones), are respectively associated with enhanced photosynthetic performance, improved hydraulic responses, and increased plant protection under recurrent stress conditions (Jacques et al., 2021).

When a plant experiences an external stimulus (stress), referred to here as ‘priming,’ it activates mechanisms associated with mitigating damage caused by this stimulus. These mechanisms may remain active or become more easily reactivated, even in the absence of the stressor (Charng et al., 2023; Lagiotis et al., 2023). Furthermore, the type and severity of the stress event can modulate the plant’s acclimation capacity and intensity (Charng et al., 2023; Lagiotis et al., 2023). In addition to short-term morphophysiological adjustments, acclimation can also occur through the modulation of key gene expression, leading to long-term epigenetic modifications (Xu et al., 2024). These epigenetic changes are primarily triggered by

DNA methylation, histone modifications, and the synthesis of non-coding RNAs, all stress-responsive processes (Akhter et al., 2021; Lagiotis et al., 2023).

In coffee cultivation, studies demonstrate that *C. canephora* plants exposed to recurrent cycles of water deficit develop a series of physiological, metabolic (Menezes-Silva et al., 2017), and molecular (Guedes et al., 2018) adjustments associated with a 'stress memory'. This phenotypic plasticity enhances their capacity to withstand future stress events. Therefore, understanding these plant strategies for stress acclimation, combined with advances in biotechnological research and genetic improvement of crops, paves the way for the development of increasingly stress-tolerant genotypes in the context of ongoing climate change (Sun et al., 2021).

2.5 Leaf-scale and whole-canopy scale gas exchange

Current research on coffee ecophysiology predominantly relies on leaf-level gas exchange measurements (photosynthesis and transpiration). To date, only two studies, one with closed system (Marur and de Faria, 2007) and one with open system (Rodrigues et al., 2016), have aimed to assess gas exchange at the canopy level in *C. arabica* and *C. canephora* genotypes.

Leaf-level gas exchange measurements provide valuable insights into the ecophysiological responses of coffee plants. However, many environmental parameters that influence photosynthesis, particularly light distribution, vary across different canopy strata (Miller et al., 1996; Niinemets, 2007; Araujo et al., 2008; Ferraz et al., 2016). Moreover, coffee plants exhibit leaf adaptation to both sun and shade conditions throughout the canopy, which can affect the plant's photosynthetic potential as well as the nitrogen distribution within these leaves (Gomez et al., 2005; Araujo et al., 2008). Consequently, measurements taken from isolated leaves may overestimate whole-canopy photosynthesis and transpiration while underestimating light compensation and saturation points compared to those observed at the whole-canopy level (Francesconi et al., 1997; Poni et al., 1997; Peña and Tarara, 2004; Katerji et al., 2015). Given these considerations, the adoption of whole-canopy gas exchange measurement techniques can enhance the understanding of gas exchange responses in coffee plants cultivated under different growing conditions, accounting for the photosynthetic variability across the canopy.

Whole-canopy gas exchange can be measured using flow chambers in an open system. These systems quantify photosynthesis and transpiration rates by precisely measuring CO_2 and H_2O vapor concentration differentials, coupled with airflow through the chamber (Takahashi et al., 2007). The CO_2 and H_2O differentials are obtained by calculating the difference between the concentrations of these gases entering and exiting the chambers. Typically, larger differentials are observed during the day, while smaller differentials occur at night (Baker et al., 2014). This approach allows for the integration of multiple environmental conditions to which the plant is exposed, including biotic and abiotic stresses, cultivation systems, training techniques, and developmental stages of the crop (Whiting and Lang, 2001).

The installation of chambers inevitably alters the microclimate surrounding the plant (Garcia et al., 1990). To minimize significant microclimatic changes, it is essential to calibrate and maintain a stable airflow rate, ensuring an air exchange time within the chamber of less than 30 seconds. This prevents the internal air temperature from exceeding approximately 3°C above the external air temperature (Peña and Tarara, 2004). Additionally, excessively high airflow rates in plants with small leaf areas may reduce measurement accuracy due to low detection differentials in gas concentrations. An optimal airflow rate should range between 3 and 4 L s^{-1} per m^2 of leaf area (Poni et al., 2014). When these operational precautions are observed, gas exchange measurements can provide valuable insights into the canopy-wide dynamics, while also enabling accurate estimations of daily carbon gain and water consumption (Escalona et al., 2016).

3. MANUSCRIPTS

3.1 The OJIP kinetics analysis reveals differential thermal tolerance responses in *Coffea canephora* clones after two recurrent cycles of soil water deficit

Abstract

In Brazil, rainfed *Coffea canephora* cultivation areas are frequently exposed to successive cycles of soil water deficit, which trigger stress responses in plants. In addition to drought stress, increased air temperature can act as a second stressor. The recurrence of these factors may induce plant tolerance mechanisms, potentially mitigating future stress responses, even of a different nature. This study tested the hypothesis that repeated cycles of soil water deficit can trigger tolerance mechanisms that make *C. canephora* leaves more resilient to supra-optimal temperatures. To test this hypothesis, young *C. canephora* plants (cv. clones 'A1' and '3V', previously classified as drought-sensitive and tolerant, respectively, considering dynamics of physiological parameters) were grown for six months, after which they were subjected to two consecutive cycles of soil water deficit ($\Psi_{mSoil} \approx$ -300 kPa) followed by rehydration. After the second cycle, leaf discs were collected from leaves formed during the two stress cycles and exposed to heat treatments (35°C, 40°C, 45°C, 50°C, and 55°C) for 15 minutes in a water bath. Chlorophyll *a* fluorescence emission was then monitored, and the results were analyzed using OJIP transient kinetics and JIP_{Test}. The increasing temperatures resulted in negative changes in both OJIP kinetics and JIP_{Test}-derived parameters. At 50°C and 55°C, mainly, there was a significant increase in F_0 and a reduction in F_m, due to changes in the steps of the OJIP curve. These changes impacted the energy connectivity and, consequently, the electron transport along its transport chain and increased energy dissipation. This was confirmed by the JIP_{Test} variables. Despite the impact of temperature, the results suggested that the recurrence of soil water deficit induced heat tolerance in clone 'A1', while it increased sensitivity in clone '3V'.

Resumo

No Brasil, áreas de cultivo de *Coffea canephora* sem sistemas de irrigação são frequentemente expostas a ciclos sucessivos de déficit hídrico no solo, que desencadeiam respostas de estresse nas plantas. Além do estresse hídrico, o aumento da temperatura do ar pode atuar como um segundo fator de estresse. A recorrência desses fatores de estresse pode induzir mecanismos de tolerância das plantas, potencialmente mitigando futuras respostas de estresse, mesmo de natureza diferente. Neste estudo, levantou-se a hipótese de que ciclos repetidos de déficit hídrico no solo podem desencadear mecanismos de tolerância que tornam as folhas de *C. canephora* mais resilientes a temperaturas supra ótimas. Para testar essa hipótese, plantas jovens de *C. canephora* (cv. clones 'A1' e '3V', previamente classificadas como sensíveis e tolerantes à seca, respectivamente, considerando a dinâmica dos parâmetros fisiológicos) foram cultivadas por seis meses, após estas foram submetidas a dois ciclos consecutivos de déficit hídrico no solo ($\Psi_{mSoil} \approx$ -300 kPa) seguidos de reidratação. Após o segundo ciclo, discos foliares foram coletados de folhas formadas durante os dois ciclos de estresse e expostos a tratamentos térmicos (35°C, 40°C, 45°C, 50°C e 55°C) por 15 minutos em banho-maria. A emissão de fluorescência da clorofila *a* foi então monitorada, e os resultados foram analisados usando a cinética transiente do OJIP e o JIP_{Test}. O aumento das temperaturas resultou em mudanças negativas tanto na cinética do OJIP quanto nos parâmetros derivados do JIP_{Test}. A 50°C e 55°C, principalmente, houve um aumento significativo em F_0 e uma redução em F_m, devido a mudanças nos degraus da curva do OJIP. Essas mudanças impactaram a conectividade de energia e, consequentemente, o transporte de elétrons ao longo da cadeia transportadora de elétrons e aumentaram a dissipação de energia. Isso foi confirmado pelas variáveis do JIP_{Test}. Apesar do impacto da temperatura, os resultados sugeriram que a recorrência do déficit hídrico do solo induziu tolerância ao calor no clone 'A1', enquanto aumentou a sensibilidade no clone '3V'.

Introduction

C. canephora is the second most cultivated and consumed coffee species worldwide. Brazil ranks second in the production and export of this species (ICO,

2025). The primary contributor to Brazilian *C. canephora* production is the Espírito Santo state, which accounts for approximately 70% of the national output (Conab, 2024). However, productivity in this region has faced ongoing challenges due to water scarcity and rising average air temperatures, particularly in non-irrigated crops (Venancio et al., 2020). Numerous studies have highlighted the negative impacts of drought and supra-optimal temperatures on the cultivation of *Coffea* spp., mainly due to stomatal and non-stomatal photosynthetic limitations (Rodrigues et al., 2016; Dubberstein et al., 2020b; Baroni et al., 2024; DaMatta et al., 2025).

Supra-optimal temperature stress directly damages the photosynthetic apparatus due to the sensitivity of photosystem II (PSII) reaction centers to heat (Zahra et al., 2023). High temperatures reduce the stability of the manganese cluster in the oxygen evolution complex (OEC), thereby limiting the electron supply to the transport chain (ETC) (Gupta, 2020). Additionally, increased membrane fluidity results in significant energy decoupling and a reduction in electron flow toward PSI, which restricts the synthesis of ATP and NADPH (Mathur et al., 2014). In *Coffea* spp., studies have shown that thermal stress decreases photochemical efficiency (Yamane et al., 2022), reduces the electron transport rate and the activity of photosynthetic and respiratory enzymes (Rodrigues et al., 2016; Dubberstein et al., 2020), and compromises the photosynthetic assimilation rate (Rodrigues et al., 2018; Dubberstein et al., 2020b) The extent of damage resulting from heat stress and the ability of plants to recover after stress relief are strongly impacted by leaf genotype and age (Marias et al., 2017a; 2017b) and by the combination of stressors such as drought and supra-optimal temperatures (Dubberstein et al., 2020; Rodrigues et al., 2024).

The simultaneous occurrence of stressful conditions, such as water scarcity combined with supra-optimal temperatures, can severely damage the photosynthetic apparatus and reduce crop productivity (Shabbir et al., 2022). However, some studies have shown that the recurrence of these stressful conditions in cultivation areas can trigger stress responses that activate certain tolerance mechanisms in plants (Bandurska, 2022; Saharan et al., 2022; Rakocevic et al., 2024). These acclimation mechanisms are associated with stress memory in plants and have been extensively studied for the development of cultivation techniques, such as priming, which enhances a plant's ability to cope with environmental stress (Liu et al., 2022). For example, it has been reported that repeated drought cycles in *Coffea* spp. can

trigger physiological adjustments that confer greater tolerance to future water deficits (Menezes-Silva et al., 2017; Baroni et al., 2024; Rakocevic et al., 2024), or that the occurrence of a previous water deficit can induce tolerance to heat stress (Zhang and Huang, 2020). The regulation of antioxidant protection and metabolic reprogramming - involving hormone metabolism, osmoregulators, protective metabolites, lipid, and fatty acid metabolism - as well as molecular responses and epigenetic changes, may all contribute to the acquisition of heat tolerance (Zhang and Huang, 2020).

In recent decades, the occurrence and severity of various types of environmental stresses on plants have been monitored in a practical, fast, and non-invasive way through the monitoring of chlorophyll *a* fluorescence emission (ChlF) (Kalaji et al., 2016; Park et al., 2024). The use of the direct fluorescence technique allows measuring the "fast kinetics" of fluorescence between the O (initial fluorescence) and P (maximum fluorescence) steps of the induction curve and is called transient fluorescence due to its momentary and unstable response (Bussotti et al., 2012). In the induction curve, when plotted on a logarithmic scale (between 0 and 1000 ms), between the O and P steps, two inflection points become evident and are known as J (2 - 3 ms) and I (20 - 30 ms) steps, which is why it is commonly called the “OJIP curve” (Bussotti et al., 2012).

By evaluating the kinetics of the OJIP transient and its conformational changes, is possible to analyze the chain of biophysical events that describe the energy flow from light energy absorption and electron transport in the PSII reaction centers (RCs) to the reduction of final photosystem I (PSI) acceptors. The rise in the induction curve between the O and J steps is mainly related to the primary photochemical stage, that is the occurrence of single turnover Q_A reduction events, where Q_A is reduced only once (Yusuf et al., 2010; Chen et al., 2016; Zhu et al., 2021). The rise between the J and I steps primarily reflects the capacity to reduce electron acceptors between photosystems, such as Q_B, plastoquinone (PQ), cytochrome b6/f (cyt), and plastocyanin (PC) (Yusuf et al., 2010; Chen et al., 2016; Zhu et al., 2021).

The rise from J to P is related to the multiple turnover Q_A reduction events to achieve the complete closure of the reaction centers, and therefore, is dominated by the biochemical stage (Yusuf et al., 2010; Chen et al., 2016). The rise between I and P is mainly related to the reduction of final PSI acceptors, especially ferredoxin (FD) and nicotinamide adenine dinucleotide phosphate (NADP) (Yusuf et al., 2010; Chen

et al., 2016; Zhu et al., 2021). In some cases, the occurrence of drought or thermal stress can trigger the appearance of the K step between O and J, which is directly related to oxygen-evolving complex damage (OEC) (Kalaji et al., 2016). In addition to OJIP kinetics analysis, numerous quantitative parameters can be derived through JIP_{Test} analysis, which is based on the theory of energy flow in biomembranes (Strasser & Strasser, 1995).

The hypothesis posited that two successive cycles of soil water deficit would induce thermal tolerance in *C. canephora* clones. It was further hypothesized that this acquired tolerance could be interpreted through the analysis of OJIP kinetics and JIP_{Test} parameters, reflecting enhanced PSII stability following exposure to supra-optimal temperatures. To test this, two *C. canephora* clones with contrasting drought sensitivity were cultivated and subjected to two cycles of soil water deficit followed by rehydration. Finally, thermal shock using a water bath was simulated for both clones, during which ChlF emission from the samples was monitored.

Material and methods

Plant material and growing conditions

The experiment was conducted in a greenhouse at the State University of the North Fluminense Darcy Ribeiro, in Campos dos Goytacazes (21º44'47” S, 41º18'24” W, at 10 m), RJ, Brazil. Fourteen plants of two *C. canephora* cv. Conilon clones, designated as ‘3V’ and ‘A1’, were cultivated. The ‘3V’ clone was previously characterized by deeper root growth (Rakocevic et al., 2023) and greater water stress tolerance, as evidenced by some physiological (Baroni et al., 2024), anatomical, and morphological (De Souza et al., 2025) parameters. Conversely, the ‘A1’ clone exhibited shallower root growth (Rakocevic et al., 2023) and higher sensitivity to water stress, based on some physiological responses (Baroni et al., 2024), but more conservative in water use, considering anatomical and morphological parameters (De Souza et al., 2025).

Five-month-old vegetatively propagated seedlings were transplanted into 31-liter PVC tubes containing a substrate of red-yellow latosol and sand in a 4:1 ratio, corrected and fertilized according to agronomic requirements. For 60 days, the plants were irrigated daily to maintain soil retention capacity. Following this establishment

period, seven plants of each clone were kept under full irrigation (WW), while the other seven were subjected to two successive cycles of soil drying and rehydration (WS), as shown in the scheme below (Figure 1). The treatments were designated as '3V'-WW and 'A1'-WW (well-watered treatments) and '3V'-WS and 'A1'-WS (water-stressed treatments).

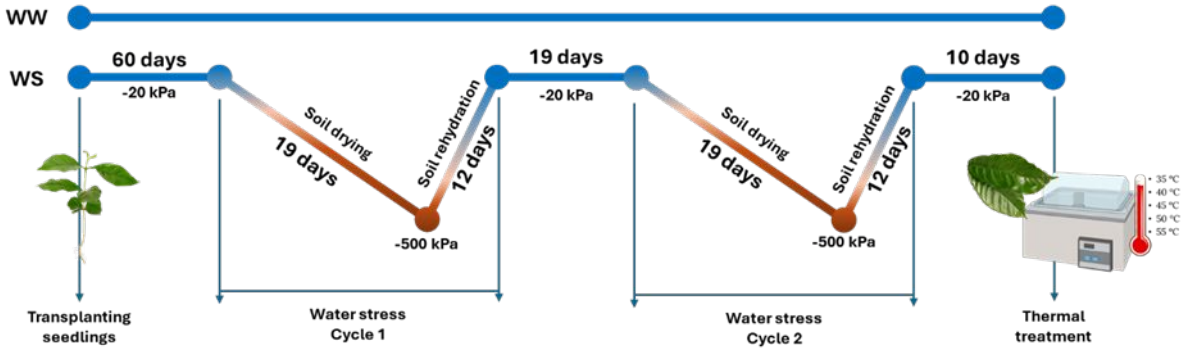

Figure 1: Experimental flow chart. Seedlings of *C. canephora* clones 'A1' and '3V' were transplanted into 31-liter pots. The plants were grown for 60 days under full irrigation (Ψ_{mSoil} ≈ -20 kPa). After this period, a group of plants was subjected to two cycles of water stress (WS; soil drying + rehydration) until reaching Ψ_{mSoil} ≈ -500 kPa, and a group was kept under full irrigation (WW). Between the two cycles of water stress, for 19 days, the plants were kept under full irrigation. Ten days after the end of the second cycle of water stress, the leaves were collected and subjected to heat treatment.

Soil matric potential (Ψ_{mSoil}) was monitored daily using Teros-21 sensors, with data stored in ZL6 Pro dataloggers (METER Group, Pullman, WA, EUA). The sensors were positioned at a soil depth of 0.1 m and 0.5 m. During the two soil drying cycles, plants were not irrigated until Ψ_{mSoil} values dropped below -500 kPa. Subsequently, the soil was re-irrigated to allow plant recovery. Each cycle of soil drying and rehydration lasted 31 days, with a 19-day recovery period between the cycles and a final recovery period of 10 days.

The plants were cultivated in a random block design. Throughout the experimental period, variables such as air temperature (T_{air}, °C), relative humidity (RH, %), and photosynthetic photon flux density (PPFD, µmol m^{-2} s^{-1}) were monitored daily using a Weather Station Watchdog 2000 (Spectrum Technologies, Plainfield, IL,

USA). Air vapor pressure deficit (VPD_{air}, kPa) was calculated based on air temperature and humidity values, as proposed by Jones (1992).

During the experimental period, the maximum and mean PPFD values were 1291.7 ± 32.1 $\mu mol.m^{-2}.s^{-1}$ and 627.6 ± 19.3 $\mu mol.m^{-2}.s^{-1}$, respectively. The maximum, mean, and minimum RH values were 89.9 ± 0.2%, 71.2 ± 0.5%, and 41.4 ± 0.9%, respectively. The maximum, mean, and minimum T_{air} were 41.6 ± 0.4°C, 29.7 ± 0.2°C, and 22.8 ± 0.2°C, respectively. The maximum, mean, and minimum VPD_{air} values were 4.9 ± 0.1 kPa, 1.7 ± 0.1 kPa, and 0.3 ± 0.01 kPa, respectively.

The minimum observed soil matric potential (Ψ_{mSoil}) values for ‘3V’-WS during the first and second cycles of water deficit were -406 kPa and -446 kPa, respectively. For ‘A1’-WS, the minimum Ψ_{mSoil} values during the first and second cycles were -332 kPa and -376 kPa, respectively. In the irrigated treatments ‘3V’-WW and ‘A1’-WW, Ψ_{mSoil} was maintained at -11 kPa and -15 kPa, respectively, throughout the experimental period.

Thermal treatment

Thermal treatments were applied following the methodology of Souza et al. (2022). Ninety days after the initiation of the first water deficit cycle, the five most vigorous plants from each of the four treatments (‘3V’-WW, ‘A1’-WW, ‘3V’-WS, and ‘A1’-WS) were selected. Fully expanded leaves developed during the successive cycles of soil drying and rehydration were collected at predawn. These leaves were placed in dark, moistened bags with wet paper towels and transported to the laboratory.

In the laboratory, under dark conditions, leaf discs (~2 cm^2) were cut from the leaf blade, avoiding the midrib. The leaf discs from the five plants were mixed to create five random samples for each genotype treatment, previously experienced water stress. These samples were subsequently exposed to short-term (15 minutes) high-temperature treatments (at 35°C, 40°C, 45°C, 50°C, and 55°C). Discs were placed in perforated plastic containers and immersed in a water bath where they were incubated independently for 15 minutes at each of five temperatures. After incubation, they were removed from the water bath, surface-dried with paper towels, and prepared for ChlF emission measurement.

Chlorophyll *a* fluorescence emission measurement

Chlorophyll fluorescence (ChlF) emission from leaf discs was monitored using a non-modulated fluorimeter model Pocket PEA (Hansatech Instruments Ltd, Pentney, King's Lynn, UK) equipped with a leaf clip. Typically, leaf clips are employed to adapt the leaf to darkness, allowing for the complete oxidation of PSII reaction centers (RCs "open") and preparing them to receive electrons. However, since the entire procedure was conducted in the dark, the dark adaptation step was not necessary.

To induce the ChlF emission curve based on OJIP transients, a pulse of saturating red light (~627 nm) with an intensity of 3500 μmol m^{-2} s^{-1} was applied to the leaf discs. The emitted ChlF was detected by a PIN photodiode, amplified, and recorded at intervals of 10 μs up to 2 ms, 100 μs between 2 and 3 ms, 1 ms between 3 and 30 ms, 10 ms between 30 and 300 ms, and 100 ms between 300 and 1000 ms. Data was recorded over a period of one second. Additionally, the basic ChlF parameters recorded at 50 μs (F_0 – initial fluorescence), 100 μs ($F_{100\mu s}$), 300 μs ($F_{300\mu s}$), 2 ms (F_J – J phase), 30 ms (F_I – I phase), and 300 ms ($F_P \sim F_m$, where F_m is the maximum fluorescence after the saturating light pulse) were used to calculate JIP_{Test} parameters (Table S1) (Strasser et al., 2004; Stirbet and Govindjee, 2011; Goltsev et al., 2016) using the PEA Plus software (Hansatech Instruments Ltd, Pentney, King's Lynn, UK).

Membrane permeability

Ten leaf discs (63.62 mm^2) were removed along the leaf blade, avoiding the midrib. These discs were washed in distilled water and placed in test tubes with 10 mL of distilled water. The tubes were partially immersed in a water bath previously adjusted to each temperature (35ºC, 40ºC, 45ºC, 50ºC, and 55ºC) and were kept incubated for 15 minutes. Two hours after removal from the water bath and stabilization, the electrical conductivity of the solution was measured with an $Edge^{EC}$ conductivity meter (model HI2003-02, Hanna Instruments, Barueri, SP, Brazil). Subsequently, the tubes were kept for 2 hours in a water bath at 90ºC, and after cooling, the total conductivity of the solution was measured again. The membrane

permeability was calculated as the percentage of the total conductivity for each temperature.

Data processing and analysis

For the OJIP transient kinetics analysis, the recorded ChlF data over the induction time were plotted on a logarithmic scale. Subsequently, the data were double-normalized between the O and P steps as $W_{OP} = (F_t – F_0)/(F_P – F_0)$ and $\Delta W_{OP} = (W_{OP(Temperature)} - W_{OP(35°C)})$; between the O and J steps as $W_{OJ} = (F_t – F_0)/(F_J – F_0)$ and $\Delta W_{OJ} = (W_{OJ(Temperature)} - W_{OJ(35°C)})$; between the O and K steps as $W_{OK} = (F_t – F_0)/(F_K – F_0)$ and $\Delta W_{OK} = (W_{OK(Temperature)} - W_{OK(35°C)})$; between the O and I steps as $W_{OI} = (F_t – F_0)/(F_I – F_0)$ and $\Delta W_{OI} = (W_{OI(Temperature)} - W_{OI(35°C)})$, for $1 < W_{OI} > 1$; and between the I and P steps as $W_{IP} = (F_t – F_I)/(F_P – F_I)$ and $\Delta W_{IP} = (W_{IP(Temperature)} – W_{IP(35°C)})$. Each plotted curve represents the average of five repetitions, each corresponding to a leaf disc. Data normalization was performed using Excel®, and graphs were plotted using OriginPro, version 2016® (OriginLab Corporation, Northampton, MA, USA).

For the JIP_{Test} and membrane permeability data, a two-way analysis of variance (ANOVA) was performed with a completely randomized design including two factors (4 x 5): four treatments (‘3V’-WW, ‘A1’-WW, ‘3V’-WS, and ‘A1’-WS) and five temperatures (35°C, 40°C, 45°C, 50°C, and 55°C), with five replications. The ANOVA was conducted using R software, version 4.4.0. In the case of statistical significance (P-value < 0.05), means were compared using the Tukey test at a 5% significance level with the agricolae package, version 1.3-7.

Results

Considering the results obtained from the analysis of the OJIP transient polyphasic curve for clones ‘3V’ and ‘A1’ under irrigated (WW) and post-water stress (WS) conditions, it is evident that the increase in temperature caused considerable changes in the phases of the curve starting from 45°C (Figure 2). However, in all treatments at 50°C and 55°C, the conformational changes in the curves are more pronounced. Notably, for clone ‘3V’, in both treatments (WW and WS) at 55°C, the values of F_0 and F_P become similar.

At the O step, the temperature increases led to the following percentage changes compared to the control (35°C): in ‘3V’-WW, increases of 7% at 45°C, 50% at 50°C, and 135% at 55°C (Figure 2a); in ‘3V’-WS, increases of 23% at 45°C, 34% at 50°C, and 202% at 55°C (Figure 1b); in ‘A1’-WW, increases of 14% at 45°C, 48% at 50°C, and 93% at 55°C (Figure 2c); in ‘A1’-WS, increases of 11% at 45°C, 69% at 50°C, and 44% at 55°C (Figure 2d).

At the K step, the temperature increases led to the following percentage changes compared to the control: in ‘3V’-WW, increases of 7% at 40°C, 11% at 45°C, 60% at 50°C, and 102% at 55°C (Figure 2a); in ‘3V’-WS, increases of 25% at 45°C, 39% at 50°C, and 164% at 55°C (Figure 2b); in ‘A1’-WW, increases of 19% at 45°C, 49% at 50°C, and 78% at 55°C (Figure 2c); in ‘A1’-WS, increases of 15% at 45°C, 67% at 50°C, and 34% at 55°C (Figure 2d).

At the J step, the temperature changes resulted in the following variations compared to the control (35°C) (Figure 2a): in ‘3V’-WW, a reduction of 9% at 45°C (Figure 2a); in ‘3V’-WS, a reduction of 5% at 50°C and an increase of 34% at 55°C (Figure 2b); in ‘A1’-WW, increases of 7% at 45°C and 14% at 55°C (Figure 2c); in ‘A1’-WS, an increase of 6% at 50°C and a reduction of 18% at 55°C (Figure 2d).

At the I step, the temperature changes led to the following variations compared to the control: in ‘3V’-WW, reductions of 9% at 40°C, 28% at 45°C, and 31% at 50°C and 55°C (Figure 2a); ‘3V’-WS, an increase of 5% at 40°C and reductions of 19% at 45°C, 38% at 50°C, and 10% at 55°C (Figure 2b); ‘A1’-WW, increases of 24% at 50°C and 9% at 55°C (Figure 2c); in ‘A1’-WS, reductions of 15% at 45°C, 23% at 50°C, and 39% at 55°C (Figure 2d).

At the P step, the temperature changes resulted in the following variations compared to the control: in ‘3V’-WW, reductions of 10% at 40°C, 11% at 45°C, 25% at 50°C, and 39% at 55°C (Figure 2a); in ‘3V’-WS, an increase of 5% at 40°C and reductions of 22% at 50°C and 25% at 55°C (Figure 2b); in ‘A1’-WW, an increase of 5% at 45°C and reductions of 18% at 50°C and 15% at 55°C (Figure 2c); in ‘A1’-WS, reductions of 22% at 50°C and 44% at 55°C (Figure 2d).

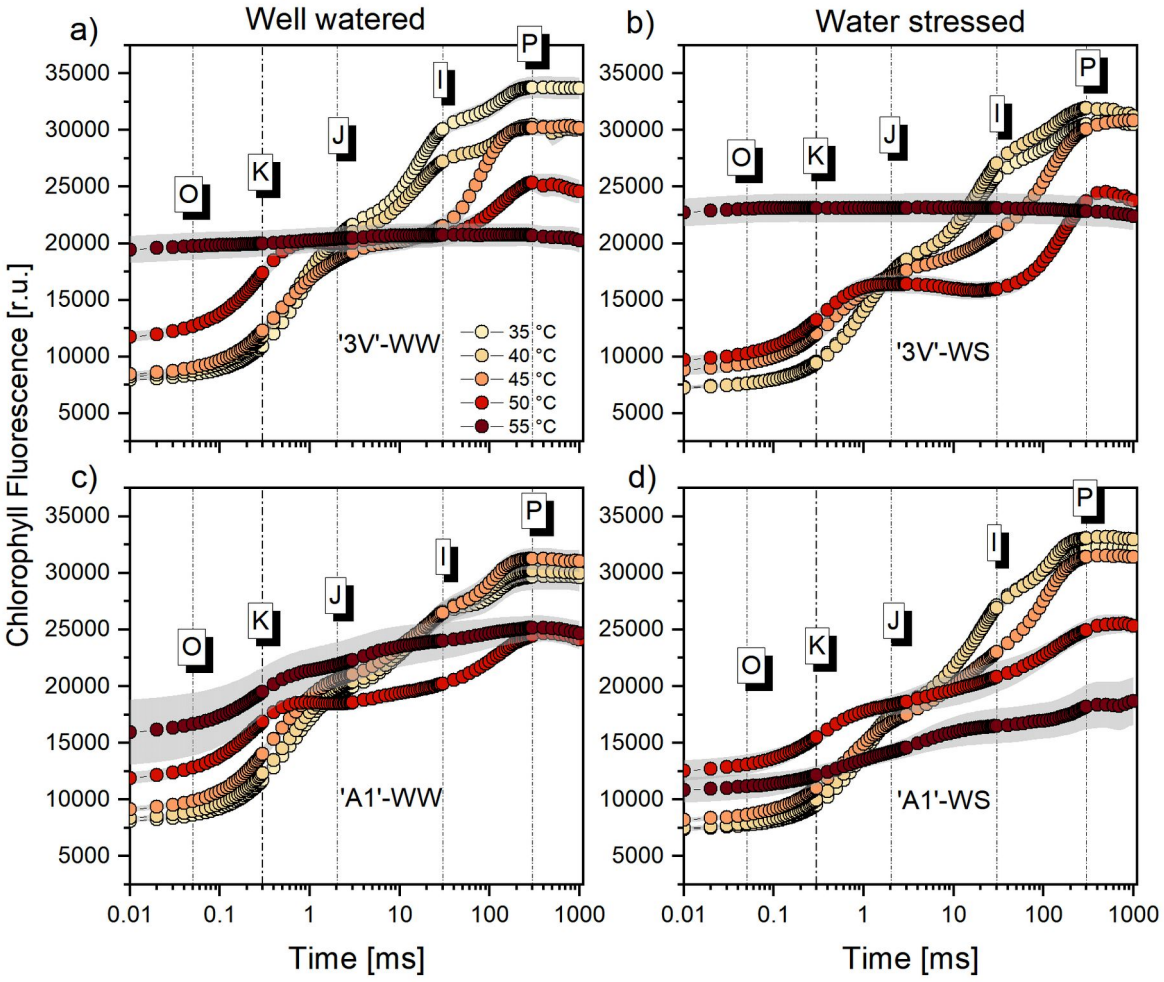

Figure 2: Transient chlorophyll *a* fluorescence induction curves in logarithmic scale, measured in leaf discs subjected to heat treatment in a water bath at different temperatures, and sampled in *C. canephora* '3V' and 'A1' clones grown under well-watered conditions (WW) and under two cycles of recurrent water stress (WS). The figure shows the treatments '3V'-WW (a), '3V'-WS (b), 'A1'-WW (c), and 'A1'-WS (d) incubated for 15 min at temperatures of 35°C, 40°C, 45°C, 50°C, and 55°C, indicated by colored symbols, where lighter colors represent lower temperatures and darker colors indicate higher temperatures. Each symbol indicates the mean of five replicates (n = 5). Within the figure, points O, K, J, I, and P represent the ChlF emission curve steps at times 50 µs, 300 µs, 2 ms, 30 ms, and 300 ms, respectively.

Considering the double normalization of W_{OP} and ΔW_{OP} (Figure 3) between the O step ($F_{50\mu s}$) and the P step (F_{300ms}) of the typical polyphasic curve, it was evident that starting from 45°C, there was a trend toward increased positive amplitude at the K step and increased negative amplitude at the I step, particularly at 50°C and 55°C.

The changes in ΔW_{OP} were the most pronounced in the following order: ‘3V’-WS (Figure 3b) > ‘3V’-WW (Figure 3a) > ‘A1’-WW (Figure 3c) > ‘A1’-WS (Figure 3d). Notably, in ‘3V’-WS at 55°C, there was a complete loss of photosynthetic apparatus function from the O step, as indicated by the high negative amplitude throughout the fluorescence increase kinetics.

The double normalization of W_{OJ} and ΔW_{OJ} (Figure 4) between the O step ($F_{50\mu s}$) and the J step (F_{2ms}) revealed the K-band, through which it can be observed that the increase in temperature to 45°C, 50°C, and 55°C led to an increase in the positive amplitude of ΔW_{OJ} in all treatments. In ‘3V’-WW, this increase began at 40°C and was highest at 55°C (Figure 4a). In ‘3V’-WS, there was a low variation at 40°C compared to 35°C; the increase at 50°C was less compared to ‘3V’-WW, but at 55°C, there was a significant rise in the amplitude of the curve, indicating severe damage to the photosynthetic apparatus (Figure 4b). In ‘A1’-WW (Figure 4c) and ‘A1’-WS (Figure 4d), an increase in amplitude due to rising temperature was observed, although less pronounced than in ‘3V’-WW and ‘3V’-WS. Additionally, the peaks in ‘A1’-WS at 50°C and 55°C are relatively smaller compared to ‘A1’-WW.

The double normalization of W_{OK} and ΔW_{OK} between the O step ($F_{50\mu s}$) and the K step ($F_{200\mu s}$) revealed the L band (Figure 5). In ‘3V’-WW, an increase in ΔW_{OK} amplitude at 50°C and 55°C is observed, indicating extreme damage at the latter (Figure 5a). In ‘3V’-WS, the peak at 50°C was reduced compared to ‘3V’-WW at the same temperature (Figure 5b). However, the high amplitude at 55°C persisted. ‘A1’-WW (Figure 5c) and ‘A1’-WS (Figure 5d) showed greater stability in ΔW_{OK}, with the peak amplitudes in ‘A1’-WS being relatively smaller compared to ‘A1’-WW at all temperatures.

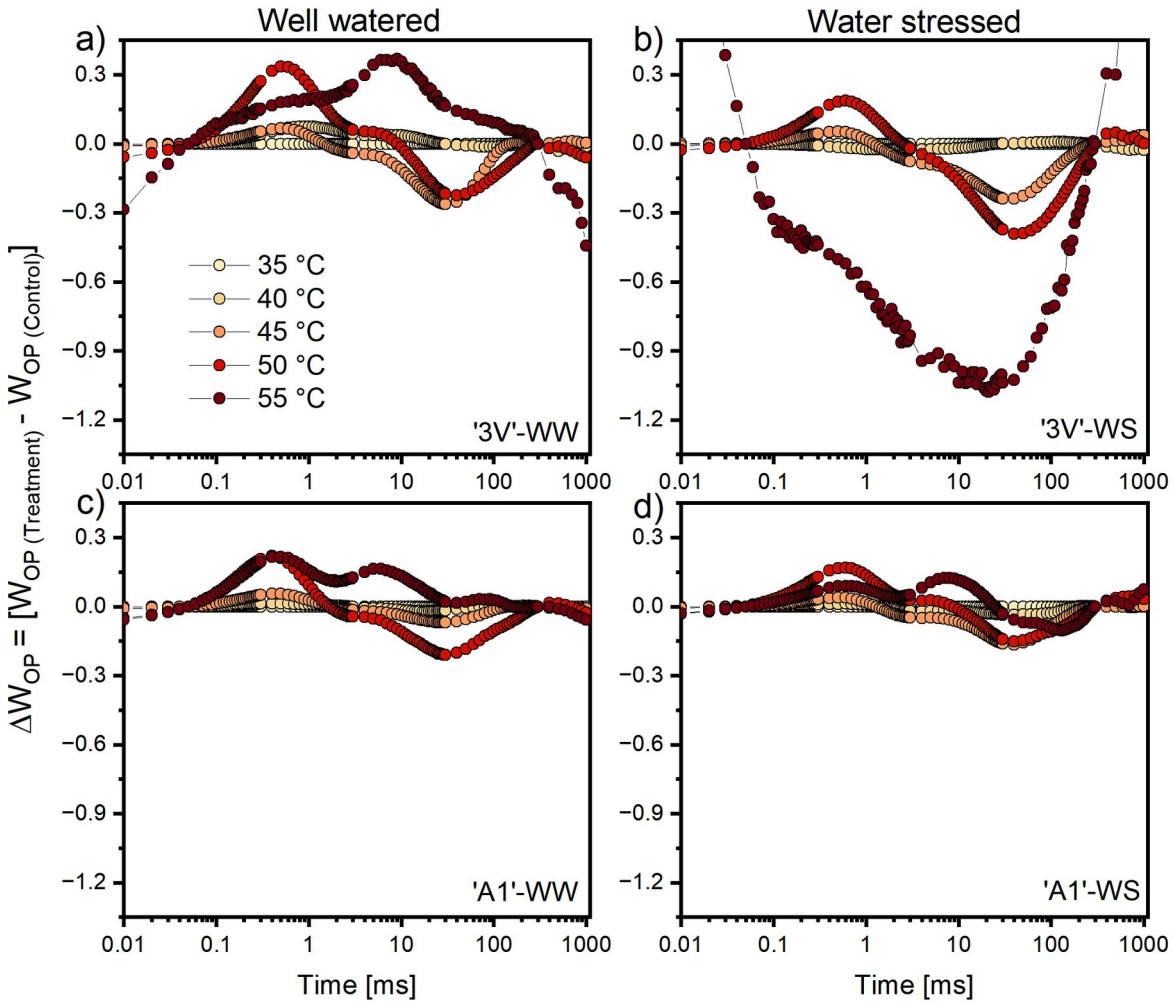

Figure 3: Differential analysis of OJIP kinetics (ΔW_{OP}), obtained by normalizing the relative fluorescence kinetics between the O and P steps (W_{OP}) in transient chlorophyll *a* fluorescence induction curves measured in leaf discs subjected to heat treatment in a water bath at different temperatures, and sampled in *C. canephora* '3V' and 'A1' clones grown under well-watered conditions (WW) and under two cycles of recurrent water stress (WS). The figure shows the treatments '3V'-WW (a), '3V'-WS (b), 'A1'-WW (c), and 'A1'-WS (d) incubated for 15 minutes at temperatures of 35°C, 40°C, 45°C, 50°C, and 55°C, indicated by colored symbols, where lighter colors indicate lower temperatures and darker colors indicate higher temperatures. Each symbol indicates the mean of five replicates (n = 5). The normalizations $W_{OP} = (F_t - F_0)/(F_P - F_0)$ and $\Delta W_{OP} = (W_{OP(Temperature)} - W_{OP(35°C)})$ were considered.

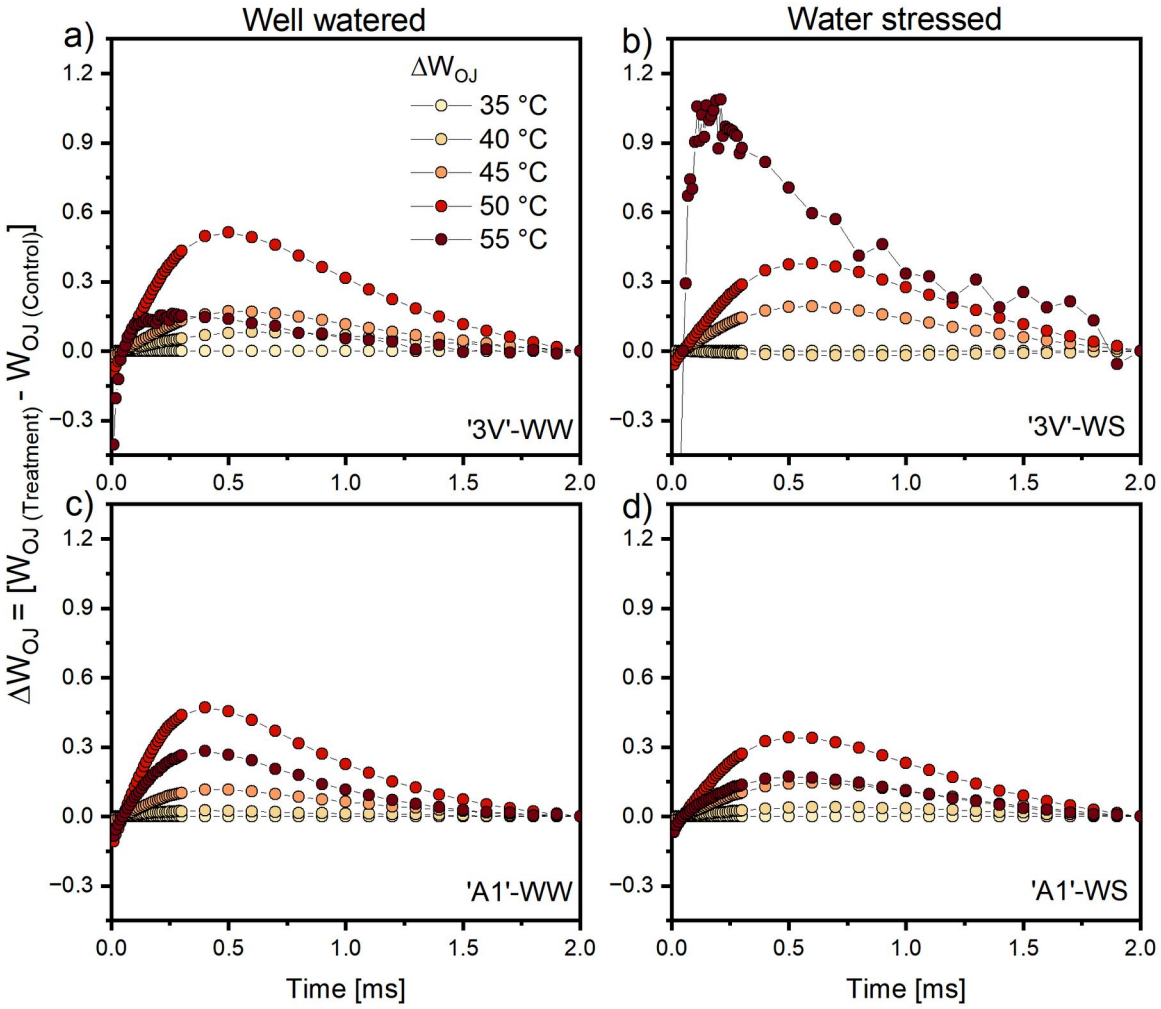

Figure 4: Differential analysis of OJIP kinetics (ΔW_{OJ}), obtained by normalizing the relative fluorescence kinetics between the O and J steps (W_{OJ}) in transient chlorophyll *a* fluorescence induction curves measured in leaf discs subjected to heat treatment in a water bath at different temperatures, and sampled in *C. canephora* '3V' and 'A1' clones grown under well-watered conditions (WW) and two cycles of recurrent water stress (WS). The figure shows the treatments '3V'-WW (a), '3V'-WS (b), 'A1'-WW (c), and 'A1'-WS (d) incubated for 15 minutes at temperatures of 35°C, 40°C, 45°C, 50°C and 55°C, indicated by colored symbols, where lighter colors represent lower temperatures, and darker colors represent higher temperatures. Each symbol represents the mean of five replicates (n = 5). The normalizations $W_{OJ} = (F_t - F_O)/(F_J - F_O)$ and $\Delta W_{OJ} = (W_{OJ(Temperature)} - W_{OJ(35°C)})$ were considered.

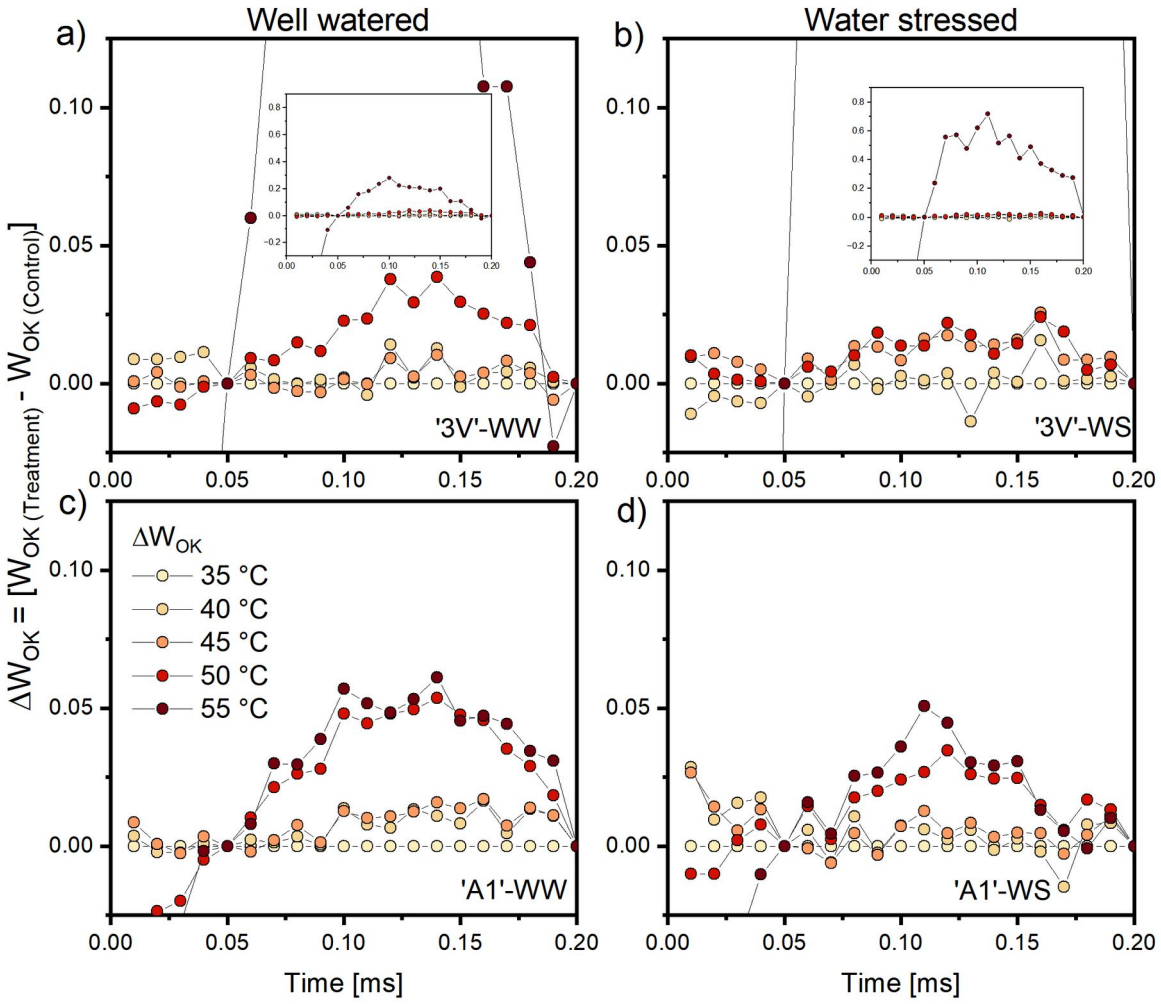

Figure 5: Differential analysis of OJIP kinetics (ΔW_{Ok}), obtained by normalizing the relative fluorescence kinetics between the O and K steps (W_{OK}) in transient chlorophyll *a* fluorescence induction curves measured in leaf discs subjected to heat treatment in a water bath at different temperatures, and sampled in *C. canephora* '3V' and 'A1' clones grown under well-watered conditions (WW) and two cycles of recurrent water stress (WS). The figure shows the treatments '3V'-WW (a), '3V'-WS (b), 'A1'-WW (c), and 'A1'-WS (d) incubated for 15 minutes at temperatures of 35°C, 40°C, 45°C, 50°C, and 55°C, indicated by colored symbols, where lighter colors represent lower temperatures, and darker colors represent higher temperatures. Each symbol represents the mean of five replicates (n = 5). The normalizations $W_{OK} = (F_t - F_O)/(F_K - F_O)$ and $\Delta W_{OK} = (W_{OK(Temperature)} - W_{OK(35°C)})$ were considered.

Considering the double normalization of W_{OI} and ΔW_{OI} ($W_{OI} < 1$) between the O step ($F_{50\mu s}$) and the I step (F_{30ms}), the amplitude of the curve that in 3V-WW at 40°C was slightly higher than at 35°C, with the greatest amplitude observed at 50°C

(Figure 6a). In ‘3V’-WS (Figure 6b), the highest amplitude with significant variation was observed at 55°C. Compared to ‘3V’, ‘A1’ (Figures 6c and 6d, respectively) exhibited reduced curve amplitudes starting from 45°C, especially in ‘A1’-WS.

Analyzing the double normalization of W_{OI} and ΔW_{OI} ($W_{OI} > 1$) in ‘3V’-WW, the highest positive amplitudes were observed at 50°C and 45°C, respectively (Figure 7a); at 55°C, a negative amplitude of the curve was noted compared to the control (35°C). In ‘3V’-WS, the highest amplitudes were at 45°C and 50°C, respectively (Figure 7b), and at 55°C, a negative amplitude was observed compared to the control (35°C). The amplitudes observed in ‘3V’-WS were greater than in ‘3V’-WW. In ‘A1’-WW, the highest amplitudes were at 45°C and 50°C, respectively (Figure 7c); and in ‘A1’-WS, they were at 50°C and 45°C, respectively (Figure 7d). In ‘A1’-WW and ‘A1’-WS, at 55°C, the negative amplitude of the curve was lower than ‘3V’-WW and ‘3V’-WS.

The analysis of the double normalization of W_{IP} and ΔW_{IP} between step I (F_{30ms}) and step P (F_{300ms}) revealed that in ‘3V’-WW (Figure 8a), the greatest positive amplitude was observed at 45°C, while the greatest negative amplitudes were observed at 40°C, 50°C, and 55°C, respectively. In ‘3V’-WS at 40°C (Figure 8b), the amplitude of the curve was slightly positive, while at 45°C, 50°C, and 55°C, negative amplitudes were observed; at 55°C, the amplitude in ‘3V’-WS was lower compared to ‘3V’-WW. In ‘A1’-WW (Figure 8c), all curves showed positive amplitude with no significant variations between temperatures. In ‘A1’-WS (Figure 8d), all curves exhibited negative amplitudes at 40°C, 45°C, 50°C, and 55°C, respectively.

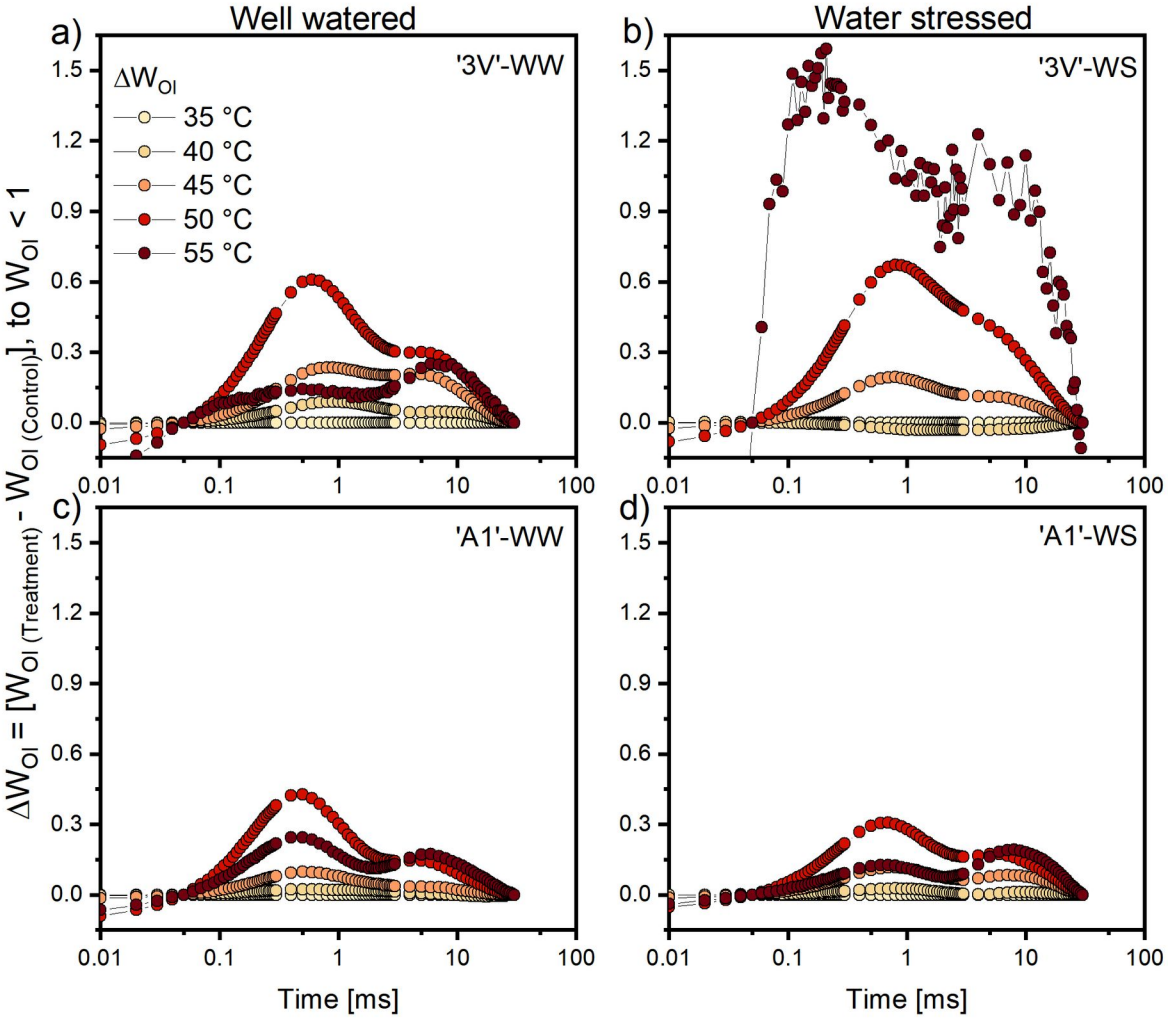

Figure 6: Differential analysis of OJIP kinetics (ΔW_{OI}, W_{OI} < 1), obtained by normalizing the relative fluorescence kinetics between the O and I steps (W_{OI} < 1) in transient chlorophyll *a* fluorescence induction curves measured in leaf discs subjected to heat treatment in a water bath at different temperatures, and sampled in *C. canephora* '3V' and 'A1' clones grown under well-watered conditions (WW) and two cycles of recurrent water stress (WS). The figure shows the treatments '3V'-WW (a), '3V'-WS (b), 'A1'-WW (c), and 'A1'-WS (d) incubated for 15 minutes at temperatures of 35°C, 40°C, 45°C, 50°C, and 55°C, indicated by colored symbols, where lighter colors represent lower temperatures, and darker colors represent higher temperatures. Each symbol represents the mean of five replicates (n = 5). The normalizations $W_{OI} = (F_t - F_O)/(F_I - F_O)$, to W_{OI} < 1 and $\Delta W_{OI} = (W_{OI(Temperature)} - W_{OI(35°C)})$ were considered.

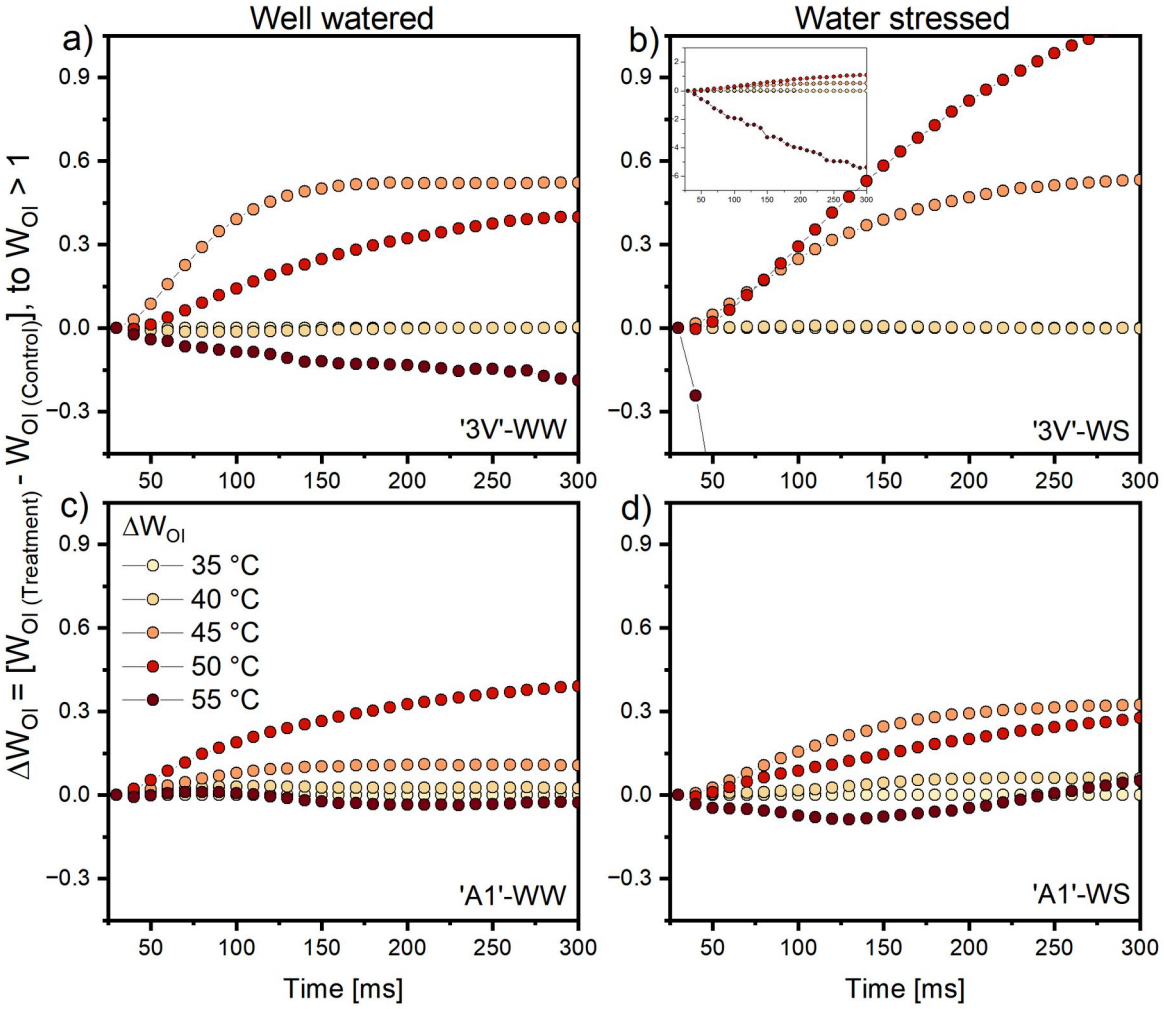

Figure 7: Differential analysis of OJIP kinetics (ΔW_{OI}, W_{OI} > 1), obtained by normalizing the relative fluorescence kinetics between the O and I steps (W_{OI} > 1) in transient chlorophyll *a* fluorescence induction curves measured in leaf discs subjected to heat treatment in a water bath at different temperatures, and sampled in *C. canephora* '3V' and 'A1' clones grown under well-watered conditions (WW) and two cycles of recurrent water stress (WS). The figure shows the treatments '3V'-WW (a), '3V'-WS (b), 'A1'-WW (c), and 'A1'-WS (d) incubated for 15 minutes at temperatures of 35°C, 40°C, 45°C, 50°C, and 55°C, indicated by colored symbols, where lighter colors represent lower temperatures, and darker colors represent higher temperatures. Each symbol represents the mean of five replicates (n = 5). The normalizations $W_{OI} = (F_t - F_O)/(F_I - F_O)$, to W_{OI} > 1 and $\Delta W_{OI} = (W_{OI(Temperature)} - W_{OI(35°C)})$ were considered.

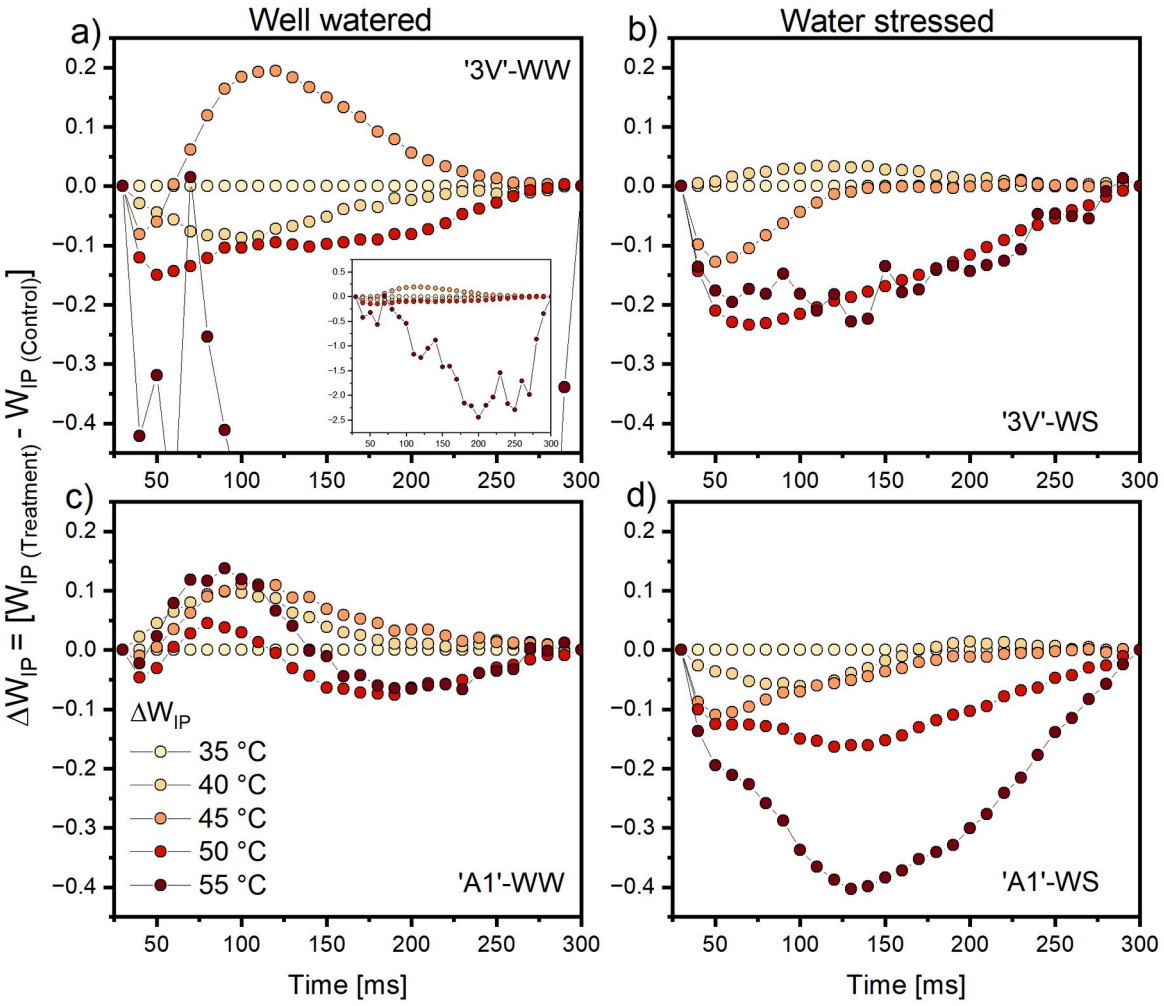

Figure 8: Differential analysis of OJIP kinetics (ΔW_{IP}), obtained by normalizing the relative fluorescence kinetics between the I and P steps (W_{IP}) in transient chlorophyll *a* fluorescence induction curves measured in leaf discs subjected to heat treatment in a water bath at different temperatures, and sampled in *C. canephora* '3V' and 'A1' clones grown under well-watered conditions (WW) and two cycles of recurrent water stress (WS). The figure shows the treatments '3V'-WW (a), '3V'-WS (b), 'A1'-WW (c), and 'A1'-WS (d) incubated for 15 minutes at temperatures of 35°C, 40°C, 45°C, 50°C and 55°C, indicated by colored symbols, where lighter colors represent lower temperatures, and darker colors represent higher temperatures. Each symbol represents the mean of five replicates (n = 5). The normalizations $W_{IP} = (F_t - F_O)/(F_I - F_P)$ and $\Delta W_{IP} = (W_{IP(Temperature)} - W_{IP(35°C)})$ were considered.

For the energy flux ratios or quantum yields, the interaction of treatment *vs.* temperature was significant for the variables φ_{Po}, φ_{Eo}, φ_{Do}, and φ_{Ro}, and not significant for Ψ_{Eo} and δ_{Ro}. Ψ_{Eo}, which showed an expressive difference for the isolated factors

treatment and temperature, and δ_{Ro} showed a significant difference only for the temperature factor (Table S2; Supplementary data A).

At 55°C there was a difference in φ_{Po} between treatments (Table 1), where ‘A1’-WW and ‘A1’-WS were similar and statistically higher than ‘3V’-WW and ‘3V’-WS, which also did not differ from each other. The φ_{Po} at temperatures between 35°C and 45°C did not differ from each other, despite the trend of reduction. At 50°C, a significant φ_{Po} reduction of 32%, 23%, 32%, and 36% was observed for ‘3V’-WW, ‘3V’-WS, ‘A1’-WW, and ‘A1’-WS, respectively. At 55°C, there was a φ_{Po} reduction of 93% and 98% for ‘3V’-WW and ‘3V’-WS, respectively, and 51% for ‘A1’-WW and ‘A1’-WS, indicating that the ‘A1’ clone had greater thermal tolerance compared to ‘3V’.

There was a significant reduction in Ψ_{Eo} only at 55°C, considering the average of all treatments (Table 1). The overall temperature Ψ_{Eo} average values indicated that the treatments ‘3V’-WS and ‘A1’-WS were approximately 25% higher when compared to ‘3V’-WW and ‘A1’-WW.

At temperatures ranging from 35°C to 45°C, there was a tendency of higher average values in φ_{Eo} in ‘3V’-WS and ‘A1’-WS compared to their counterparts ‘3V’-WW and ‘A1’-WW, respectively (Table 1). At 50°C, only the φ_{Eo} of ‘3V’-WS was higher than ‘3V’-WW. At 55°C, there was a φ_{Eo} reduction of 95%, 99%, 60%, and 49% in ‘3V’-WW, ‘3V’-WS, ‘A1’-WW, and ‘A1’-WS, respectively. At 50°C and 55°C, the lowest values of φ_{Eo} were observed in all treatments, with emphasis on clone ‘3V’ at 55°C.

For φ_{Do} a response inversely proportional to that observed in φ_{Po} is noted (Table 1). The φ_{Do} in treatments only differed from each other at 55°C, where ‘A1’-WW and ‘A1’-WS were lower than ‘3V’-WW and ‘3V’-WS. Between 35°C and 45°C, there was no difference in φ_{Do} for any treatment, but at 50°C and 55°C, the highest averages were observed, with emphasis on clone ‘3V’ at 55°C.

A considerable increase in δ_{Ro} was observed from 45°C, with the highest average observed at 55°C (Table 1). Higher general means of φ_{Ro} were observed at 45°C and 50°C, and for the treatments ‘3V’-WS and ‘A1’-WS, when compared to their counterparts ‘3V’-WW and ‘A1’-WW. At 50°C, ‘3V’-WS presented a higher δ_{Ro} mean value compared to the other treatments. At 55°C, the φ_{Ro} of the clone ‘3V’ was lower than that of ‘A1’.

Table 1: Quantum efficiency or energy flux ratios parameters derived from the analysis of OJIP transients using JIP_{Test}, for treatments '3V'-WW, '3V'-WS, 'A1'-WW, and 'A1'-WS incubated at different temperatures (35°C, 40°C, 45°C, 50°C, and 55°C) for 15 minutes. φ_{Po}, maximum quantum yield of primary PSII photochemistry; Ψ_{Eo}, probability with which a PSII trapped electron is transferred from Q_A to Q_B; φ_{Eo}, quantum yield of electron transport flux from Q_A to Q_B; φ_{Do}, quantum yield of energy dissipation; δ_{Ro}, probability with which an electron from Q_B is transferred until PSI acceptors; φ_{Ro}, quantum yield of electron transport flux until the PSI acceptors.

Parameter	Treatment	Temperature					
		35 °C	40 °C	45 °C	50 °C	55 °C	Means
φ_{Po}	'3V'-WW	0.75 aA	0.71 aA	0.70 aA	0.51 aB	0.05 bC	0.55 b
	'3V'-WS	0.75 aA	0.76 aA	0.70 aAB	0.58 aB	0.01 bC	0.56 b
	'A1'-WW	0.71 aA	0.70 aA	0.68 aA	0.48 aB	0.35 aB	0.59 ab
	'A1'-WS	0.76 aA	0.76 aA	0.73 aA	0.49 aB	0.37 aB	0.62 a
	Means	0.74 A	0.74 A	0.70 A	0.51 B	0.20 C	
Ψ_{Eo}	'3V'-WW	0.53	0.46	0.56	0.43	0.32	0.46 b
	'3V'-WS	0.58	0.61	0.64	0.57	0.57	0.59 a
	'A1'-WW	0.49	0.49	0.49	0.51	0.36	0.47 b
	'A1'-WS	0.61	0.62	0.65	0.57	0.66	0.62 a
	Means	0.56 AB	0.55 AB	0.59 A	0.52 AB	0.48 B	
φ_{Eo}	'3V'-WW	0.40 abA	0.34 bA	0.39 abA	0.22 bB	0.02 bC	0.27 c
	'3V'-WS	0.44 abAB	0.46 aA	0.45 aA	0.33 aB	0.003 bC	0.34 b
	'A1'-WW	0.35 bA	0.34 bA	0.34 bA	0.25 abA	0.14 aB	0.29 c
	'A1'-WS	0.47 aA	0.48 aA	0.47 aA	0.28 abB	0.24 aB	0.39 a
	Means	0.41 A	0.40 A	0.41 A	0.27 B	0.10 C	
φ_{Do}	'3V'-WW	0.25 aC	0.29 aC	0.30 aC	0.49 aB	0.95 aA	0.46 a
	'3V'-WS	0.25 aC	0.24 aC	0.30 aBC	0.42 aB	0.99 aA	0.44 a
	'A1'-WW	0.29 aB	0.30 aB	0.32 aB	0.52 aA	0.65 bA	0.42 ab
	'A1'-WS	0.24 aB	0.24 aB	0.28 aB	0.51 aA	0.63 bA	0.38 b
	Means	0.26 C	0.27 C	0.30 C	0.49 B	0.80 A	
δ_{Ro}	'3V'-WW	0.28	0.31	0.75	0.85	1.15	0.67
	'3V'-WS	0.37	0.34	0.73	1.05	1.99	0.89
	'A1'-WW	0.32	0.35	0.45	0.68	0.22	0.41
	'A1'-WS	0.35	0.39	0.58	0.59	2.34	0.85
	Means	0.33 B	0.35 B	0.63 AB	0.79 AB	1.43 A	
φ_{Ro}	'3V'-WW	0.11 aB	0.11 aB	0.29 aA	0.19 bB	0.01 bC	0.14 b
	'3V'-WS	0.16 aB	0.16 aB	0.32 aA	0.35 aA	0.01 bC	0.19 a
	'A1'-WW	0.11 aAB	0.12 aAB	0.15 bA	0.18 bA	0.05 abB	0.12 b
	'A1'-WS	0.16 aB	0.19 aAB	0.27 aA	0.18 bAB	0.13 aB	0.19 a
	Means	0.14 B	0.14 B	0.26 A	0.23 A	0.05 C	

The means for each treatment are shown (n = 5). ANOVA P-values < 0.05 were considered significant; Means followed by the same lowercase letters compare means of treatments and the uppercase letters compare temperatures according to the Tukey test at 95% confidence.

All phenomenological energy flow parameters per leaf cross-section and performance indices were significantly impacted by the interaction between treatment and temperature (Table S2; Supplementary data A).

Higher temperatures induced higher mean values of ABS/CS_0 for this parameter, especially at 55°C (Table 2). At this temperature, a difference among treatments in ABS/CS_0 was observed, with the following order: 'A1'-WS < 'A1'-WW < '3V'-WW < '3V'-WS.

At 55°C, there were reductions of 84%, 97%, 20%, and 36% for '3V'-WW, '3V'-WS, 'A1'-WW and 'A1'-WS, respectively, in TR_0/CS_0 (Table 2). The exception was 'A1'-W, where the highest TR_0/CS_0 average was observed at 45°C. The treatments differed from each other only at 55°C, where the TR_0/CS_0 means of 'A1'-WW and 'A1'-WS remained significantly higher than those of '3V'-WW and '3V'-WS.

At 55°C, reductions of 89%, 97%, 39%, and 34% in ET/CS_0 (Table 2) were observed for '3V'-WW, '3V'-WS, 'A1'-WW, and 'A1'-WS, respectively. Furthermore, as observed, the general ET/CS_0 means for 'A1'-WW and 'A1'-WS remained significantly higher than those for '3V'-WW and '3V'-WS.

The highest mean values in DI_0/CS_0 were observed (Table 2) at 55°C for most treatments, except for 'A1'-WS, which showed higher DI_0/CS_0 values at both 50°C and 55°C. At this temperature, the treatments differed from each other, with 'A1'-WS < 'A1'-WW < '3V'-WW < '3V'-WS.

Differences in RC/CS_0 were observed starting at 45°C (Table 2) for all treatments. Both '3V'-WW and '3V'-WS showed RC/CS_0 mean reductions of 35%, 62%, and 95% at 45°C, 50°C, and 55°C, respectively. 'A1'-WW exhibited a reduction in RC/CS_0, approximately 60% at 50°C and 55°C. 'A1'-WS showed RC/CS_0 reductions of 32% at 45°C and an average of 60% at both 50°C and 55°C. At 50°C, 'A1'-WS was higher than 'A1'-WW, with no differences among the other treatments. At 55°C, the RC/CS_0 of 'A1'-WW and 'A1'-WS was significantly higher than of '3V'-WW and '3V'-WS.

For each temperature, starting at 40°C, '3V'-WW and 'A1'-WW showed lower mean values of SFI_{abs} (Table 2) compared to their counterparts, '3V'-WS and 'A1'-WS. Overall, there was a SFI_{abs} reduction of 39% at 45°C and an average of 86% at both 50°C and 55°C. Additionally, in general terms, the order observed in SFI_{abs} was 'A1'-WS = '3V'-WS > '3V'-WW > 'A1'-WW.

Temperatures above 40°C caused reductions in PI_{abs} for all treatments, except ‘A1’-WW (Table 2). ‘3V’-WW showed PI_{abs} reductions of approximately 50% at 40°C and 45°C, and 97% at both 50°C and 55°C. ‘3V’-WS exhibited PI_{abs} reductions of 42%, 85%, and approximately 99% at 45°C, 50°C, and 55°C, respectively. ‘A1’-WS showed PI_{abs} reductions of 44%, 93%, and 88% at 45°C, 50°C, and 55°C, respectively. Overall, the average PI_{abs} values for ‘3V’-WS and ‘A1’-WS were 1.5-fold higher compared to their counterparts ‘3V’-WW and ‘A1’-WW.

Membrane permeability was impacted by the interaction between treatments and temperatures (Figure 9). Up to 45ºC there was no difference between treatments, and there was no significant increase in membrane permeability. At 50ºC and 55ºC there was an increase in membrane permeability and '3V'-WS was lower than the other treatments at 50ºC. Only at 55ºC, the membrane permeability of 'A1'-WS was higher than '3V'-WS.

Table 2: Phenomenological energy fluxes parameters and photosynthetic indices derived from the analysis of OJIP transients using JIP_{Test}, for treatments '3V'-WW, '3V'-WS, 'A1'-WW, and 'A1'-WS incubated at different temperatures (35°C, 40°C, 45°C, 50°C, and 55°C) for 15 minutes. ABS/CS_0, absorbed energy; TR_0/CS_0, energy flux trapped by PSII reaction centers; ET_0/CS_0, energy flux through PSII; DI_0/CS_0, thermal dissipation of energy in PSII; RC/CS_0, density of reaction centers capable of Q_A reduction; described per unit of leaf cross-section (CS). SFI_{abs}, structure-function index; PI_{abs}, PSII performance index normalized by absorbed energy.

Parameter	Treatment	Temperature					
		35 °C	40 °C	45 °C	50 °C	55 °C	Means
ABS/CS_0	'3V'-WW	8392.60 aC	8738.20 aC	9016.00 aC	12662.20 aB	19739.60 bA	11709.72 a
	'3V'-WS	7639.60 aB	7600.80 aB	9356.80 aB	10266.20 aB	23038.00 aA	11580.28 a
	'A1'-WW	8624.20 aC	8943.80 aC	9855.60 aBC	12781.00 aB	16631.80 cA	11367.28 a
	'A1'-WS	7735.40 aC	7889.00 aBC	8651.60 aBC	13103.00 aA	11141.60 dAB	9704.12 b
	Means	8097.95 C	8292.95 C	9220.00 C	12203.10 B	17637.75 A	
TR_0/CS_0	'3V'-WW	6301.85 aA	6214.69 aA	6337.67 aA	6381.49 aA	964.96 bB	5240.13 bc
	3V'-WS	5743.22 aA	5790.85 aA	6472.87 aA	5961.78 aA	150.79 bB	4823.91 c
	'A1'-WW	6116.47 aAB	6285.96 aAB	6729.75 aA	6038.36 aAB	4882.09 aB	6010.53 a
	'A1'-WS	5880.77 aA	6012.08 aA	6266.27 aA	6267.92 aA	3721.96 aB	5629.80 ab
	Means	6010.58 A	6075.90 A	6451.64 A	6162.39 A	2429.95 B	
ET_0/CS_0	'3V'-WW	3313.21 aA	2917.74 aA	3512.52 aA	2745.16 aA	380.24 bB	2573.77 b
	'3V'-WS	3347.42 aA	3489.57 aA	4146.22 aA	3395.96 aA	79.45 bB	2891.72 b
	'A1'-WW	3034.40 aA	3077.89 aA	3348.56 aA	3114.16 aA	1855.98 aB	2886.20 b
	'A1'-WS	3602.86 aA	3735.38 aA	4039.67 aA	3601.48 aA	2367.08 aB	3469.30 a
	Means	3324.47 AB	3305.15 AB	3761.74 A	3214.19 B	1170.69 C	
DI_0/CS_0	'3V'-WW	2090.76 aB	2523.50 aB	2678.33 aB	6280.71 aB	18774.64 bA	6469.59 a
	'3V'-WS	1896.38 aB	1809.95 aB	2883.93 aB	4304.42 aB	22887.21 aA	6756.38 a
	'A1'-WW	2507.73 aB	2657.85 aB	3125.85 aB	6742.64 aB	11749.70 cA	5356.75 ab
	'A1'-WS	1854.63 aB	1876.92 aB	2385.33 aB	6835.08 aA	7419.64 dA	4074.32 b
	Means	2087.37 C	2217.05 C	2768.36 C	6040.71 B	15207.80 A	
RC/CS_0	'3V'-WW	7476.30 aA	5865.72 bcB	4720.02 aB	2517.65 abC	709.82 bD	4257.90 bc
	'3V'-WS	7308.72 aA	7760.59 aA	4890.05 aB	3120.03 abC	43.65 bD	4624.61 b
	'A1'-WW	5342.02 bA	5136.70 cA	4399.97 aA	2117.97 bB	2263.18 aB	3851.97 c
	'A1'-WS	7873.84 aA	7079.50 abA	5385.53 aB	3527.75 aC	2816.76 aC	5336.68 a
	Means	7000.22 A	6460.63 A	4848.89 B	2820.85 C	1458.35 D	
SFI_{abs}	'3V'-WW	3.55 bA	2.28 bB	2.08 bcB	0.45 aC	0.02 bC	1.67 b
	'3V'-WS	4.19 abA	4.71 aA	2.45 abB	1.03 aC	0.0001 bD	2.48 a
	'A1'-WW	2.18 cA	2.01 bA	1.56 cA	0.44 aB	0.27 abB	1.29 c
	'A1'-WS	4.79 aA	4.28 aA	2.93 aB	0.75 aC	0.90 aC	2.73 a
	Means	3.68 A	3.32 A	2.26 B	0.67 C	0.29 C	
PI_{abs}	'3V'-WW	31.47 bA	15.47 bB	16.50 bB	1.82 aBC	0.04 aC	13.06 b
	'3V'-WS	41.82 abA	51.30 aA	24.04 abB	6.01 aC	0.0002 aC	24.63 a
	'A1'-WW	15.02 cA	13.77 bA	10.33 bA	2.10 aA	0.95 aA	8.43 b
	'A1'-WS	54.55 aA	49.04 aA	30.84 aB	3.91 aC	6.48 aC	28.97 a
	Means	35.71 A	32.40 A	20.43 B	3.46 C	1.87 C	

The means for each treatment are shown (n = 5). ANOVA P-values < 0.05 were considered significant; Means followed by the same lowercase letters compare means of treatments, and the uppercase letters compare temperatures according to the Tukey test at 95% confidence.

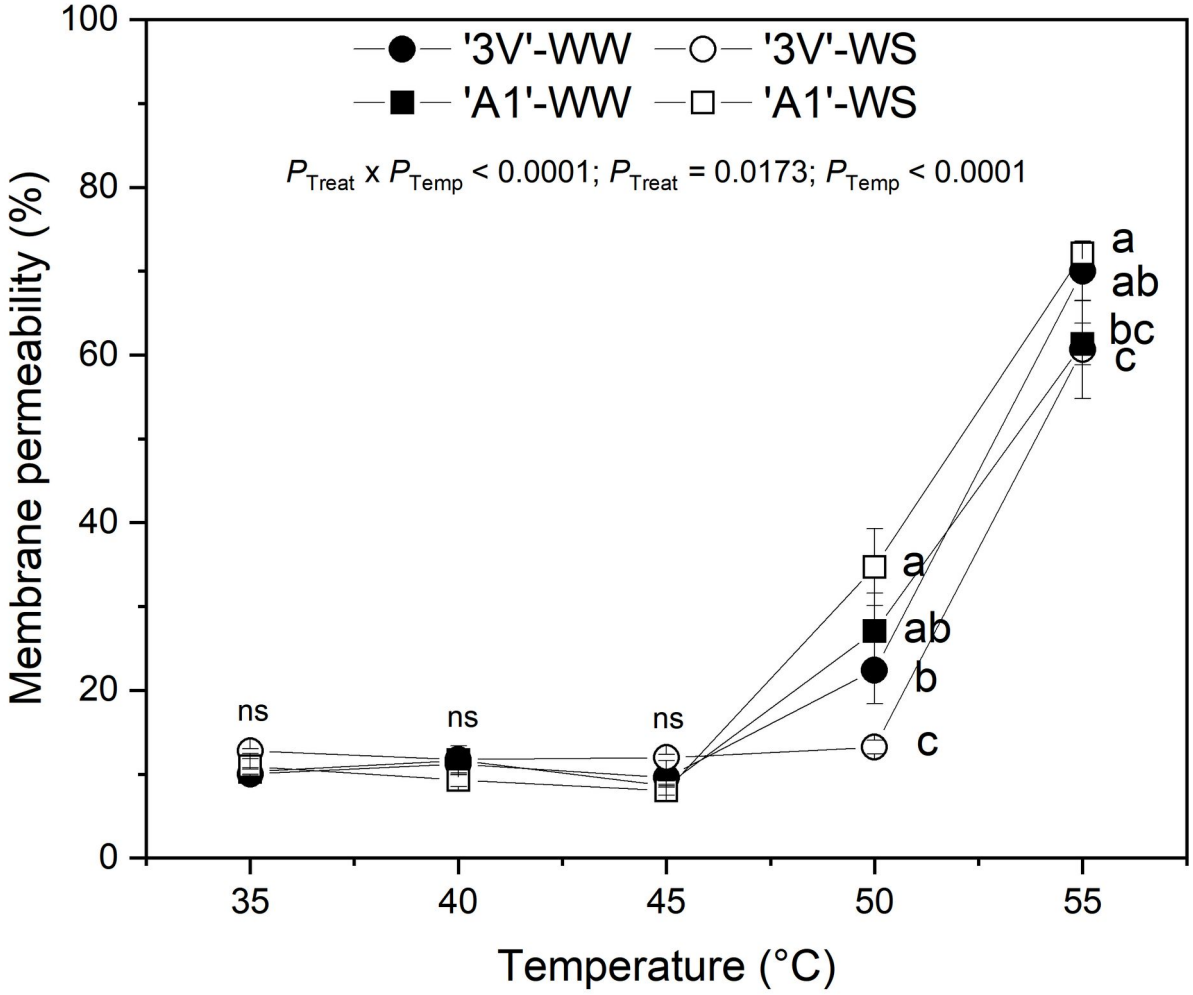

Figure 9: Membrane permeability (%) determined in leaf discs subjected to heat treatment in a water bath at different temperatures and sampled in *C. canephora* '3V' and 'A1' clones grown under well-watered conditions (WW) and under two cycles of recurrent water stress (WS). The figure shows the treatments '3V'-WW, '3V'-WS, 'A1'-WW, and 'A1'-WS incubated for 15 minutes at temperatures of 35°C, 40°C, 45°C, 50°C, and 55°C. Each symbol represents the mean (n = 5), and the vertical bars represent the standard error (SE). ANOVA P-values < 0.05 were considered significant; Means followed by the same lowercase letters compare means of treatments in each temperature according to the Tukey test at 95% confidence. The "ns" indicates no difference among treatments.

Discussion

This study investigated the effects of two recurrent drought events on the induction of heat stress tolerance in *C. canephora* clones, '3V' and 'A1', grown in a greenhouse and exposed to mean and maximum temperatures of up to 30ºC and 41ºC, respectively. The analysis focused on conformational changes in the OJIP kinetics of chlorophyll fluorescence *a* (ChlF) emission curves and utilized quantitative assessments based on JIP_{Test} parameters. Previous findings indicated that, based on certain physiological (Baroni et al., 2024) and morphological traits - particularly root growth (De Souza et al., 2025) - clone '3V' exhibited drought tolerance following two cycles of drought stress.

In contrast, clone 'A1' displayed greater sensitivity in physiological parameters (Baroni et al., 2024) but demonstrated a more conservative water-use strategy for growth (De Souza et al., 2025). Results revealed that both OJIP kinetics and JIP_{Test} parameters effectively differentiated the thermal tolerance levels between the two clones. While the '3V' genotype showed greater drought tolerance, its photosynthetic apparatus became more susceptible to supra-optimal temperatures after repeated drought cycles. Conversely, clone 'A1' recurrent drought stress appeared to function as a priming mechanism, enhancing the tolerance of its photosynthetic apparatus to thermal stress.

The W_{OP} normalization denotes the relative variable fluorescence at each point *t* between the O and P steps, also called V_t (Bussotti et al., 2012). The ΔW_{OP} normalization indicated the subtraction of the variable fluorescence (V) of the control sample (here 35°C) from the treated samples. This normalization reveals more bands and information usually hidden in the fluorescence rise kinetics (Chen et al., 2016). A more pronounced peak at the J step and a less pronounced peak at the I step indicate a slowdown in electron transport between these two phases (Bussotti et al., 2012). Results indicated a greater amplitude of variation in ΔW_{OP} for clone ‘3V’, especially after water stress (Figure 3).

In plants, increased cellular membrane fluidity is the main effect that triggers damage to the photosynthetic apparatus and, consequently, carbon fixation (Cano-Ramirez et al., 2021; Prasertthai et al., 2022; P. Sharma et al., 2023). In Figure 9, it is possible to observe an increase in membrane permeability at 50°C and 55°C, indicating an improvement in membrane fluidity, but PSII is reported to be more

sensitive to heat than membrane stability (Marias et al., 2017b). Non-stomatal effects, related to limitations in the photochemical stage, are strongly impacted by supra-optimal temperatures. These photochemical reactions occur in the thylakoid membranes, whose lipid composition confers sensitivity to temperature increases (Mathur et al., 2014; Kulke et al., 2023). Supra-optimal temperatures cause the dissociation of pigment-protein complexes, such as light-harvesting centers of PSII (LHCII) and PSII, and other components of the ETC, such as OEC and cyt b6f (Nievola et al., 2017; Hu et al., 2020). This compromises electron flow and the generation of reducing power (ATP and NADPH) (Nievola et al., 2017).

In ChlF, the dissociation between LHCII and PSII was evidenced by the increase in F_0 or the O step in the OJIP transient, associated with increased ChlF emission by the antenna complexes and reduced excitation energy transfer to PSII (Srivastava et al., 1997; Goltsev et al., 2016; Kalaji et al., 2016). Outcomes indicated an increase in F_0, $F_{50\mu s}$ (Table S3; Supplementary data A), and the O step (Figure 2) at temperatures above 45°C; however, at 55°C, clone ‘3V’ is more sensitive compared to clone ‘A1’. Additionally, lower values were observed in the ‘3V’-WS treatments at 50°C and ‘A1’-WS at 55°C.

These results were supported by those observed in the double normalization W_{OK} and ΔW_{OK} (Figure 5), where the positive amplitude of the kinetics is related to the loss of energy connectivity among the structural components of PSII, i.e. LHC and antenna core coupled to RC, and RC (Bussotti et al., 2012). This increase is evidenced at high temperatures (Martinazzo et al., 2012; Bednaříková et al., 2020). Greater amplitudes in ΔW_{OK} were observed at 55°C in ‘3V’-WW and ‘3V’-WS, while the lowest amplitudes were at 50°C in ‘3V’-WS and ‘A1’-WS compared to their counterparts, ‘3V’-WW and ‘A1’-WW (Figure 5). These results may indicate a possible acclimatization of the photosynthetic apparatus in both clones, triggered by the recurring water deficit under moderate to high temperatures in the growing environment.

The thermal stress caused the appearance of an additional K step between the O and J points, known as the K-band (Figure 2), which becomes visible at 200–300 µs (Srivastava et al., 1997; Li et al., 2009). The emergence of this K step is primarily related to a limitation in the efficiency of the OEC electron donor (Yusuf et al., 2010; Bussotti et al., 2012). The double normalization, W_{OJ} and ΔW_{OJ} (Figure 3), revealed the appearance of the K-band, and its positive amplitude is associated with

greater inactivation of the OEC and limitation in the supply of electrons to the ETC (Chen et al., 2016). Certainly, temperatures above 35°C resulted in a significant reduction in O_2 release in *Carica papaya* L. (Souza et al., 2022). However, in *Coffea* spp., up to 42ºC, no significant impact is observed on thermotolerance for O_2 release (Dubberstein et al., 2020b). Findings indicated a greater amplitude of the ΔW_{OJ} curve at 50°C for all treatments, except for ‘3V’-WS, where the greatest amplitude was observed at 55°C (Figure 4). Furthermore, significant differences between irrigated and non-irrigated treatments for this variable were not observed, indicating that water deficit did not induce greater stability of the OEC.

The inactivation of the OEC leads to the emergence of alternative electron donors, such as proline, which promote the rapid reduction of Q_A and an increase in fluorescence at 300 µs (De Ronde et al., 2004). Alternative electron donors are not able to maintain a continuous flow of electrons beyond Q_B, leading to the accumulation of $P680^+$ and a consequent reduction in fluorescence yield between the J and P steps (F_m) (Tóth et al., 2007). When examining the double normalization W_{OI} and ΔW_{OI}, for $W_{OI} < 1$ (Figure 6), its positive amplitude could be related to the blockage of electrons from PSII to plastoquinone (Chen et al., 2016).

Results showed a significant increase in the amplitude of $\Delta W_{OI} < 1$ starting at 45°C in ‘3V’-WW and ‘3V’-WS, while the amplitudes for ‘A1’-WW and ‘A1’-WS were lower. Additionally, the lower amplitudes of ‘A1’-WS compared to ‘A1’-WW may indicate the ability to maintain electron flow beyond Q_A even under the WS. The values of Ψ_{Eo}, φ_{Eo} (Table 1), and ET_0/CS_0 (Table 2), parameters related to electron transport along the ETC, did not show clear differences among treatments. However, for these parameters, the mean values for ‘A1’-WS might indicate that this treatment performed better than '3V'-WW, '3V'-WS and ‘A1’-WW in maintaining energy transport beyond Q_A.

The double normalization of W_{OI} and ΔW_{OI} to $W_{OI} > 1$ reflects the size of the final PSI electron acceptor pool due to the electron flow driven by PSI beyond PQH_2 (Yusuf et al., 2010; Chen et al., 2016). Therefore, the positive amplitude of the ΔW_{OI} curve ($W_{OI} > 1$) is related to a larger pool of active final PSI acceptors. Outcomes showed that temperatures of 45°C and 50°C induce greater activity of final PSI acceptors in all treatments, more evident in ‘3V’-WW and ‘3V’-WS (Figure 7). In fact, higher temperatures are associated with increased PSI activity, stimulating intersystem electron flow (Havaux et al., 1991; Sharkey, 2005; Ivanov et al., 2017). In

addition, it is reported that activation of cyclic electron flow (CEF) is associated with greater tolerance in *Coffea* spp. genotypes (Dubberstein et al., 2020b).

However, the negative amplitude of ΔW_{OI} ($W_{OI} > 1$) at 55°C indicated damage to the reduction capacity of final acceptors. These results were related to φ_{Ro} (Table 1), which showed similar responses at 45°C and 50°C with high mean values. The double normalization of W_{IP} and ΔW_{IP} reflects the rate of reduction of final PSI acceptors (Martinazzo et al., 2013). As observed, the negative amplitudes in ΔW_{IP} (Figure 8) indicated that the increase in temperatures tended to decrease the rate of reduction of final PSI acceptors, primarily due to the blockage of electrons along the ETC. Even with increased PSI activity, the rate of reduction of final acceptors decreased.

The parameter ABS/CS_0 is related to the absorption of light energy per unit of leaf area and the functional size of the antenna (Chen et al., 2016; Souza et al., 2022). Results indicated that clone ‘A1’ had a lower capacity for energy absorption by the antenna complex than clone ‘3V’, especially after the occurrence of water deficit (Table 2). The parameter φ_{Po} is related to the maximum capacity of PSII to reduce Q_A from the absorbed energy (Souza et al., 2022). In that regard, there was a significant reduction of φ_{Po} only at 50°C and 55°C, with clone ‘A1’ showing higher average values compared to ‘3V’ only at 55°C (Table 1).

A similar response was observed for TR_0/CS_0 (Table 2), which is related to the capture of excitation energy by PSII (Çiçek et al., 2020). The opposite responses in φ_{Do} (Table 1) and DI_0/CS_0 (Table 2) were observed, indicating increased energy dissipation in response to increased temperature, while ‘A1’-WW and ‘A1’-WS showed lower dissipation compared to ‘3V’-WW and ‘3V’-WS at 55 °C. The lower energy absorption by the antenna complex, followed by its lower dissipation by PSII, is related to greater energy utilization efficiency (Chen et al., 2016; Souza et al., 2022; Ferraz et al., 2025). Therefore, the higher values of φ_{Po} and TR_0/CS_0 at 55 °C for clone A1, in both WW and WS treatments, may be related to the lower energy absorption, which resulted in lower dissipation of the excitation energy.

The progressive increase in supra-optimal temperatures triggers the inactivation of PSII reaction centers (Mathur et al., 2014). The parameter RC/CS_0 (Table 2) describes the density of active reaction centers capable of reducing Q_A, so its reduction is related to greater inactivation of RCs (Zhang et al., 2018; Doğru, 2021; Souza et al., 2022). Results suggested lower inactivation of RCs for clone ‘A1’

at higher temperatures, especially after water deficit experience (A1'-WS). This lower inactivation of RCs is directly related to greater efficiency in energy capture and transport, and lower non-photochemical dissipation (Doğru, 2021; Souza et al., 2022), as observed in the results.

The parameters SFI_{abs} and PI_{abs} are the indices that simplify the description of energy flow along the ETC. SFI_{abs} is related to the structure and function of the ETC components (Tsimilli-Michael et al., 1999). In general, 3V'-WS and 'A1'-WS showed higher SFI_{abs} values compared to '3V'-WW and 'A1'-WW. PIabs is an index of PSII performance that summarizes the components of energy absorption, capture, and transport (Stirbet and Govindjee, 2011). In *C. canephora*, greater reductions in PI_{abs} at temperatures above 40°C were observed in all treatments. In 'A1'-WS, reductions were smaller than in 'A1'-WW, while '3V'-WS showed greater reductions than '3V'-WW. The reduction of SFI_{abs} and PI_{abs} is directly related to the level of damage to the photosynthetic apparatus in processes involving its structure and activity (Kalaji et al., 2016; Doğru, 2021; Souza et al., 2022). The results observed in SFI_{abs} and PI_{abs} suggested that the exposure of *C. canephora* plants to recurrent cycles of water stress may result in possible mitigation of the effects of heat stress, especially for clone A1.

The analysis of the OJIP kinetics, as well as the JIP_{Test}, were effective in detecting the differential response of *C. canephora* clones subjected to two recurrent soil water deficit cycles and, subsequently, to thermal stress. In fact, the hypothesis that pre-existing water stress would result in the induction of thermal stress tolerance responses was confirmed. However, it was possible to observe that those responses were genotype-dependent. Specifically, results suggested that clone 'A1' seemed to have acquired tolerance, while clone '3V' appeared more sensitive to supra-optimal temperatures which followed two water stress cycles. It was observed that Ψ_{mSoil} values *ca.* 15% lower in '3V'-WS when compared to 'A1'-WS, but findings imply that this increased sensitivity at '3V' was inherent to the clone and not due to this small difference in Ψ_{mSoil}. These results indicated the potential to further explore the mechanisms involved in acquiring tolerance in different genotypes, to understand the possibility of improving *Coffea spp*. hardening techniques.

Conclusions

The selection of *Coffea* spp. genotypes with tolerance to water and heat stresses are an important tool for the more resilient cultivation of *C. canephora* to environmental stresses.

In this work, it was observed that the imposition of supra-optimal temperatures through heat shock in *C. canephora* clones ‘3V’ and ‘A1’ caused changes in the kinetics of the OJIP of ChlF emission, indicating damage to the photosynthetic apparatus.

The occurrence of two recurrent cycles of water stress before heat stress appeared to act as a priming effect in clone ‘A1’, making it more tolerant to temperature increases. In contrast, clone ‘3V’ was more sensitive to supra-optimal temperatures, both with and without previous water stress.

The results observed through changes in the kinetics of the OJIP and the quantitative analysis of the JIP_{Test} lead the analyses to conclude that the increase in heat tolerance promoted by water stress is genotype-dependent.

References

Bandurska, H. (2022). Drought Stress Responses: Coping Strategy and Resistance. *Plants*, *11*(7), 922. https://doi.org/10.3390/plants11070922

Baroni, D. F., De Souza, G. A. R., Bernado, W. D. P., Santos, A. R., Barcellos, L. C. D. S., Barcelos, L. F. T., Correia, L. Z., De Almeida, C. M., Verdin Filho, A. C., Rodrigues, W. P., Ramalho, J. C., Rakočević, M., Campostrini, E. (2024). Stomatal and Non-Stomatal Leaf Responses during Two Sequential Water Stress Cycles in Young *Coffea canephora* Plants. *Stresses*, *4*(3), 575–597. https://doi.org/10.3390/stresses4030037

Bussotti, F., Kalaji, M. H., Desotgiu, R., Pollastrini, M., Loboda, T., Bosa, K. (2012). *Misurare la Vitalità Delle Piante Per Mezzo Della Fluorescenza Della Clorofilla* (1° ed, Vol. 137). Firenze University Press. https://doi.org/10.36253/978-88-6655-216-1

Cano-Ramirez, D. L., Carmona-Salazar, L., Morales-Cedillo, F., Ramírez-Salcedo, J., Cahoon, E. B., Gavilanes-Ruíz, M. (2021). Plasma Membrane Fluidity: An Environment Thermal Detector in Plants. *Cells*, *10*(10), 2778. https://doi.org/10.3390/cells10102778

Chen, S., Yang, J., Zhang, M., Strasser, R. J., Qiang, S. (2016). Classification and Characteristics of Heat Tolerance in *Ageratina adenophora* Populations Using Fast Chlorophyll a Fluorescence Rise O-J-I-P. *Environmental and Experimental Botany*, *122*, 126–140. https://doi.org/10.1016/j.envexpbot.2015.09.011

Çiçek, N., Kalaji, H. M., Ekmekçi, Y. (2020). Probing the Photosynthetic Efficiency of Some European and Anatolian Scots Pine Populations Under UV-B Radiation Using Polyphasic Chlorophyll a Fluorescence Transient. *Photosynthetica*, *58*(SPECIAL ISSUE), 468–478. https://doi.org/10.32615/ps.2019.151

Conab – Companhia Nacional de Abastecimento (2024). *Produção De Café De 2024 é Estimada Em 54,79 Milhões de Sacas, Influenciada por Clima*. Available in:

https://www.conab.gov.br/ultimas-noticias/5740-producao-de-cafe-de-2024-e-estimada-em-54-79-milhoes-de-sacas-influenciada-por-clima; Accessed on February 02, 2025.

DaMatta, F. M., Martins, S. C. V., Ramalho, J. D. C. (2025). Ecophysiology of Coffee Growth and Production in a Context of Climate Changes. In *Advances in Botanical Research* (Vol. 114, p. 97–139). Elsevier. https://doi.org/10.1016/bs.abr.2024.07.004

De Ronde, J. A., Cress, W. A., Krüger, G. H. J., Strasser, R. J., Van Staden, J. (2004). Photosynthetic Response of Transgenic Soybean Plants, Containing an *Arabidopsis* P5CR Gene, During Heat and Drought Stress. *Journal of Plant Physiology*, *161*(11), 1211–1224. https://doi.org/10.1016/j.jplph.2004.01.014

De Souza, G. A. R., Baroni, D. F., Bernado, W. D. P., Santos, A. R., Barcellos, L. C. D. S., Barcelos, L. F. T., Correia, L. Z., De Almeida, C. M., Verdin Filho, A. C., Rodrigues, W. P., Ramalho, J. C., Rakočević, M., Campostrini, E. (2025). Leaf to Root Morphological and Anatomical Indicators of Drought Resistance in *Coffea canephora* After Two Stress Cycles. *Agriculture*, *15*(6), 574. https://doi.org/10.3390/agriculture15060574

Doğru, A. (2021). Effects of heat stress on photosystem II activity and antioxidant enzymes in two maize cultivars. *Planta*, *253*(4), 85. https://doi.org/10.1007/s00425-021-03611-6

Dubberstein, D., Lidon, F. C., Rodrigues, A. P., Semedo, J. N., Marques, I., Rodrigues, W. P., Gouveia, D., Armengaud, J., Semedo, M. C., Martins, S., Simões-Costa, M. C., Moura, I., Pais, I. P., Scotti-Campos, P., Partelli, F. L., Campostrini, E., Ribeiro-Barros, A. I., DaMatta, F. M., Ramalho, J. C. (2020). Resilient and Sensitive Key Points of the Photosynthetic Machinery of *Coffea* spp. To the Single and Superimposed Exposure to Severe Drought and Heat Stresses. *Frontiers in Plant Science*, *11*, 1049. https://doi.org/10.3389/fpls.2020.01049

Ferraz, T. M., De Oliveira Maia Júnior, S., De Souza, G. A. R., Baroni, D. F., Rodrigues, W. P., De Sousa, E. F., Penchel, R., Loos, R., De Assis Figueiredo, F. A. M. M., Rakocevic, M., Campostrini, E. (2025). Clonal Differences in Ecophysiological Responses to Imposed Drought in Selected *Eucalyptus grandis* × *E. urophylla* Hybrids. *Tree Physiology*, *45*(1), tpae160. https://doi.org/10.1093/treephys/tpae160

Goltsev, V. N., Kalaji, H. M., Paunov, M., Bąba, W., Horaczek, T., Mojski, J., Kociel, H., Allakhverdiev, S. I. (2016). Variable Chlorophyll Fluorescence and Its Use for Assessing Physiological Condition of Plant Photosynthetic Apparatus. *Russian Journal of Plant Physiology*, *63*(6), 869–893. https://doi.org/10.1134/S1021443716050058

Gupta, R. (2020). The Oxygen-Evolving Complex: a Super Catalyst for Life on Earth, in Response to Abiotic Stresses. *Plant Signaling Behavior*, *15*(12), 1824721. https://doi.org/10.1080/15592324.2020.1824721

Havaux, M., Greppin, H., Strasser, Reto, J. (1991). Functioning Of Photosystems I And II In Pea Leaves Exposed to Heat Stress in the Presence or Absence of Light: Analysis Using In-Vivo Fluorescence, Absorbance, Oxygen and Photoacoustic Measurements. *Planta*, *186*(1). https://doi.org/10.1007/BF00201502

Hu, S., Ding, Y., Zhu, C. (2020). Sensitivity and Responses of Chloroplasts to Heat Stress in Plants. *Frontiers in Plant Science*, *11*, 375. https://doi.org/10.3389/fpls.2020.00375

ICO (2025). International Coffee Organization - Coffee Market Report. Available in: https://ico.org/; Accessed on February 02, 2025.

Ivanov, A. G., Velitchkova, M. Y., Allakhverdiev, S. I., Huner, N. P. A. (2017). Heat Stress-Induced Effects of Photosystem I: An Overview of Structural and Functional Responses. *Photosynthesis Research*, *133*(1–3), 17–30. https://doi.org/10.1007/s11120-017-0383-x

Jones, H. G. (1992). *Plants and Microclimate: A Quantitative Approach to Environmental Plant Physiology* (3º ed). Cambridge University Press. https://doi.org/10.1017/CBO9780511845727

Kalaji, H. M., Jajoo, A., Oukarroum, A., Brestic, M., Zivcak, M., Samborska, I. A., Cetner, M. D., Łukasik, I., Goltsev, V., Ladle, R. J. (2016). Chlorophyll a Fluorescence as a Tool to Monitor Physiological Status of Plants Under Abiotic Stress Conditions. *Acta Physiologiae Plantarum*, *38*(4), 102. https://doi.org/10.1007/s11738-016-2113-y

Kulke, M., Weraduwage, S. M., Sharkey, T. D., Vermaas, J. V. (2023). Nanoscale Simulation of the Thylakoid Membrane Response to Extreme Temperatures. *Plant, Cell Environment*, *46*(8), 2419–2431. https://doi.org/10.1111/pce.14609

Li, P., Cheng, L., Gao, H., Jiang, C., Peng, T. (2009). Heterogeneous Behavior of PSII in Soybean (*Glycine max*) Leaves with Identical PSII Photochemistry Efficiency Under Different High Temperature Treatments. *Journal of Plant Physiology*, *166*(15), 1607–1615. https://doi.org/10.1016/j.jplph.2009.04.013

Liu, H., Able, A. J., Able, J. A. (2022). Priming Crops for the Future: Rewiring Stress Memory. *Trends in Plant Science*, *27*(7), 699–716. https://doi.org/10.1016/j.tplants.2021.11.015

Marias, D. E., Meinzer, F. C., Still, C. (2017a). Impacts of Leaf Age and Heat Stress Duration on Photosynthetic Gas Exchange and Foliar Nonstructural Carbohydrates in *Coffea arabica*. *Ecology and Evolution*, *7*(4), 1297–1310. https://doi.org/10.1002/ece3.2681

Marias, D. E., Meinzer, F. C., Still, C. (2017b). Leaf Age and Methodology Impact Assessments of Thermotolerance of *Coffea arabica*. *Trees*, *31*(3), 1091–1099. https://doi.org/10.1007/s00468-016-1476-4

Martinazzo, E. G., Ramm, A., Bacarin, M. A. (2013). The Chlorophyll A Fluorescence as An Indicator of the Temperature Stress in the Leaves of *Prunus persica*. *Brazilian Journal of Plant Physiology*, *24*(4), 237–246. https://doi.org/10.1590/S1677-04202013005000001

Mathur, S., Agrawal, D., Jajoo, A. (2014). Photosynthesis: Response to High Temperature Stress. *Journal of Photochemistry and Photobiology B: Biology*, *137*, 116–126. https://doi.org/10.1016/j.jphotobiol.2014.01.010

Menezes-Silva, P. E., Sanglard, L. M. V. P., Ávila, R. T., Morais, L. E., Martins, S. C. V., Nobres, P., Patreze, C. M., Ferreira, M. A., Araújo, W. L., Fernie, A. R., DaMatta, F. M. (2017). Photosynthetic and Metabolic Acclimation to Repeated Drought Events Play Key Roles in Drought Tolerance in Coffee. *Journal of Experimental Botany*, *68*(15), 4309–4322. https://doi.org/10.1093/jxb/erx211

Nievola, C. C., Carvalho, C. P., Carvalho, V., Rodrigues, E. (2017). Rapid Responses of Plants to Temperature Changes. *Temperature*, *4*(4), 371–405. https://doi.org/10.1080/23328940.2017.1377812

Park, B., Wi, S., Chung, H., Lee, H. (2024). Chlorophyll Fluorescence Imaging for Environmental Stress Diagnosis in Crops. *Sensors*, *24*(5), 1442. https://doi.org/10.3390/s24051442

Prasertthai, P., Paethaisong, W., Theerakulpisut, P., Dongsansuk, A. (2022). High Temperature Alters Leaf Lipid Membrane Composition Associated with Photochemistry of PSII and Membrane Thermostability in Rice Seedlings. *Plants*, *11*(11), 1454. https://doi.org/10.3390/plants11111454

Rakocevic, M., Baroni, D. F., De Souza, G. A. R., Bernado, W. D. P., De Almeida, C. M., Matsunaga, F. T., Rodrigues, W. P., Ramalho, J. C., Campostrini, E. (2023). Correlating *Coffea Canephora* 3D Architecture to Plant Photosynthesis at a Daily Scale and Vegetative Biomass Allocation. *Tree Physiology*, *43*(4), 556–574. https://doi.org/10.1093/treephys/tpac138

Rakocevic, M., Costes, E., Campostrini, E., Ramalho, J. C., Ribeiro, R. V. (2024). Drought Responses in *Coffea arabica* as Affected by Genotype and Phenophase. II – Photosynthesis at Leaf and Plant Scales. *Experimental Agriculture*, *60*, e22. https://doi.org/10.1017/S0014479724000164

Rodrigues, A. P., Pais, I. P., Leitão, A. E., Dubberstein, D., Lidon, F. C., Marques, I., Semedo, J. N., Rakocevic, M., Scotti-Campos, P., Campostrini, E., Rodrigues, W. P., Simões-Costa, M. C., Reboredo, F. H., Partelli, F. L., DaMatta, F. M., Ribeiro-Barros, A. I., Ramalho, J. C. (2024). Uncovering the Wide Protective Responses in *Coffea* spp. Leaves to Single and Superimposed Exposure of Warming and Severe Water Deficit. *Frontiers in Plant Science*, *14*, 1320552. https://doi.org/10.3389/fpls.2023.1320552

Rodrigues, W. P., Machado Filho, J. A., Da Silva, J. R., De Assis Figueiredo, F. A. M. M., Ferraz, T. M., Ferreira, L. S., Da Silva Bezerra, L. B., De Abreu, D. P., De Paula Bernado, W., Cespom Passos, L., De Sousa, E. F., Glenn, D. M., Ramalho, J. C., Campostrini, E. (2016). Whole-Canopy Gas Exchanges in *Coffea* spp. is Affected by Supra-Optimal Temperature and Light Distribution Within the Canopy: The Insights From an Improved Multi-Chamber System. *Scientia Horticulturae*, *211*, 194–202. https://doi.org/10.1016/j.scienta.2016.08.022

Rodrigues, W. P., Martins, M. Q., Fortunato, A. S., Rodrigues, A. P., Semedo, J. N., Simões-Costa, M. C., Pais, I. P., Leitão, A. E., Colwell, F., Goulao, L., Máguas, C., Maia, R., Partelli, F. L., Campostrini, E., Scotti-Campos, P., Ribeiro-Barros, A. I., Lidon, F. C., DaMatta, F. M., Ramalho, J. C. (2016). Long-Term Elevated Air [CO_2] Strengthens Photosynthetic Functioning and Mitigates the Impact of Supra-Optimal Temperatures in Tropical *Coffea arabica* and *C. canephora* Species. *Global Change Biology*, *22*(1), 415–431. https://doi.org/10.1111/gcb.13088

Rodrigues, W. P., Silva, J. R., Ferreira, L. S., Filho, J. A. M., Figueiredo, F. A. M. M. A., Ferraz, T. M., Bernado, W. P., Bezerra, L. B. S., De Abreu, D. P., Cespom, L., Ramalho, J. C., Campostrini, E. (2018). Stomatal and Photochemical

Limitations of Photosynthesis in Coffee (*Coffea* spp.) Plants Subjected to Elevated Temperatures. *Crop and Pasture Science*, *69*(3), 317. https://doi.org/10.1071/CP17044

Saharan, B. S., Brar, B., Duhan, J. S., Kumar, R., Marwaha, S., Rajput, V. D., Minkina, T. (2022). Molecular and Physiological Mechanisms to Mitigate Abiotic Stress Conditions in Plants. *Life*, *12*(10), 1634. https://doi.org/10.3390/life12101634

Shabbir, R., Singhal, R. K., Mishra, U. N., Chauhan, J., Javed, T., Hussain, S., Kumar, S., Anuragi, H., Lal, D., Chen, P. (2022). Combined Abiotic Stresses: Challenges and Potential for Crop Improvement. *Agronomy*, *12*(11), 2795. https://doi.org/10.3390/agronomy12112795

Sharkey, T. D. (2005). Effects of Moderate Heat Stress on Photosynthesis: Importance of Thylakoid Reactions, Rubisco Deactivation, Reactive Oxygen Species, and Thermotolerance Provided by Isoprene. *Plant, Cell Environment*, *28*(3), 269–277. https://doi.org/10.1111/j.1365-3040.2005.01324.x

Sharma, P., Lakra, N., Goyal, A., Ahlawat, Y. K., Zaid, A., Siddique, K. H. M. (2023). Drought and Heat Stress Mediated Activation of Lipid Signaling in Plants: A Critical Review. *Frontiers in Plant Science*, *14*, 1216835. https://doi.org/10.3389/fpls.2023.1216835

Souza, G. A. R. D., Neves, D. D. A., Ruas, K. F., Baroni, D. F., Santos, K. D. D., Bernado, W. D. P., Miranda, R. M. D. S. N. D., Almeida, C. M. D., Santos, A. R., Rodrigues, W. P., Rakocevic, M., Campostrini, E. (2022). Supra-Optimal Temperatures Induce Photochemical Leaf Damage and Reduce Photosynthetic O_2 Evolution in *Carica papaya* L. *Environmental and Experimental Botany*, *203*, 105051. https://doi.org/10.1016/j.envexpbot.2022.105051

Srivastava, A., Guissé, B., Greppin, H., Strasser, R. J. (1997). Regulation of Antenna Structure and Electron Transport in Photosystem II of *Pisum sativum* Under Elevated Temperature Probed by the Fast Polyphasic Chlorophyll a

Fluorescence Transient: OKJIP. *Biochimica et Biophysica Acta (BBA) - Bioenergetics*, *1320*(1), 95–106. https://doi.org/10.1016/S0005-2728(97)00017-0

Stirbet, A. Govindjee. (2011). On the Relation Between the Kautsky Effect (Chlorophyll a Fluorescence Induction) and Photosystem II: Basics and Applications of the OJIP Fluorescence Transient. *Journal of Photochemistry and Photobiology B: Biology*, *104*(1–2), 236–257. https://doi.org/10.1016/j.jphotobiol.2010.12.010

Strasser, B. J., Strasser, R. J. (1995). Measuring Fast Fluorescence Transients to Address Environmental Questions: The JIP-Test. In *Photosynthesis: From Light to Biosphere* (p. 4869–4872). Springer Netherlands. https://doi.org/10.1007/978-94-009-0173-5_1142

Strasser, R. J., Tsimilli-Michael, M., Srivastava, A. (2004). Analysis of the Chlorophyll a Fluorescence Transient. In *Chlorophyll a Fluorescence* (Vol. 19, p. 321–362). Springer Netherlands. https://doi.org/10.1007/978-1-4020-3218-9_12

Tóth, S. Z., Schansker, G., Garab, G., Strasser, R. J. (2007). Photosynthetic Electron Transport Activity in Heat-Treated Barley Leaves: The Role of Internal Alternative Electron Donors to Photosystem II. *Biochimica et Biophysica Acta (BBA) - Bioenergetics*, *1767*(4), 295–305. https://doi.org/10.1016/j.bbabio.2007.02.019

Tsimilli-Michael, M., Pêcheux, M., Strasser, R. J. (1999). Light and Heat Stress Adaptation of the Symbionts of Temperate and Coral Reef Foraminifers Probed in Hospite by the Chlorophyll a Fluorescence Kinetics. *Zeitschrift Für Naturforschung C*, *54*(9–10), 671–680. https://doi.org/10.1515/znc-1999-9-1009

Venancio, L. P., Filgueiras, R., Mantovani, E. C., Do Amaral, C. H., Da Cunha, F. F., Dos Santos Silva, F. C., Althoff, D., Dos Santos, R. A., Cavatte, P. C. (2020). Impact of Drought Associated with High Temperatures on *Coffea canephora*

Plantations: A Case Study in Espírito Santo State, Brazil. *Scientific Reports*, *10*(1), 19719. https://doi.org/10.1038/s41598-020-76713-y

Yamane, K., Nishikawa, M., Hirooka, Y., Narita, Y., Kobayashi, T., Kakiuchi, M., Iwai, K., Iijima, M. (2022). Temperature Tolerance Threshold and Mechanism of Oxidative Damage in the Leaf of *Coffea arabica* 'Typica' Under Heat Stress. *Plant Production Science*, *25*(3), 337–349. https://doi.org/10.1080/1343943X.2022.2064309

Yusuf, Mohd. A., Kumar, D., Rajwanshi, R., Strasser, R. J., Tsimilli-Michael, M., Govindjee, Sarin, N. B. (2010). Overexpression of Γ-Tocopherol Methyl Transferase Gene in Transgenic *Brassica juncea* Plants Alleviates Abiotic Stress: Physiological and Chlorophyll a Fluorescence Measurements. *Biochimica et Biophysica Acta (BBA) - Bioenergetics*, *1797*(8), 1428–1438. https://doi.org/10.1016/j.bbabio.2010.02.002

Zahra, N., Hafeez, M. B., Ghaffar, A., Kausar, A., Zeidi, M. A., Siddique, K. H. M., Farooq, M. (2023). Plant Photosynthesis Under Heat Stress: Effects and Management. *Environmental and Experimental Botany*, *206*, 105178. https://doi.org/10.1016/j.envexpbot.2022.105178

Zhang, K., Chen, B., Hao, Y., Yang, R., Wang, Y. (2018). Effects Of Short-Term Heat Stress on PSII And Subsequent Recovery for Senescent Leaves of *Vitis Vinifera* L. cv. Red Globe. *Journal of Integrative Agriculture*, *17*(12), 2683–2693. https://doi.org/10.1016/S2095-3119(18)62143-4

Zhang, X., Huang, B. (2020). Drought Priming-Induced Heat Tolerance: Metabolic Pathways and Molecular Mechanisms. In *Priming-Mediated Stress and Cross-Stress Tolerance in Crop Plants* (p. 149–160). Elsevier. https://doi.org/10.1016/B978-0-12-817892-8.00009-X

Zhu, L., Wen, W., Thorpe, M. R., Hocart, C. H., Song, X. (2021). Combining Heat Stress with Pre-Existing Drought Exacerbated the Effects on Chlorophyll Fluorescence Rise Kinetics in Four Contrasting Plant Species. *International*

Journal of Molecular Sciences, *22*(19), 10682. https://doi.org/10.3390/ijms221910682

3.2. Gas exchange in *Coffea canephora* under recurrent water deficit stress: from leaf to whole-canopy scales

Abstract

The intensification of global climate change has led to an increase in average air temperatures and a higher frequency of drought events in many *Coffea canephora* cultivation regions. These drought events, often accompanied by supra-optimal temperatures, can trigger stress responses that compromise photosynthetic metabolism, particularly leaf gas exchange. Moreover, recurrent drought events may induce physiological adjustments in these plants, enhancing their tolerance to future water deficit conditions. In this study, 10-month-old *C. canephora* plants underwent three recurrent cycles of soil drying and rewetting, and gas exchange was monitored at both the leaf and whole-canopy levels during cycles 1 and 3. Whole-canopy gas exchange variables (A_C, E_C, and g_C) were strongly influenced by micrometeorology, with A_C and E_C displaying a bell-shaped pattern throughout the day, while g_C decreased between 09:00 and 18:00. Both leaf-level (A_{net}, E, and g_s) and whole-canopy ($A_{C\text{-}max}$ and $E_{C\text{-}max}$) gas exchange decreased as water stress intensified. During cycles 1 and 3, $A_{C\text{-}max}$ and $E_{C\text{-}max}$ showed a more evident recovery compared to A_{net} and E after soil rewetting. The reduction in $A_{C\text{-}max}$ and $E_{C\text{-}max}$ due to water stress impacted the daily carbon gain (A_{daily}) and water loss (E_{daily}) per unit leaf area; however, these variables recovered following soil rewetting. Nevertheless, when considering daily carbon gain and water loss per plant, there was a significant decline in the soil drying cycles (WS-1 and WS-3), and recovery in REC-1 and REC-3 was impaired due to leaf shedding and a reduction in leaf area. Despite the decline in whole-canopy gas exchange in cycle 3 compared to cycle 1, water use efficiency (WUE) increased while water footprint (WFP) decreased. These results indicate that, despite the damage caused by severe water stress, *C. canephora* plants that experienced recurrent drought cycles developed physiological adjustments, enhancing resilience to initial mild to moderate drought conditions. Finally, whole-canopy gas exchange measurements proved to be an effective tool for monitoring dynamic stress responses.

Resumo

A intensificação das mudanças climáticas globais levou a um aumento nas temperaturas médias do ar e a uma maior frequência de eventos de seca em muitas regiões de cultivo de *Coffea canephora*. A ocorrência desses eventos de seca, frequentemente acompanhados por temperaturas supra ótimas, pode desencadear respostas de estresse que comprometem o metabolismo fotossintético, particularmente a troca gasosa foliar. Além disso, eventos recorrentes de seca podem induzir ajustes fisiológicos nessas plantas, aumentando sua tolerância a futuras condições de déficit hídrico. Neste estudo, foram utilizadas plantas de *C. canephora* com 10 meses de idade a três ciclos recorrentes de secagem e re-umedecimento do solo e monitorou-se as trocas gasosas nos níveis foliar e de planta inteira durante os ciclos 1 e 3. Observou-se que as variáveis de troca gasosa de planta inteira (A_C, E_C e g_C) foram fortemente influenciadas por variáveis micrometeorológicas, com A_C e E_C exibindo um padrão em forma de sino ao longo do dia, enquanto g_C exibiu uma tendência decrescente entre 09:00h e 18:00h. As trocas gasosas no nível foliar (A_{net}, E e g_s) e na planta inteira ($A_{C\text{-}max}$ e $E_{C\text{-}max}$) diminuíram conforme o estresse hídrico se intensificou. Durante os ciclos 1 e 3, $A_{C\text{-}max}$ e $E_{C\text{-}max}$ mostraram uma recuperação mais evidente em comparação com *A*net e *E* após o re-umedecimento do solo. A redução em $A_{C\text{-}max}$ e $E_{C\text{-}max}$ devido ao estresse hídrico impactou o ganho diário de carbono (A_{daily}) e a perda de água (E_{daily}) por unidade de área foliar; no entanto, essas variáveis se recuperaram após o re-umedecimento do solo. No entanto, ao considerar o ganho diário de carbono e a perda de água por planta, houve um declínio significativo nos ciclos de secagem do solo (WS-1 e WS-3), e a recuperação em REC-1 e REC-3 foi prejudicada devido à queda de folhas e à redução na área foliar. Apesar do declínio nas trocas gasosas da planta inteira no ciclo 3 em comparação ao ciclo 1, foi observado um aumento na eficiência do uso da água (EUA) e uma diminuição na pegada hídrica (PH). Esses resultados indicam que, apesar dos danos causados pelo estresse hídrico severo, as plantas de *C. canephora* submetidas a ciclos recorrentes de seca desenvolvem ajustes fisiológicos que lhes permitem lidar mais efetivamente com condições iniciais de seca leve a moderada. Além disso, medir a troca gasosa da planta inteira provou ser uma

ferramenta eficaz para monitorar as respostas dinâmicas das plantas sob condições de estresse.

Introduction

Coffee, the world's second most consumed beverage (Gil-Gómez et al., 2024), has experienced a surging global demand in recent years, particularly in Asian countries (Wei, 2024). This demand is primarily met by the cultivation of *Coffea arabica* L. and *C. canephora* Pierre ex A. Froehner (Dubberstein et al., 2018; Mannino et al., 2023). However, global climate change has negatively impacted the yields of both species, diminishing supply and increasing costs (Ebisa, 2017; Bilen et al., 2022; De Freitas et al., 2024). Rising temperatures have altered rainfall patterns, increasing the frequency of extreme droughts in key production regions (Wagner et al., 2021). Furthermore, climate change-induced frost events and, increased pest and disease incidence are significant factors, contributing to yield losses (Dias et al., 2024). Consequently, many regions once suitable for cultivating current *Coffea* spp. genotypes are becoming unsuitable (Ngolo et al., 2018; Lorençone et al., 2023), forcing producers to migrate to more favorable areas and adopt sustainable agricultural practices (Bracken et al., 2023).

C. canephora, originating from regions with lower altitudes and higher temperatures, is typically cultivated in such environments compared to *C. arabica* (Salvador et al., 2025). Despite its greater thermal tolerance, *canephora* coffee-growing regions in Brazil (Venancio et al., 2020) and Vietnam (Byrareddy et al., 2021) have been severely affected by rising air temperatures and intensifying droughts. These conditions induce plant stress, reducing yield (DaMatta and Ramalho, 2006). Drought, especially when coupled with high temperatures during the reproductive phase, directly impacts production through floral abortion and poor grain filling (Venancio et al., 2020). Moreover, water scarcity during the vegetative phase limits root and shoot growth, restricting photosynthetic carbon assimilation and the plant's energy reserves (Borgo et al., 2024). Additionally, soil water deficit impairs photosynthesis, including stomatal closure, photochemical damage, and oxidative stress (Borgo et al., 2024).

Early studies investigating the physiological responses of *Coffea* spp. genotypes to soil water deficit primarily utilized single drought cycles, often followed

by re-irrigation (Menezes-Silva et al., 2017). These studies provided foundational insights into coffee plant physiology under drought stress. However, the prevalence of multiple drying and rewetting cycles, coupled with elevated air temperatures, under contemporary climate change scenarios requires a shift in research focus. Consequently, recent investigations have increasingly explored plant responses to recurrent soil water deficit cycles (Menezes-Silva et al., 2017; Guedes et al., 2018; Baroni et al., 2024; Rakocevic et al., 2024). These studies, across several crops, have demonstrated that repeated drought events induce morphophysiological, hydraulic, and molecular adaptations, enhancing tolerance to subsequent drought or other environmental stressors (Pritzkow et al., 2021; Rowland et al., 2023). Such adaptations are often attributed to a "stress memory" mechanism, which improves survival, photosynthetic capacity, and yield in both natural and agricultural settings (Kashyap et al., 2024; Siddique et al., 2024).

Photosynthesis in coffee plants is generally highly sensitive to soil water deficit (DaMatta and Ramalho, 2006). The primary response to mild to severe water deficit is stomatal closure, mediated by abscisic acid (ABA) synthesis and signaling in roots and leaves (Avila et al., 2020; Almeida et al., 2021). Furthermore, stomatal sensitivity increases under reduced soil water availability and elevated air vapor pressure deficit (VPD_{air}), leading to reduced stomatal conductance (g_s) (Dubberstein et al., 2018; Baroni et al., 2024; Sarzynski et al., 2024). This stomatal closure acts as a protective mechanism against water loss, evidenced by decreased xylem sap flow (Sarzynski et al., 2024) and leaf transpiration rate (E) (Baroni et al., 2024). Consequently, CO_2 uptake and fixation at ribulose-1,5-bisphosphate carboxylase/oxygenase (RUBISCO) carboxylation sites are restricted, resulting in a decline in net CO_2 assimilation (A_{net}) (Martins et al., 2019; Semedo et al., 2021).

Diffusional limitations are often cited as the primary constraints on photosynthesis in *Coffea* spp. (Martins et al., 2019; Almeida et al., 2021; Semedo et al., 2021). However, under severe water deficit, photochemical limitations, indicated by reductions in maximum (F_V/F_M) and effective (Φ_{PSII}) quantum yield, as well as electron transport rate (ETR), are also observed (Dubberstein et al., 2020a; Almeida et al., 2021). Biochemical limitations may contribute to the reduction of net photosynthetic rate (A_{net}), although to a lesser extent, under severe water stress (Martins et al., 2019; Dubberstein et al., 2020; Almeida et al., 2021).

Leaf gas exchange analysis is crucial for understanding the ecophysiological responses of *Coffea* spp. to drought at the leaf level. However, the limitations of long-term leaf-level monitoring hinder the comprehension of dynamic plant responses to water deficit. Whole-canopy gas exchange studies offer a promising approach to better interpret these dynamic stress responses and provide insights into the relation between leaf and canopy-level gas exchange (Ferraz et al., 2016; Leonardos and Grodzinski, 2017). Whole-canopy gas exchange is significantly influenced by canopy-wide factors such as light dynamics, branch angle, nutritional status, and leaf age (Wang et al., 2014; Niinemets, 2016; Rodrigues et al., 2016). Consequently, whole-canopy measurements more accurately reflect the integrated plant responses to the cultivation environment compared to single-leaf chamber measurements (Leonardos and Grodzinski, 2017). Furthermore, extrapolating leaf-level gas exchange data to the entire plant can introduce errors and overestimations due to canopy heterogeneity (Tarara and Perez Peña, 2015; Ferraz et al., 2016). Functional-architectural 3D modeling can mitigate these errors (Leonardos and Grodzinski, 2017) but requires complex computational programming and detailed plant architecture assessments (Prieto et al., 2020; Rakocevic et al., 2023). Previous studies (Marur and de Faria, 2007; Rodrigues et al., 2016) have demonstrated that whole-canopy gas exchange measurements in coffee, particularly using multi-chamber open systems (Rodrigues et al., 2016), enhance the ecophysiological understanding under stress.

This study aimed to elucidate the dynamic ecophysiological responses of *C. canephora* plants subjected to three recurring soil drying and rewetting cycles, using single-leaf and whole-canopy gas exchange. Therefore, the hypotheses were: although soil water deficit limits gas exchange at both the leaf and canopy levels, (1) whole-canopy gas exchange values would be significantly lower than those at the leaf level; (2) gas exchange in individual leaves and the whole canopy may show differential responses throughout the recurrent drying and rewetting cycles; (3) whole-canopy gas exchange would be strongly influenced by the growing environment; and (4) the whole-canopy gas exchange system would provide a more comprehensive understanding of carbon gain and water loss over a growing cycle in coffee plants.

Material and methods

Plant material and growth conditions

The experiment was conducted in a greenhouse at the State University of the North Fluminense Darcy Ribeiro, located in Campos dos Goytacazes (21º44'47" S, 41º18'24" W; 10 m altitude), RJ, Brazil. Sixteen *C. canephora* plants from the LB1 clone were used. Five-month-old seedlings with three to four pairs of fully expanded leaves were provided by the Instituto Capixaba de Pesquisa, Assistência Técnica e Extensão Rural (INCAPER, Marilândia, ES, Brazil). These seedlings were transplanted into 80 L high-density polyethylene (HDPE) pots, filled with a substrate composed of yellow-red latosol and sand in a 3:1 ratio. The substrate was pre-corrected and fertilized with 5 $g.L^{-1}$ of limestone and 3.75 $g.L^{-1}$ of single superphosphate, following recommendations based on the substrate's chemical analysis. The plants were cultivated for 12 months, from August 2022 to August 2023, maintaining one orthotropic stem under optimal irrigation and nutritional management conditions. A controlled-release fertilizer, Basacote® Plus 6M (COMPO EXPERT GmbH, Münster, NW, Germany), was applied, supplemented by phytosanitary management as needed. After this period, the plants underwent drastic pruning (August 14 2023), and upon the induction of lateral shoots, two orthotropic stems were maintained growing for ten months, until June 2024. During this growth phase, plants received full irrigation twice a day (at 06:00 and 18:00) for 30 minutes at a flow rate of 2.8 $L.h^{-1}$. The irrigation duration varied throughout the cultivation cycle to maintain water availability close to the substrate's retention capacity. Nutritional management was maintained using the controlled-release fertilizer Basacote® Plus 6M, applied at three-month intervals.

Application of recurrent soil drying and rewetting cycles

Starting in June 2024 (308 days after the drastic pruning), recurrent soil drying and rewetting cycles were applied. To this finality, the 16 plants were divided into two groups: WW (well-watered, maintained under full irrigation throughout the experimental period) and WS (water-stressed, subjected to three recurrent soil drying and rewetting cycles), with eight plants in each group. Water stress was induced by completely suspending irrigation. Three drying cycles, designated as WS-1, WS-2,

and WS-3, were applied, followed by three soil rewetting cycles, designated as REC-1, REC-2, and REC-3. In Cycle 1 (WS-1 + REC-1), irrigation was suspended from June 17 to July 2, 2024 (14 days), and the soil was re-irrigated until it reached its maximum water-holding capacity. In Cycle 2 (WS-2 + REC-2), irrigation was suspended from July 23 to August 3, 2024 (10 days), followed by soil re-irrigation. In Cycle 3 (WS-3 + REC-3), irrigation was suspended from August 24 to September 8, 2024 (14 days), followed by soil re-irrigation. The cultivation scheme, application of soil drying and rewetting cycles, and gas exchange measurements are exposed in Figure S5 (Supplementary data B).

Monitoring of micrometeorological conditions and soil moisture

Throughout the cultivation cycle, micrometeorological variables [photosynthetic photon flux density (PPFD, µmol m^{-2} s^{-1}), temperature (°C), and relative air humidity (%)] inside the greenhouse were monitored using a WatchDog Model 2475 mini weather station (Spectrum Technologies, Inc., Aurora, IL, USA), positioned among the plants while avoiding shading effects. Using the collected temperature and relative humidity data, the air vapor pressure deficit (VPD_{air}) was calculated according to the equation proposed by Jones (1992). The micrometeorological data recorded between June 1, 2024, and September 28, 2024, are presented in Figure S1. In general, during Cycle 1, the maximum and average PPFD were 705.5 ± 29.6 µmol.m^{-2}.s^{-1} and 372.5 ± 19.2 µmol.m^{-2}.s^{-1}, respectively (Figure S1a; Supplementary data B); the maximum, average, and minimum temperatures were 33.2 ± 0.7°C, 23.9 ± 0.3°C, and 18.5 ± 0.3°C, respectively (Figure S1b; Supplementary data B); the maximum, average, and minimum relative humidity values were 95.6 ± 0.8%, 72.4 ± 0.5%, and 33.4 ± 1.9%, respectively (Figure S1c; Supplementary data B); and the maximum, average, and minimum VPD_{air} values were 3.47 ± 0.2 kPa, 1.1 ± 0.1 kPa, and 0.1 ± 0.02 kPa, respectively (Figure S1d; Supplementary data B).

During Cycle 3, the maximum and average PPFD were 894.5 ± 53.5 µmol.m^{-2}.s^{-1} and 452.28 ± 28.5 µmol.m^{-2}.s^{-1}, respectively (Figure 1a); the maximum, average, and minimum temperatures were 33.2 ± 0.9°C, 23.9 ± 0.5°C, and 18.8 ± 0.5°C, respectively; the maximum, average, and minimum relative humidity values were 90.1 ± 1.4%, 65.3 ± 1.1%, and 31.5 ± 2.3%, respectively; and the maximum,

average, and minimum VPD_{air} values were 3.6 ± 0.2 kPa, 1.3 ± 0.1 kPa, and 0.2 ± 0.03 kPa, respectively. During the same period, the soil matric potential (Ψ_{mSoil}) and soil temperature were monitored in five randomly selected plants per treatment using MPS-6 and Teros-21 sensors, with data recorded on EM-50 and ZL6 dataloggers (METER Group, Pullman, WA, USA). The sensors were positioned 0.3 m below the soil surface at the center of the pot. The recorded Ψ_{mSoil} data over the experimental period are shown in Figure S2 (Supplementary data B). Throughout the three cycles, Ψ_{mSoil} in the WW treatment remained at an average of -8.8 kPa. In the WS treatment, the minimum values reached -1538.3 ± 465.7 kPa and -1096.3 ± 292.9 kPa in WS-1 and WS-3, respectively. The soil temperatures in both treatments (WW and WS) were maintained in 24.3 ± 0.02ºC and 24.6 ± 0.03ºC (data does not show), in Cycles 1 and 3, respectively.

Single-leaf gas exchange measurements

Aiming to evaluate how *C. canephora* plants respond after a single cycle of water stress and after three recurrent cycles of water stress, single-leaf gas exchange measurements were conducted during soil drying and rewetting in Cycles 1 and 3. These measurements were taken at two diurnal time points: in the morning, between 07:00 and 09:00, and in the afternoon, between 12:00 and 14:00. A total of 11 measurements were performed at two-day intervals throughout each cycle. Gas exchange was measured using an infrared gas analyzer (IRGA), model LI-6400XT (LI-COR® Environmental, Lincoln, NE, USA), equipped with an LED light source (6400-40).

Measurement chamber conditions were set to a photosynthetic photon flux density (PPFD) of 1000 $\mu mol.m^{-2}.s^{-1}$, an external CO_2 supply of 420 $\mu mol.mol^{-1}$, an airflow rate of 300 $\mu mol.s^{-1}$, and the block temperature maintained between 25°C and 30°C in the morning and between 35°C and 40°C in the afternoon. The monitored variables included net CO_2 assimilation rate (A_{net}, $\mu mol\ CO_2.m^{-2}.s^{-1}$), leaf transpiration rate (E, $mmol.m^{-2}.s^{-1}$), and stomatal conductance (g_s, $mol.m^{-2}.s^{-1}$).

During Cycle 1, fully expanded leaves located at the third or fourth node from the apex of plagiotropic branches in the upper third of the plants were selected. For measurements in Cycle 3, fully expanded leaves formed during Cycles 1 and 2 were selected. These leaves were marked, preferably on the same 2nd order plagiotropic

axes used in Cycle 1 measurements, and their growth was monitored by measuring the midrib length at two-day intervals until reaching maximum size. At gas exchange measurements onset, these leaves were positioned between the second and third node from the branch apex. Measurements were taken on the same leaves from the beginning to the end of each cycle, at all-time points whenever possible. For each plant, gas exchange was measured on two individual leaves from opposite branches, and the average value was considered representative of the plant.

Whole-canopy gas exchange measurements

For whole-canopy gas exchange measurements, each plant was individually enclosed in a cylindrical chamber [1 m (diameter) × 1.30 m (height), volume ≈ 1 m^3], constructed of a transparent polyester film (Mylar®, DuPont Teijin Films, Wilmington, DE, USA) with 50 µm thickness and an approximate PPFD transmittance of 90% (Ferraz et al., 2016). Each chamber featured a lateral opening sealed with Velcro® (Velcro Companies, Manchester, NH, UK) to allow access to the plant, a fan (inlet, Ø = 0.12 m) mounted at the lower part of the chamber to control airflow, and an upper opening (outlet, Ø = 0.095 m) for air exhaust. A total of 16 chambers were used during the experiment, with eight assigned to well-watered plants (WW) and eight to water-stressed plants (WS).

The airflow velocity through the chambers was monitored using a digital anemometer (Extech 45118, Extech Instruments, Townsend West Nashua, NH, USA). This velocity (m s^{-1}) was multiplied by the cross-sectional area (0.0071 m^2) of the upper opening to estimate the airflow rate ($m^3.s^{-1}$) through the chamber. Throughout the experiment, the average airflow rate was maintained at 5.2 ± 1.4 $L.s^{-1}.m^{-2}$ of leaf area (mean ± standard deviation), with a complete air renewal rate inside the cylinder chamber of approximately 55 seconds.

The gas exchange measurement system (Figure 3) was designed for air sampling via independent plastic tubes (Ø = 0.004 m) connected to a vacuum pump system (AIRPOTM D2028B, SparkFun Electronics, Niwot, CO, USA). This system sucked simultaneously and independently reference air (inlet air) and sample air (outlet air) from each chamber. The vacuum pumps were automatically controlled using a 16-channel AC/DC relay controller (SDM-CD16AC, Campbell Scientific®,

Logan, UT, USA). The sampled air was expelled into independent buffers for homogenization, from which it was continuously sucked by the infrared gas analyzer pumping system (IRGA, CIRAS-DC, PP Systems, Amesbury, MA, USA). The CIRAS-DC continuously measured CO_2 concentration (ppm) and water vapor pressure (mbar) at the same time in both reference and sample air, allowing for the calculation of CO_2 and water vapor differentials between the chamber inlet and outlet. The data were automatically recorded using a CR1000 datalogger (Campbell Scientific®, Logan, UT, USA) connected to the CIRAS-DC. Each complete measurement cycle of the 16 chambers lasted one hour, alternating between treatments. Each chamber was automatically sampled 20 times over 3.75 minutes, with the final measurement calculated as the average of the last five samplings. Measurements were conducted continuously for 24 hours and 21 days in Cycles 1 (June 17 to July 7, 2024) and 3 (August 24 to September 13, 2024), unless system maintenance was required. The temperature and relative humidity inside the chambers were monitored using a datalogger (AK172, AKSO®, São Leopoldo, RS, Brazil) placed inside a representative chamber for each treatment (WW and WS).

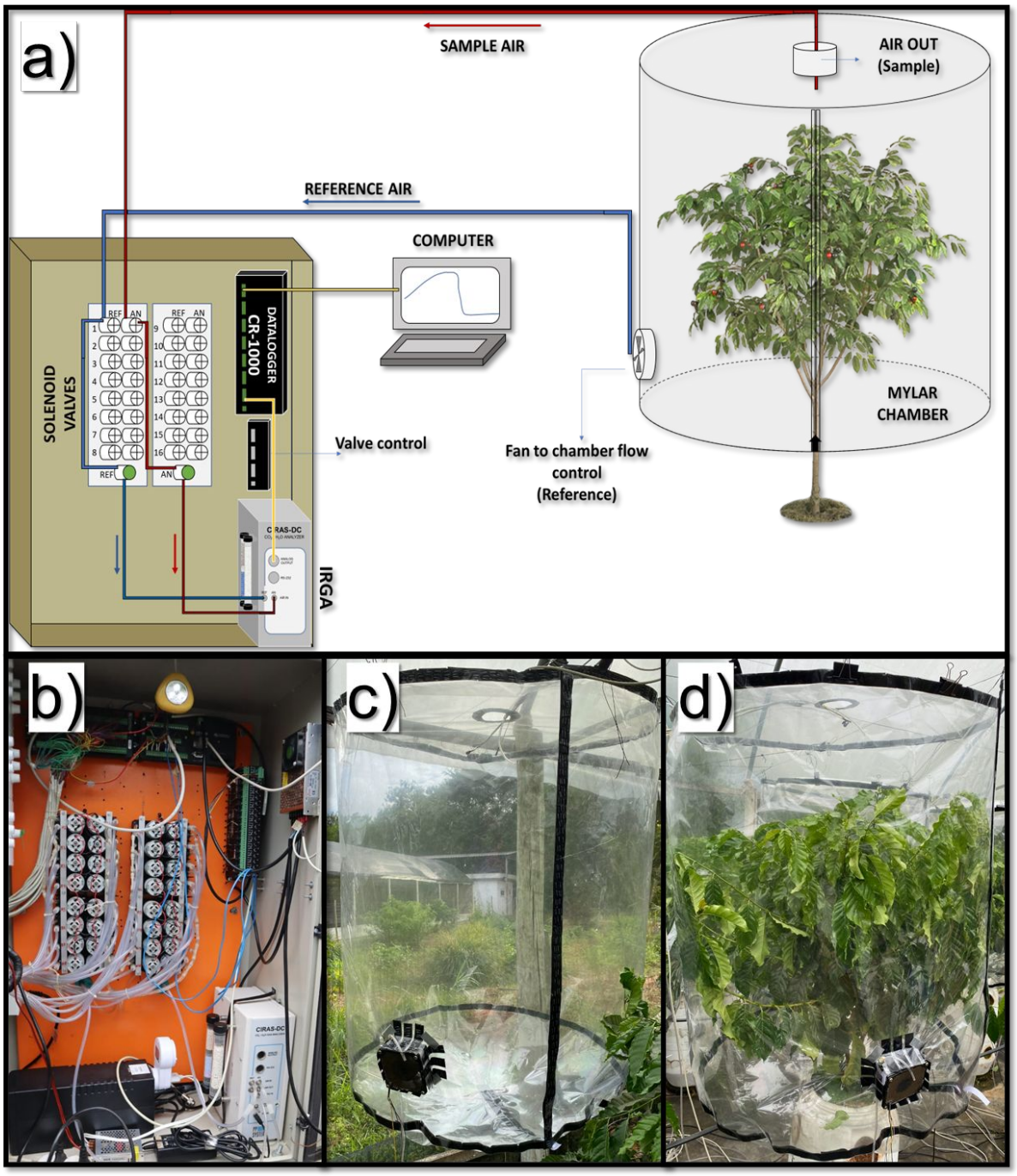

Figure 1: a) Schematic representation of the whole-canopy gas exchange system. b) Manual system for controlling the flow of balloons and automated vacuum pump system connected to the CIRAS-DC infrared gas analyzer and CR1000 datalogger. c) Cylindrical Mylar® chamber (≈ 1 m^3) with air circulation fan and top outlet. d) Cylindrical chamber surrounding a *C. canephora* clone LB1 (≈ 10 months old and with two orthotropic axes).

For the calculation of gas exchange-related variables, the following modified equations of Hall et al. (1993) were used:

$$F = V_{air} * CSA_{out} * 60 * 10^3 \quad \text{(Eq. 1)}$$

where:

F = airflow ($L.min^{-1}$ or $L.h^{-1}$) through the chamber; V_{air} = air velocity ($m.s^{-1}$); CSA_{out} = cross-section area of the air outlet (m^2); 60 = conversion factor from seconds to minutes; 10^3 = conversion factor from m^3 to liters.

$$D_{air} = \frac{P_{atm}}{287.05 * (273.15 + T_{air}¿}¿$$

(Eq. 2)

where:

D_{air} = air density at 20°C ($kg.m^{-3}$); P_{atm} = atmospheric pressure (Pa); 287.05 = specific gas constant for dry air [$J\ (kg.K^{-1})^{-1}$]; T_{air} = air temperature (°C); 273.15 = conversion factor from °C to K.

$$VPD\,air = 0.61137\,e^t * \frac{1 - RH}{100} \quad \text{(Eq. 3)}$$

where:

VPD_{air} = vapor pressure deficit (kPa); RH = relative humidity (%); and

$$t = \frac{17.502 * (T_{air})}{(240.97 + T_{air})} \quad \text{(Eq. 4)}$$

where:

T_{air} = air temperature.

$$F_{mol} = \frac{\frac{F}{60 * 10^{-3}} * \frac{P_{atm}}{10}}{8.314 * (273.15 + T_{air})}$$

(Eq. 5)

where:

F_{mol} = molar flow rate ($mol.s^{-1}$); F = Airflow through the chamber ($L.min^{-1}$); 60 = conversion factor from $L.min^{-1}$ to $L.s^{-1}$; 10^{-3} = conversion factor from $L.s^{-1}$ to $m^3.s^{-1}$; P_{atm} = atmospheric pressure (mbar); 10 = conversion factor from mbar to Pascals (Pa); 8.314 = ideal gas constant; 273.15 = conversion factor from °C to K; T_{air} = air temperature (°C).

$$A_C = \frac{\frac{\Delta CO_2}{(22.4 * \frac{(273+Temp)}{273})}}{\frac{60}{AF}} * F * (-1)$$

(Eq. 6)

where:

A_C = canopy net assimilation ($\mu mol.m^{-2}.s^{-1}$); F = Air flow ($L.min^{-1}$); ΔCO_2 = CO_2 differential between reference and sample (ppm); 22.4 = molar volume of an ideal gas under standard conditions ($L.mol^{-1}$); T_{air} = air temperature (°C); 273.15 = conversion factor from °C to K; 60 = conversion factor from minutes to seconds; AF = estimated leaf area (m^2).

$$CG = \frac{D_{air} * \Delta CO_2 * F}{10^6} * (-1)$$

(Eq. 7)

where:

CG = carbon gain ($g.h^{-1}.plant^{-1}$); D_{air} = air density at 20°C ($kg.m^{-3}$); ΔCO_2 = CO_2 differential between reference and sample (ppm); F = airflow ($L.h^{-1}$); 10^6 = conversion factor from ppm to grams.

$$EC = \frac{\Delta H_2O * F_{mol}}{AF * 10^3}$$

(Eq. 8)

where:

E_C = canopy transpiration rate (mmol.m^{-2}.s^{-1}); ΔH_2O = water vapor differential between reference and sample (mbar); F_{mol} = airflow through the chamber (mol.s^{-1}); AF = estimated leaf area (m^2); 10^3 = conversion factor from mol to mmol.

$$WL = \frac{D_{ar} * \frac{mM_{Vapor}}{mM_{ArSeco}} * \Delta H_2O}{P_{atm}} * F$$

(Eq. 9)

where::

WL = water loss (g.h^{-1}.plant^{-1}); D_{air} = air density at 20°C (kg.m^{-3}); mM_{Vapor} / $mM_{Dry\ air}$ = ratio of molar mass of water vapor (18.015 g.mol^{-1}) to dry air (28.97 g.mol^{-1}), approximately 0.622; ΔH_2O = water vapor differential between reference and sample (mb); P_{atm} = atmospheric pressure (mbar); F = airflow (L.h^{-1}).

$$g_C = \frac{EC}{VPD_{air}} * P_{atm} \qquad \text{(Eq. 10)}$$

where::

g_C = canopy conductance (mmol.m^{-2}.s^{-1}), calculated according to (Campbell & Norman, 1998); E_C = canopy transpiration rate, calculated using the previous equation (converted to mmol m^{-2}.s^{-1}); VPD_{air} = vapor pressure deficit at inlet air (kPa); P_{atm} = atmospheric pressure (kPa).

From the original data (Figure S3; Supplementary data B), the following variables were obtained: $A_{C\text{-}max}$ (µmol.m^{-2}.s^{-1}), representing the maximum value of net CO_2 assimilation rate by canopy; $E_{C\text{-}max}$ (mmol.m^{-2}.s^{-1}), representing the maximum value of daily transpiration rate by canopy; R_{dark} (µmol.m^{-2}.s^{-1}), representing the nighttime respiration rate, calculated as the average CO_2 release between 19:00 and 05:00; A_{daily} (g.m^{-2}.day^{-1}), representing the daily net CO_2 assimilation, calculated as

the integral of the area under the daily assimilation curve using the integrate function on OriginPro® software (OriginLab Corporation, Northampton, MA, USA); and E_{daily} ($g.m^{-2}.day^{-1}$), representing the daily H_2O transpiration, calculated as the integral of the area under the daily transpiration curve. Whenever possible, the data were normalized per plant, considering its leaf area, and/or per hectare (ha), assuming a high-density planting of 5000 $plants.ha^{-1}$ (Ferrão et al., 2017).

Leaf area estimation

To calculate the variables related to whole-canopy gas exchange, it is necessary to determine the leaf area responsible for CO_2 assimilation and H_2O loss. This leaf area was determined by estimation performed by multiplying the total number of leaves per plant by the average leaf area of a single leaf.

To calculate the average leaf area (LA_{mean}) of a single leaf, a representative plant grown under the same conditions prior to the experiment was selected. The total number of leaves (NL) and the plant's total leaf area (TLA) were measured using a leaf area meter (LI-3100C, LI-COR® Environmental, Lincoln, NE, USA). The ratio between TLA and NL resulted in LA_{mean} = 0.0049 m^2. This value was considered constant for all plants and, when multiplied by the total number of leaves per plant, provided the estimated leaf area.

Estimations were performed for both treatments (WW and WS) before the initiation of Cycles 1 and 3. After irrigation resumed in both cycles, and due to leaf shedding in water-stressed plants, the leaf area estimation for the WS treatment was repeated to adjust the whole-canopy gas exchange calculations. The estimated average LA is presented in Table S1 (Supplementary data B).

Biometry and final biomass accumulation

At the end of the experiment, plants from each treatment were used to determine plant height (PH), orthotropic branch diameter (OBD), number of leaves (NL), and total plant leaf area (TLA). PH was obtained as the average height of each orthotropic branch, measured using a graduated ruler from the plant collar to the apex of each branch. OBD was determined as the average diameter of each orthotropic branch, measured at the collar height using a digital caliper (JOMARCA,

Guarulhos, SP, Brazil). NF was determined by simply counting all leaves, while TLA was measured using a leaf area meter LI-3100C (LI-COR® Environmental, Lincoln, NE, USA).

Finally, total dry mass (TDM) was determined separately for leaves (LDM), plagiotropic branches (PBDM), and orthotropic branches (OBDM). Each plant component was separated and dried in a forced-air circulation oven (model 320/5, ELETROlab, Vila Dom Pedro II, SP, Brazil) at 65°C for 72 hours. The dry mass was then weighed using a semi-analytical balance (model BL3200H, SHIMADZU CORPORATION, Nakagyo-ku, KY, Japan).

Data processing and analysis

The experiment was conducted in a completely randomized design with two treatments [well-watered (WW) and water-stressed (WS)] and eight replicates (plants) per treatment (n = 8).

For the comparative analysis of the diurnal trend of meteorological conditions, data were subjected to a two-way analysis of variance (ANOVA), considering the time of day and treatment (growth environment) as factors. Tukey's test at a 5% significance level was used to compare the mean values of the environments at each hour of the day (n = 42).

For the comparative analysis of the diurnal trend in whole-canopy gas exchange, data were subjected to a two-way ANOVA, considering the time of day and treatment (WW and WS) as factors. Tukey's test at a 5% significance level was used to compare the mean values of the treatments at each hour of the day (n = 168).

For the comparative analysis of leaf and whole-canopy gas exchange over time, data were subjected to a two-way ANOVA, considering days and treatment (WW and WS) as factors. Tukey's test at a 5% significance level was used to compare the mean values of the treatments on each measurement day, and Scott-Knott's test at a 5% significance level was applied to group the daily means for each treatment (n = 8).

ANOVAs and mean comparison (Tukey) and clustering (Scott-Knott) tests were performed using the 'ExpDes.pt' package in R software version 4.4.0.

Graphs and linear and nonlinear regression analyses of quantitative data, when necessary, were conducted using OriginPro® software version 2024.

Results

Daily trend of environmental variables

The micrometeorological variables exhibited the expected bell-shaped pattern throughout the day (Figure 2), with significant differences in PPFD, relative air humidity, and VPD_{air} (Table S2; Supplementary data B). In Figure 2a, differences in PPFD between the three environments were observed between 08:00 and 16:00. The greenhouse intercepted approximately 30% of external irradiance, while the chamber intercepted about 15% of the incident irradiance within the greenhouse. Throughout the day, no differences in air temperature were detected between the greenhouse and the interior of the treatment chambers (WW and WS) (Figure 2b). However, between 11:00 and 17:00, differences in relative air humidity were observed within the chambers. In the WW treatment, humidity remained approximately 9% higher than outside the chamber. In contrast, in the WS treatment, humidity was 16% lower compared to WW and 9% lower compared to outside the chamber (Figure 2c). This variation in relative air humidity resulted in differences in VPD_{air} between 11:00 and 16:00. Specifically, VPD_{air} in WS was 30% higher compared to WW and 14% higher compared to outside the chamber (Figure 2d).

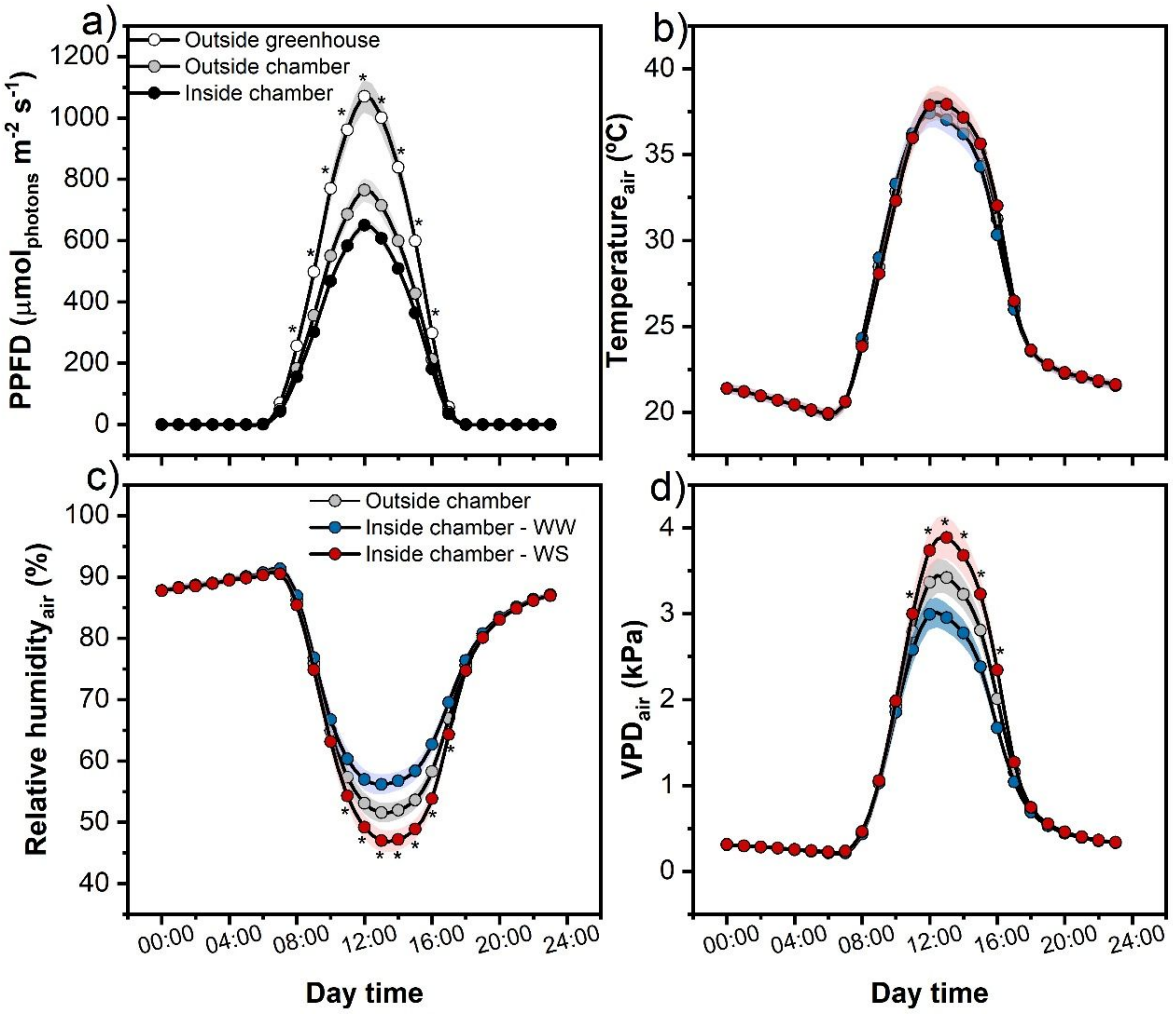

Figure 2: Daily trends of micrometeorological variables measured during the cultivation of *C. canephora* clone LB1 under recurring cycles of soil drying and rewetting in a greenhouse: (a) photosynthetic photon flux density (PPFD, $\mu mol.m^{-2}.s^{-1}$), where white symbols represent measurements outside the greenhouse, gray symbols represent measurements inside the greenhouse, and black symbols represent measurements inside whole-canopy chambers; (b) air temperature (°C); (c) relative air humidity (%); (d) vapor pressure deficit (VPD_{air}, kPa), where gray symbols represent measurements outside the whole-canopy chamber, blue symbols represent measurements inside the whole-canopy chamber for the irrigated treatment (WW), and red symbols represent measurements inside the whole-canopy chamber for the non-irrigated treatment (WS). Each symbol represents the hourly mean over 42 days (n = 42), and the shaded area indicates the standard error. Symbols marked with an asterisk denote significant differences between environments at each time point, with means compared by Tukey's test (P-value < 0.05).

Daily trend of whole-canopy gas exchange

During Cycles 1 and 3, the daily trends of A_C (canopy net CO_2 assimilation) and E_C (transpiration) followed a bell-shaped curve like the responses observed for micrometeorological variables, with significant differences between the WW (irrigated) and WS (non-irrigated) treatments (Table S3; Supplementary data B). At Cycle 1, A_C in WS differed from WW between 08:00 and 16:00 (Figure 3a), and E_C differed between 09:00 and 16:00 (Figure 3c). On average, A_C in WS was 35% lower than in WW between 09:00 and 14:00, and E_C was 27% lower than in WW. At Cycle 3, A_C in WS differed from WW between 06:00 and 15:00 (Figure 3b), and E_C differed between 07:00 and 16:00 (Figure 3d). On average, A_C in WS was 40% lower than in WW between 09:00 and 14:00, and E_C was 37% lower. Both cycles (1: Figure 3e; and 3: Figure 3f) showed that g_C followed a decreasing trend from 09:00 to 17:00 for both treatments (WW and WS), with WS values being lower than WW across all times, except at 09:00 in Cycle 1.

Relationship between whole-canopy gas exchange and micrometeorological variables

Among the measured micrometeorological variables, PPFD showed the best fit (R^2 = 0.91) for A_C responses observed during Cycles 1 and 3, based on a nonlinear model (Figure 4a). For E_C responses, both PPFD (Figure 4b; R^2 = 0.93) and temperature (Figure 7d; R^2 = 0.82) displayed a strong second-degree polynomial correlation with the response variable, while there was a reasonable linear fit (R^2 = 0.63) with VPD_{air} (Figure 4h). The relationships between A_C and temperature (Figure 7b), relative humidity (Figure 4c), and VPD_{air} (Figure 4g), as well as E_C and relative humidity (Figure 4f), showed a fit below 50% (R^2 < 0.50).

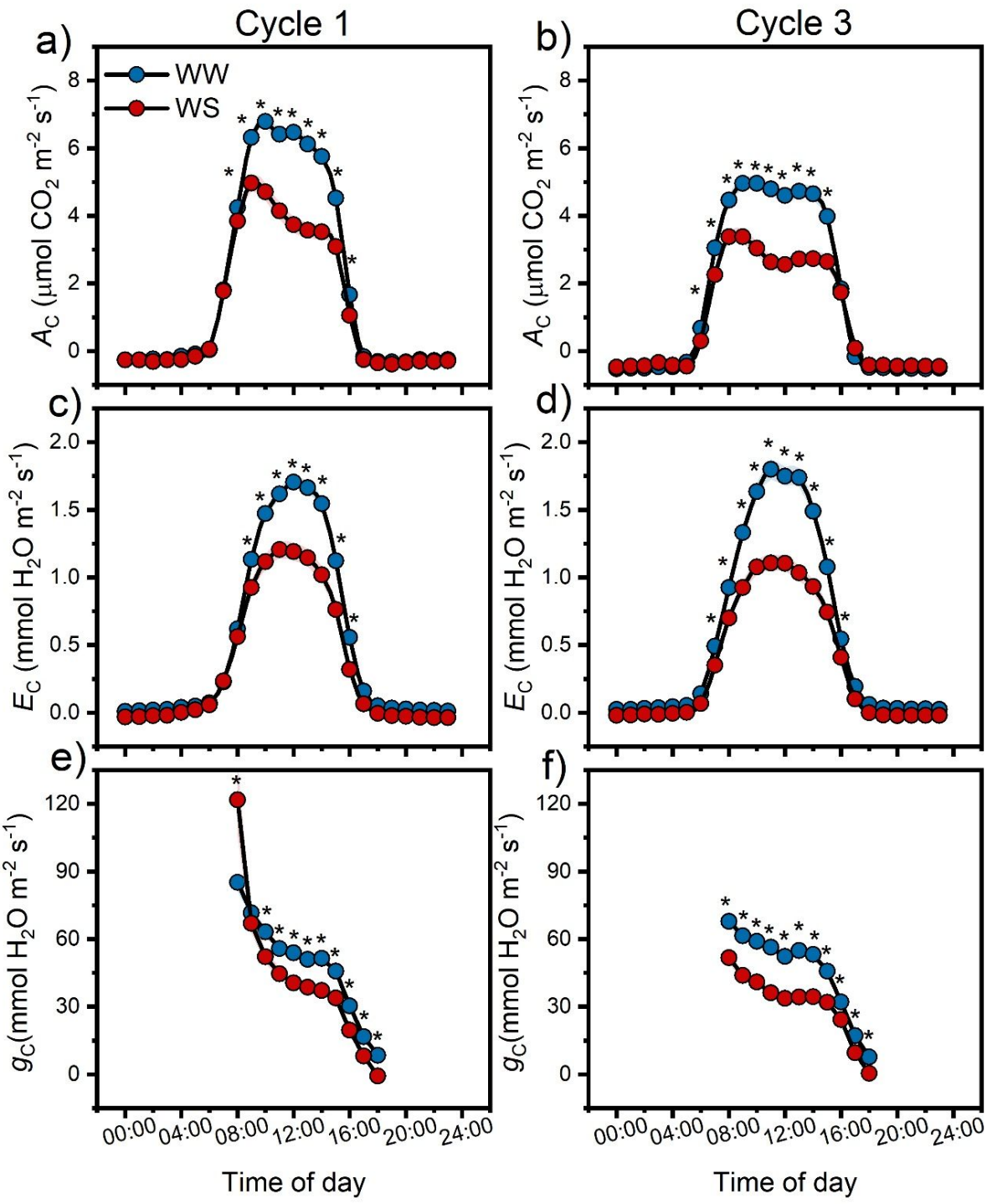

Figure 3: Whole-canopy gas exchange daily trend in *C. canephora* clone LB1 subjected to three recurrent cycles of soil drying and rewetting in a greenhouse. a) net canopy photosynthetic rate (A_C, µmol CO_2.m^{-2}.s^{-1}) during Cycle 1 of water stress (WS-1); b) net canopy photosynthetic rate (A_C, µmol CO_2.m^{-2}.s^{-1}) during Cycle 3 of water stress (WS-3); c) canopy transpiration rate (E_C, mmol H_2O.m^{-2}.s^{-1}) during Cycle 1 of water stress (WS-1); d) canopy transpiration rate (E_C, mmol H_2O.m^{-2}.s^{-1}) during Cycle 3 of water stress (WS-3); e) canopy conductance (g_C, mmol H_2O.m^{-2}.s^{-1}) during

Cycle 1 of water stress (WS-1); f) canopy conductance (g_C, mmol $H_2O.m^{-2}.s^{-1}$) during Cycle 3 of water stress (WS-3). Blue symbols represent measurements for the irrigated treatment (WW), and red symbols represent measurements for the non-irrigated treatment (WS). Each symbol represents the hourly mean of eight plants over 21 days (n = 168), with the shaded area indicating the standard error. Symbols with an asterisk indicate a significant difference between environments at each time point (P-value < 0.05).

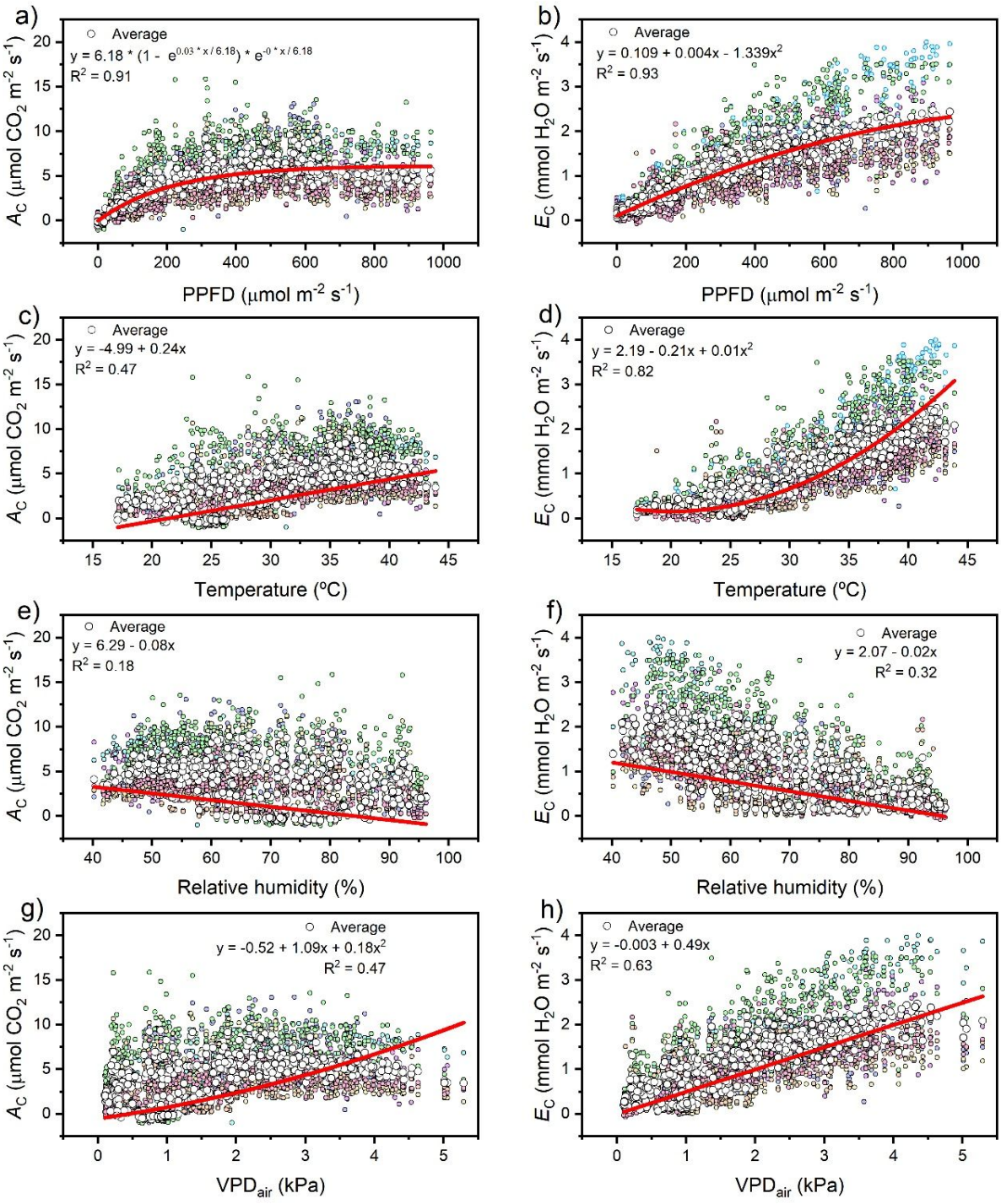

Figure 4: Linear and non-linear regressions between whole-canopy gas exchange parameters and the micrometeorological variables measured inside the chambers. a) net canopy photosynthetic rate (A_C, μmol $CO_2.m^{-2}.s^{-1}$) *versus* photosynthetic photon flux density (PPFD, μmol.$m^{-2}.s^{-1}$); b) canopy transpiration rate (E_C, mmol $H_2O.m^{-2}.s^{-1}$) *versus* photosynthetic photon flux density (PPFD, μmol.$m^{-2}.s^{-1}$); c) net canopy photosynthetic rate (A_C, μmol $CO_2.m^{-2}.s^{-1}$) *versus* temperature (°C); d) canopy transpiration rate (E_C, mmol $H_2O.m^{-2}.s^{-1}$) *versus* temperature (°C); e) net canopy photosynthetic rate (A_C, μmol $CO_2.m^{-2}..s^{-1}$) *versus* relative humidity (%); f) canopy transpiration rate (E_C, mmol $H_2O.m^{-2}.s^{-1}$) *versus* relative humidity; g) net canopy photosynthetic rate (A_C, μmol $CO_2.m^{-2}.s^{-1}$) *versus* vapor pressure deficit (VPD_{air}, kPa); h) canopy transpiration rate (E_C, mmol $H_2O.m^{-2}.s^{-1}$) *versus* vapor pressure deficit (VPD_{air}, kPa). White symbols (n = 8) represent the hourly mean of eight plants (colored symbols) from the irrigated treatment (WW) during Cycles 1 and 3 of soil drying and rewetting. Data measured between 07:00 and 17:00 were considered.

Seasonal responses of leaf gas exchange

Figure 5 presents the results for A_{net}, E, and g_s measured between 07:00 and 09:00, and it is evident that all these variables were impacted by the interaction between the evaluation days and the treatments (Table S4; Supplementary data B). During Cycle 1 (Figure 5a), in WW, A_{net} values remained around 12 μmol.$m^{-2}.s^{-1}$, despite small variations over the days. In WS, the initial average of A_{net} was 11.06 μmol.$m^{-2}.s^{-1}$ for the first two measurements (June 17 and June 19), which showed a reduction from the third measurement (June 21), reaching ≈ 70% decrease compared to the initial values and WW by the 8th measurement (July 1). In the third measurement (July 7) after irrigation in REC-1, A_{net} reached values close to those observed at the beginning of WS-1 but remained lower than WW. WS differed from WW from the 4th to the 11th measurement. During WS-3 (Figure 5b), the reduction of A_{net} in WS was observed starting from the 4th measurement (June 23), reaching ≈ 80% decrease compared to its initial values and to WW. In WS, after irrigation in REC-3, even in the third measurement (September 13), A_{net} did not show full recovery. A_{net} in WS differed from WW between the 6th and 11th evaluations (from September 3 to September 13). The average A_{net} for WW during Cycle 3 remained around 9 μmol.$m^{-2}.s^{-1}$.

Considering the *E* values measured in the morning, during Cycle 1, WW showed an overall average of 2.78 $mmol.m^{-2}.s^{-1}$ (Figure 5c). In WS-1, the initial average of *E* for WS was 2.60 $mmol.m^{-2}.s^{-1}$, which differed from WW starting from the 4th measurement (June 23), reaching a reduction of 70% compared to its initial values and 65% compared to WW (Figure 5c). After irrigation in REC-1, in the second measurement (July 5) of WS, *E* recovered values like those of WW. During Cycle 3 (Figure 5d), both WW and WS showed low *E* values, and in WW, there was a tendency for an increase from the 5th measurement (September 1), with an overall average of around 1.76 $mmol.m^{-2}.s^{-1}$. In WS, starting from the 6th measurement (September 3), *E* showed a reduction of approximately 30% compared to the initial measurements and 50% compared to WW, and even after irrigation in REC-3, it did not reach values like those observed in WW.

During Cycle 1 (Figure 5e), in WW, g_s values remained around 0.20 $mol.m^{-2}.s^{-1}$, and in WS, the initial g_s values were 0.18 $mol.m^{-2}.s^{-1}$. In WS, reductions of g_s were observed from the 4th measurement (June 23) until reaching about a 75% decrease by the 8th measurement (July 1). After irrigation of WS in REC-1, in the 2nd measurement (July 5), g_s values began to recover. During Cycle 3 (Figure 5f), in both WW and WS, a reduction in g_s values was observed between the 1st and 3rd measurements (from August 24 to August 28), after which g_s increased in WW, with an overall average of 0.18 $mol.m^{-2}.s^{-1}$. In WS, at the 8th measurement, there was a reduction of approximately 55% compared to the first measurement and 65% compared to WW. Even after irrigation of WS in REC-3, in the 3rd measurement, g_s values remained about 38% lower than those observed in WW.

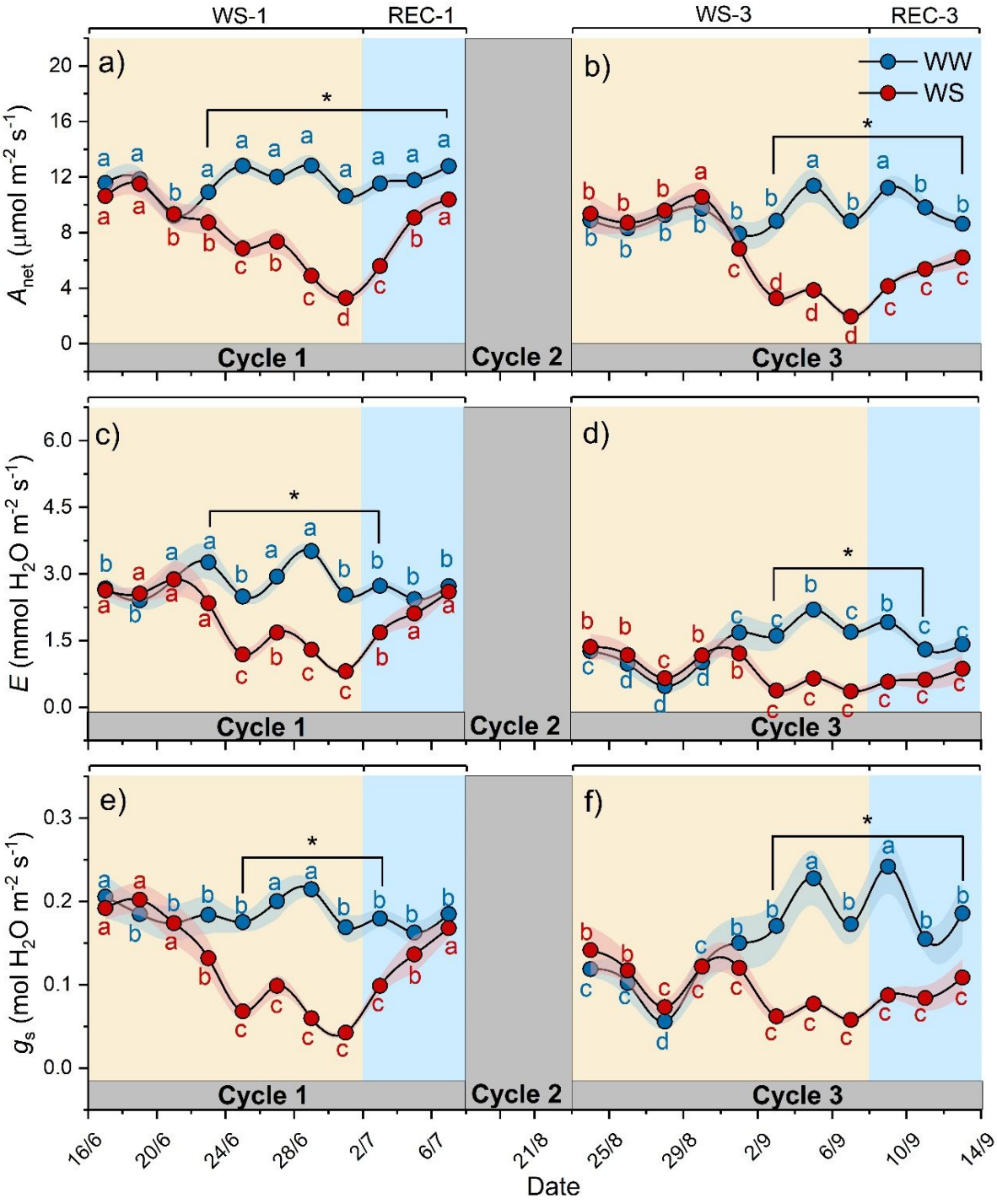

Figure 5: Single-leaf gas exchange measured between 07:00 and 09:00 in *C. canephora* clone LB1 plants subjected to three recurring cycles of soil drying and rewetting in a greenhouse. a) Leaf net photosynthetic rate (A_{net}, µmol.m^{-2}.s^{-1}) during Cycle 1, and b) during Cycle 3 of soil drying and rewetting. c) Leaf transpiration rate (E, mmol.m^{-2}.s^{-1}) during Cycle 1, and d) during Cycle 3 of soil drying and rewetting. e) Leaf stomatal conductance (g_s, mol.m^{-2}.s^{-1}) during Cycle 1, and f) during Cycle 3 of soil drying and rewetting. Eleven measurements were performed over 21 days, eight during drying (WS-1 and WS-3, indicated by the yellow background) and three after

soil rewetting (REC-1 and REC-3, indicated by the blue background). Blue symbols represent the irrigated condition (WW), and red symbols represent the non-irrigated condition (WS). Lowercase letters indicate significant differences over time for each water condition (blue for WW and red for WS), grouped by the Scott-Knott test (P-value < 0.05). Days marked below the bracket or with an asterisk indicate significant differences between water conditions for each measurement day, compared by the Tukey test (P-value < 0.05). Each symbol represents the mean ± standard error (shaded area) of eight plants (n = 8).

Figure 6 presents the results of gas exchange measurements between 12:00 and 14:00 in *C. canephora* clone LB1 plants subjected to three recurring cycles of soil drying and rewetting in a greenhouse. The results of A_{net}, E, and g_s show that all of them were impacted by the interaction between the evaluation days and the treatments (Table S4; Supplementary data B). In Cycle 1 (Figure 6a), in WW, A_{net} had an overall mean of 9.05 $\mu mol.m^{-2}.s^{-1}$, with a tendency to increase from the 1st to the 11th measurement (from June 17 to July 7). In WS, A_{net} started with an average value of 6.05 $\mu mol.m^{-2}.s^{-1}$ until the 3rd measurement (June 21), and from the 4th to the 8th measurement, a reduction of up to 85% was observed in comparison to the initial measurements and a decrease of 90% in relation to WW. In the 3rd measurement (July 07), after irrigation in REC-1, WS returned to values even higher than those observed at the beginning of WS-1 but 30% lower compared to WW. During Cycle 3 (Figure 6b), A_{net} varied throughout the days, but in WW, the overall mean was 5.93 $\mu mol.m^{-2}.s^{-1}$. In WS, A_{net} reduced by approximately 95% from the 6th measurement (September 3) compared to the initial values and WW. Even in the 3rd measurement after irrigation in REC-3 (13/09), A_{net} was 65% lower in WS compared to WW.

Regarding the E responses at noon, during Cycle 1, in WW, the overall mean was 2.95 $mmol.m^{-2}.s^{-1}$, with variations across the measurement days (Figure 6c). In WS, the initial E values were, on average, 2.35 $mmol.m^{-2}.s^{-1}$, and in the 4th measurement (June 23), a significant reduction of around 75% was observed until the 10th measurement. After irrigation in REC-1, WS recovered E values, but they remained approximately 45% lower compared to WW. E values in WS differed from WW from the 4th to the 11th measurement (from August 8 to September 11). During Cycle 3 (Figure 6d), E was reduced between the 1st and 4th measurements for both treatments, and after the 5th measurement (September 1), E values in WW remained

around 3.38 mmol.m^{-2}.s^{-1}. In WS, *E* decreased by about 80% from the 6th to the 9th measurement (from September 3 to September 9) compared to the 1st measurement and WW. In the 2nd measurement after irrigation in REC-3 (September 11), WS recovered *E* values similar to those of WW.

Considering the g_s values in Cycle 1 (Figure 6e), in WW, there was considerable variation across the days, but the overall mean was 0.10 mol m^{-2} s^{-1}. In WS, g_s values reduced by about 70% from the 4th to the 9th measurement (from June 23 to July 3). After irrigation in REC-1, g_s values in WS recovered compared to the initial measurements but were approximately 38% lower compared to WW. During Cycle 3 (Figure 6f), WW had an average g_s of around 0.08 mol.m^{-2}.s^{-1}. In WS, g_s began to decrease from the 3rd measurement (August 28) and differed from WW starting from the 5th measurement (September 09), reaching a reduction of about 80% compared to the initial measurements. After irrigation in REC-3, in WS, g_s only matched WW in the second measurement, differing in the subsequent measurements.

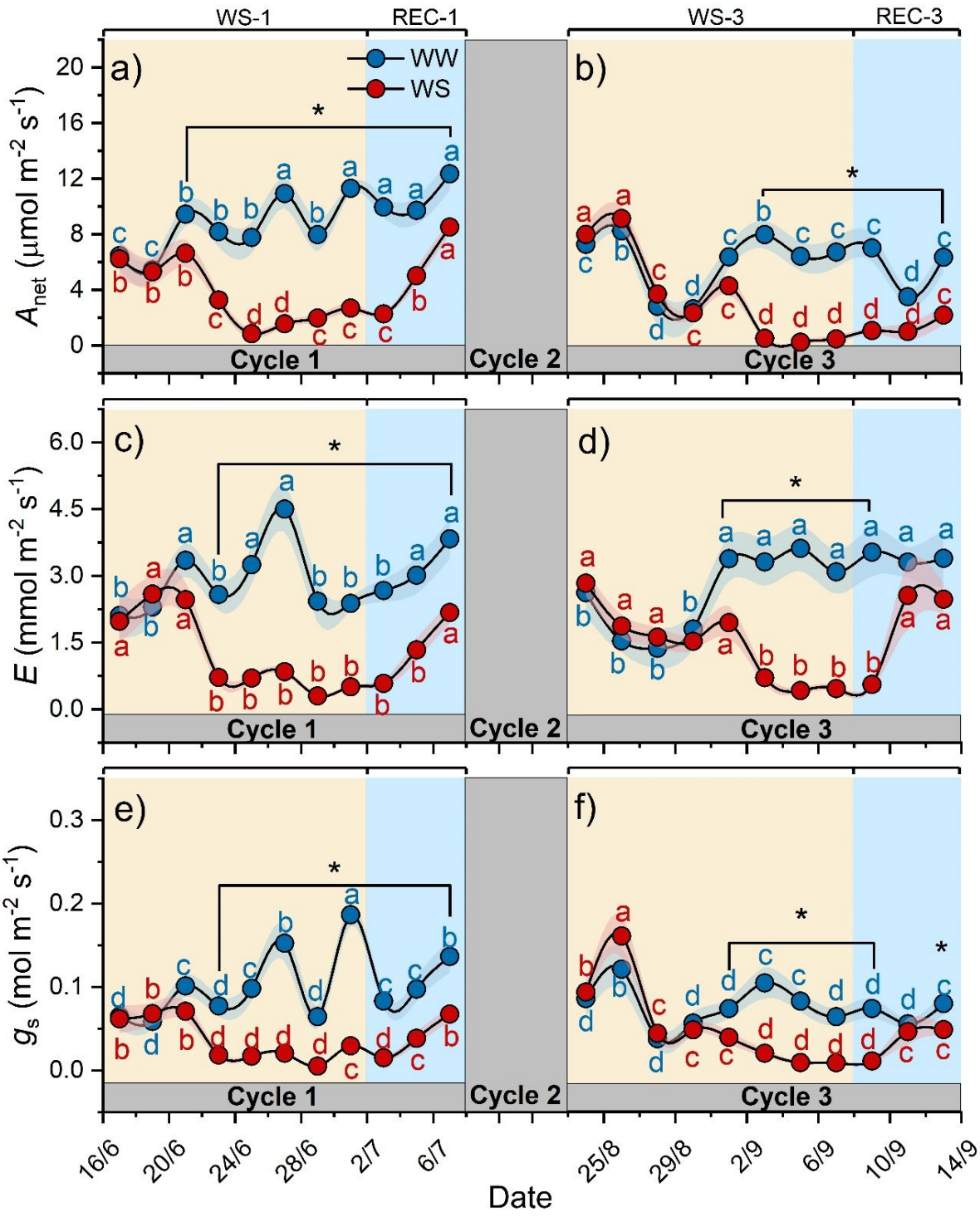

Figure 6: Single-leaf gas exchange measurements taken between 12:00 and 14:00 in *C. canephora* clone LB1 plants subjected to three recurring cycles of soil drying and rewetting in a greenhouse. a) Leaf net photosynthetic rate (A_{net}, µmol.m^{-2}.s^{-1}) during Cycle 1 and b) during Cycle 3 of soil drying and rewetting. c) Leaf transpiration rate (E, mmol.m^{-2}.s^{-1}) during Cycle 1 and d) during Cycle 3 of soil drying and rewetting. e) Leaf stomatal conductance (g_s, mol.m^{-2}.s^{-1}) during Cycle 1 and f) during Cycle 3 of soil drying and rewetting. A total of 11 measurements were

performed over 21 days, with eight measurements during soil drying (WS-1 and WS-3, indicated by yellow background) and three measurements after soil rewetting (REC-1 and REC-3, indicated by blue background). Blue symbols represent the irrigated condition (WW), and red symbols represent the non-irrigated condition (WS). Lowercase letters indicate significant differences across days for each water condition (blue for WW and red for WS), grouped by the Scott-Knott test (P-value < 0.05). Days marked below the bracket or overlaid with an asterisk indicate significant differences between the water conditions for each measurement day, compared to using the Tukey test (P-value < 0.05). Each symbol represents the mean ± standard error (shaded area) of eight plants (n = 8).

Seasonal responses of whole-canopy gas exchange

Analysis of $A_{C\text{-}max}$ and $E_{C\text{-}max}$ responses showed a significant effect of the interaction between the evaluated dates and treatments (Table S5; Supplementary data B). During Cycle 1 (Figure 7a), in WW, $A_{C\text{-}max}$ remained at an average value of 7.85 $\mu mol.m^{-2}.s^{-1}$. In WS, the initial $A_{C\text{-}max}$ value was around 6.66 $\mu mol.m^{-2}.s^{-1}$, and its reduction was observed starting from the 8th day of stress (June 23), reaching a decline of more than 70% by the 16th day (July 2). Compared to WW, the observed reduction in WS was 77%. After two days of irrigation in REC-1 (July 4), the $A_{C\text{-}max}$ values in WS returned to an average of 7.93 $\mu mol.m^{-2}.s^{-1}$, similar to those observed in WW. During WS-3 (Figure 7b), in WW, the overall mean $A_{C\text{-}max}$ was 5.94 $\mu mol.m^{-2}.s^{-1}$. In WS, the reduction in $A_{C\text{-}max}$ started from the 9th day of stress (September 1) and reached a decline of more than 80% by the 16th day (September 8), both in comparison to its initial values and to WW. After three days of irrigation in REC-3, $A_{C\text{-}max}$ returned to an average value of 5.52 $\mu mol.m^{-2}.s^{-1}$, similar to the values observed in WW.

During Cycle 1, in WW, $E_{C\text{-}max}$ maintained an average of 1.85 $mmol.m^{-2}.s^{-1}$ (Figure 7c). In WS, reductions in $E_{C\text{-}max}$ were observed starting from the 7th day of stress (June 22), reaching a decline of about 80% by the 16th day (July 2) compared to its initial values and WW values. In WS, the average value of 2.42 $mmol.m^{-2}.s^{-1}$ for $E_{C\text{-}max}$ was restored after two days of irrigation in REC-1 (July 4), reaching values like those observed in WW. During WS-3, in WW, the overall mean $E_{C\text{-}max}$ was 2.16 $mmol.m^{-2}.s^{-1}$ (Figure 7d). In WS, the reduction in $E_{C\text{-}max}$ was observed starting from

the 9th day of stress (September 1), compared to WW, and from the 10th day (September 2) compared to the initial WS values. After 16 days of stress (September 8), $E_{C\text{-}max}$ showed a reduction of about 70% compared to its initial values and 80% compared to WW. Recovery of $E_{C\text{-}max}$ was observed after three days of irrigation in REC-3, reaching an average value of 2.04 mmol.m^{-2}.s^{-1}, close to that observed in WW (2.49 mmol.m^{-2}.s^{-1}).

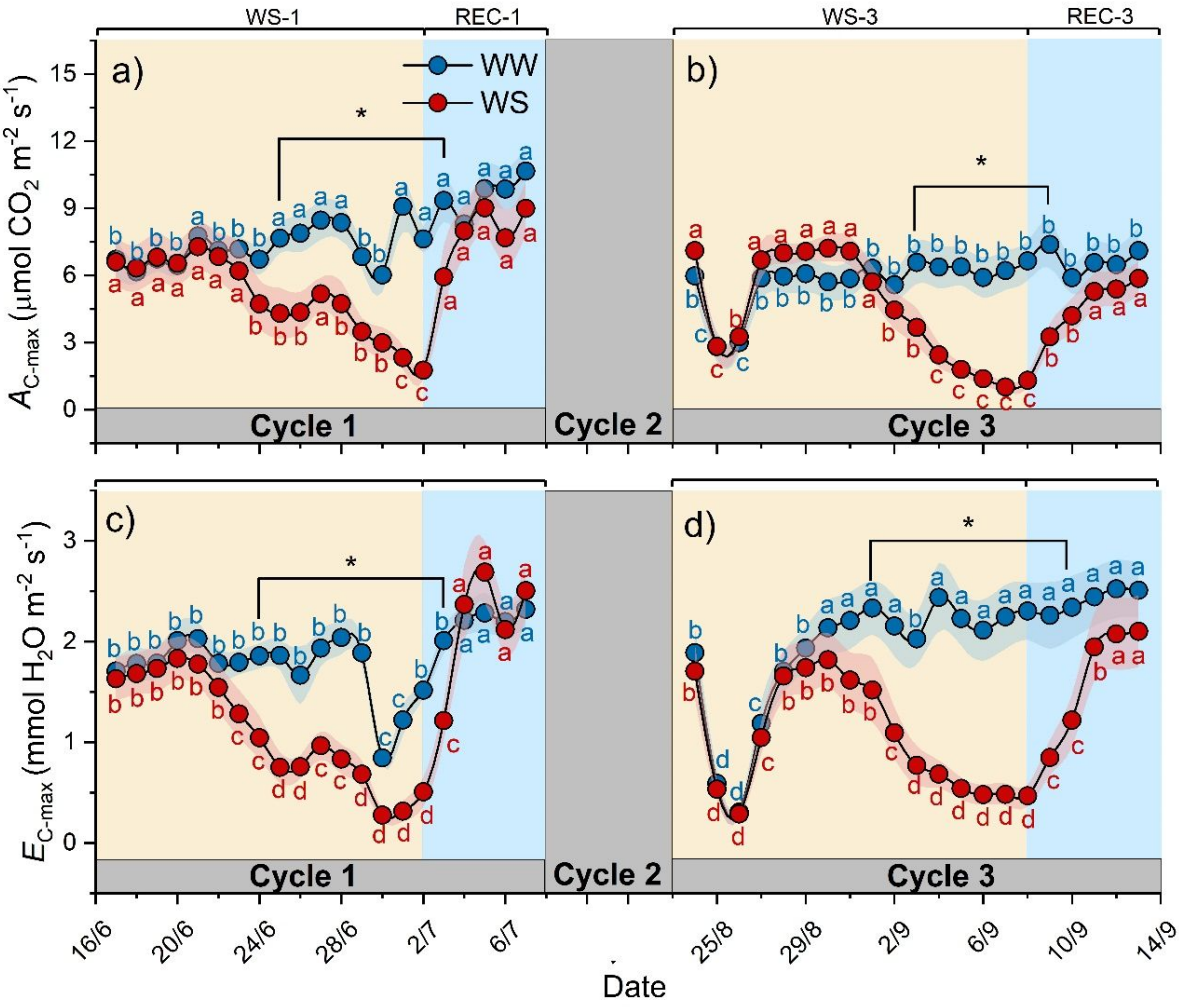

Figure 7: Whole-canopy gas exchanges in *C. canephora* clone LB1 plants subjected to three recurrent cycles of soil drying and rewetting in a greenhouse. a) maximum value of net CO_2 assimilation rate by the canopy ($A_{C\text{-}max}$, µmol CO_2.m^{-2}.s^{-1}) during Cycle 1 and b) during Cycle 3 of soil drying and rewetting. c) Maximum value of canopy transpiration rate ($E_{C\text{-}max}$, mmol H_2O.m^{-2}.s^{-1}) during Cycle 1 and d) during Cycle 3 of soil drying and rewetting. Each cycle lasted 21 days, with 16 days of drying (WS-1 and WS-3, indicated by yellow background) and 5 days of soil rewetting (REC-1 and REC-3, indicated by blue background). Blue symbols represent the

irrigated condition (WW), and red symbols represent the non-irrigated condition (WS). Lowercase letters indicate significant differences over the days for each water condition (blue for WW and red for WS), grouped by the Scott-Knott test (P value < 0.05). Days marked below the bracket or overlaid with an asterisk indicate significant differences between water conditions for each measurement day, compared to the Tukey test (P value < 0.05). Each symbol represents the mean ± standard error (shaded area) of eight plants (n = 8).

The linear regressions plotted between $A_{C\text{-}max}$ and $E_{C\text{-}max}$ (WUE) for Cycles 1 and 3 of soil drying and rewetting are shown in Figure 8. In Cycle 1 (Figure 8a), for WW, the slope of the line was 1.65 (R2 = 0.14), and for WS the slope was 3.12 (R2 = 0.89). In Cycle 3 (Figure 8b), for WW, the slope of the line was 1.69 (R2 = 0.87), and for WS the slope was 3.85 (R2 = 0.83).

The linear regressions plotted between $A_{C\text{-}max}$ and Ψ_{mSoil} (Figure 9a) and between $E_{C\text{-}max}$ and Ψ_{mSoil} (Figure 9b) are both considering only the WS treatment. In WS-1 the values of the slope and interception of the line are 0.004 and 7.23, respectively (Figure 9a); and in WS-3 the values are 0.005 and 5.82, for the slope and interception of the line, respectively (Figure 9a). In WS-1 the values of the slope and interception of the line are 0.001 and 1.68, respectively (Figure 9b); and in WS-3 the values are 0.001 and 1.52, for the slope and interception of the line, respectively (Figure 9b).

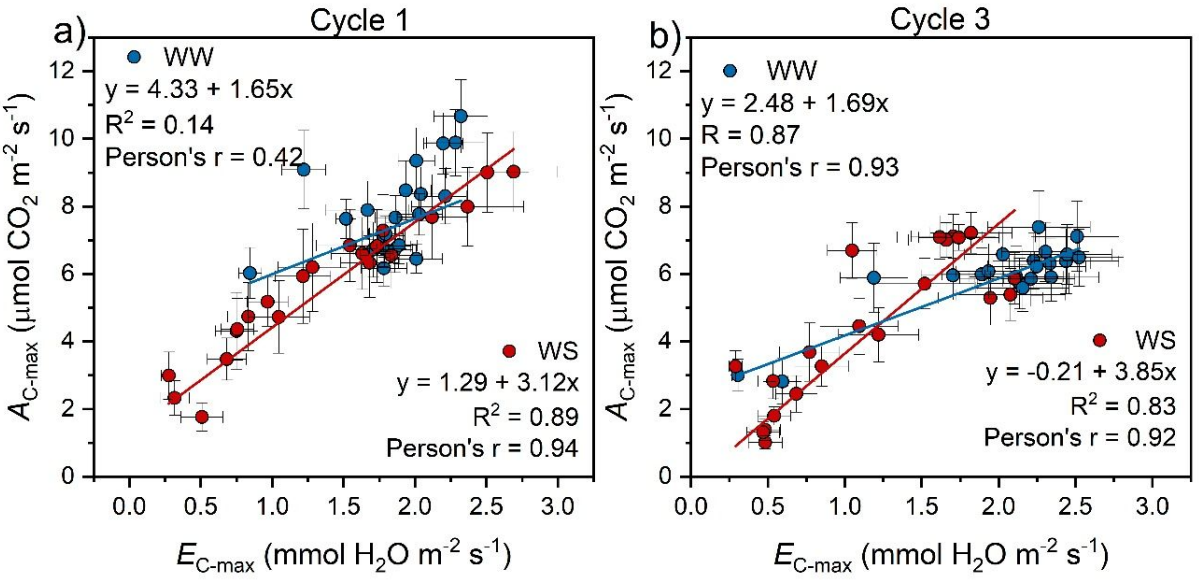

Figure 8: Linear regressions plotted between $A_{C\text{-}max}$ and $E_{C\text{-}max}$, for Cycles 1 and 3 of soil drying and rewetting. The equation, the coefficient of determination (R^2), and Pearson's correlation coefficient (r) of the lines are shown for the irrigated (WW, in blue) and non-irrigated (WS, in red) conditions, for Cycles a) 1 and b) 3. Each symbol represents the mean of eight plants (n = 8), and the horizontal and vertical bars indicate the standard error of the x and y axes, respectively.

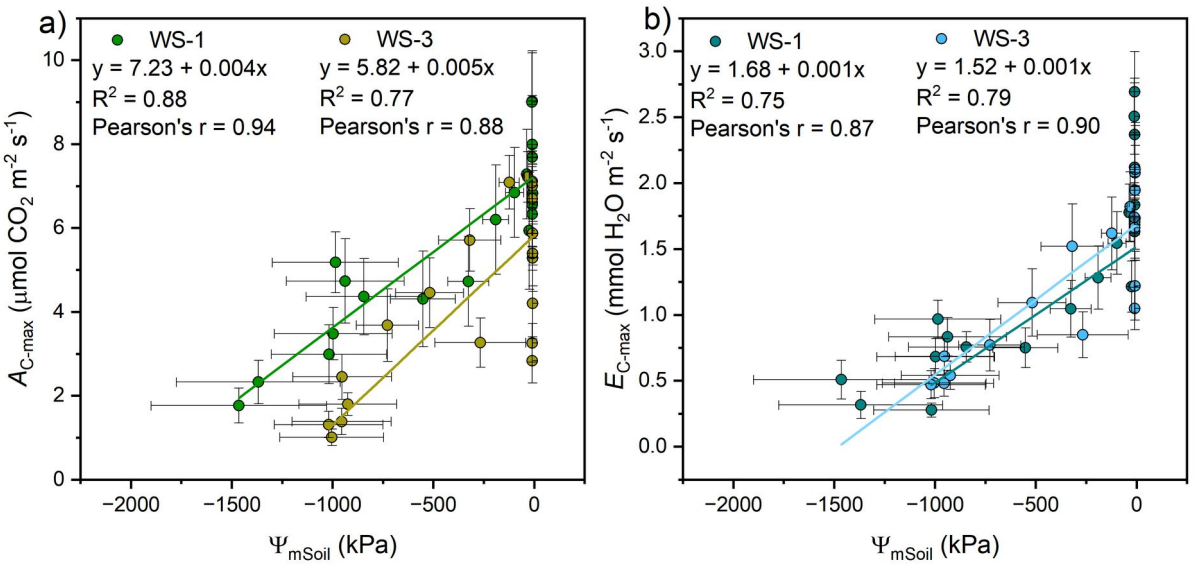

Figure 9: Linear regressions plotted between (a) $A_{C\text{-}max}$ and Ψ_{mSoil} and between (b) $E_{C\text{-}max}$ and Ψ_{mSoil} for Cycles 1 (WS-1) and 3 (WS-3) of soil drying. The equation, the coefficient of determination (R^2), and Pearson's correlation coefficient (r) of the lines are shown for each water stress cycle. Each symbol represents the mean of eight plants (n = 8), and the horizontal and vertical bars indicate the standard error of the x

and y axes, respectively. The $A_{C\text{-}max}$ and $E_{C\text{-}max}$ were commonly recorded between 11:00 and 13:00.

The linear regressions of the relation between $A_{C\text{-}max}$ and A_{leaf} (or A_{net}), measured in the morning (Figure 10a), between $A_{C\text{-}max}$ and A_{leaf}, measured at midday (Figure 10b), $E_{C\text{-}max}$ and E_{leaf}, measured in the morning (Figure 10c), and $E_{C\text{-}max}$ and E_{leaf}, measured at midday (Figure 10d) were presented. In all cases, except for $A_{C\text{-}max}$ and A_{leaf}, measured in the morning (Figure 10a), the fitting degree between the leaf-level and whole-canopy gas exchange variables was less than 50% ($R^2 < 0.50$), even though positive correlations ($r > 0.50$) were observed between them. Additionally, in all cases, the slopes of the linear regression were less than 1, indicating an underestimation of whole-canopy gas exchange variables compared to leaf-level gas exchange measurements.

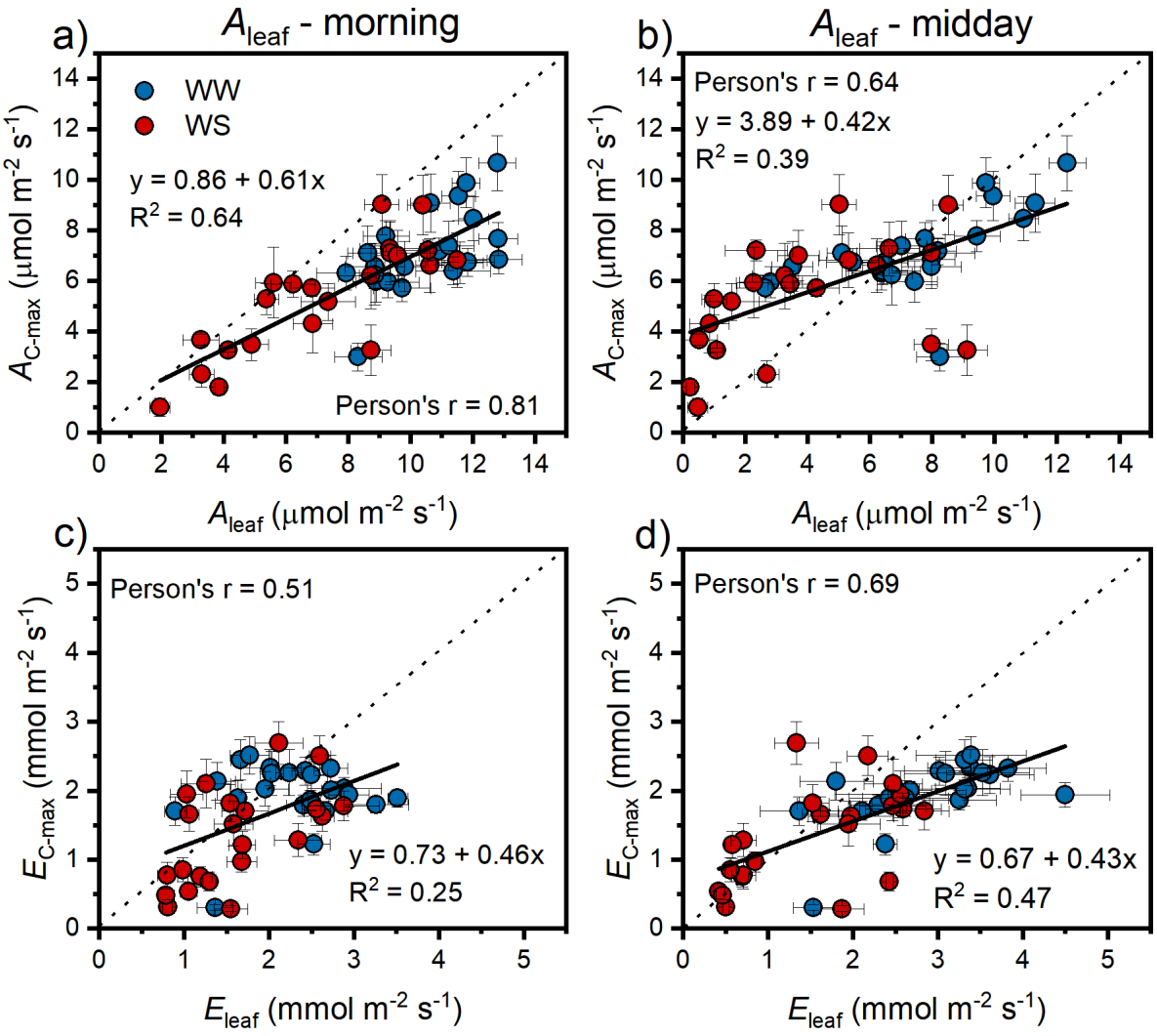

Figure 10: Linear regressions plotted between whole-canopy gas exchange and single-leaf gas exchange in *C. canephora* clone LB1 plants subjected to three recurrent cycles of soil drying and rewetting in a greenhouse. a) $A_{C\text{-}max}$ (µmol.m^{-2}.s^{-1}) *versus* A_{leaf} (µmol.m^{-2}.s^{-1}), considering A_{leaf} measured in the morning; b) $A_{C\text{-}max}$ (µmol.m^{-2}.s^{-1}) *versus* A_{leaf} (µmol.m^{-2}.s^{-1}), considering A_{leaf} measured at midday; c) $E_{C\text{-}max}$ (mmol.m^{-2}.s^{-1}) *versus* E_{leaf} (mmol.m^{-2}.s^{-1}), considering E_{leaf} measured in the morning; and d) $E_{C\text{-}max}$ (mmol.m^{-2}.s^{-1}) *versus* E_{leaf} (mmol.m^{-2}.s^{-1}), considering E_{leaf} measured at midday. In the figures, the equation, the coefficient of determination (R^2), and Pearson's correlation coefficient (r) of the regression lines are shown. Each symbol represents the mean of eight plants (n = 8), and the horizontal and vertical bars indicate the standard error of the x and y axes, respectively. Dotted lines indicate R^2 = 1, and solid lines indicate the linear plot among the estimated means by regression analysis.

The values of R_{dark} measured between 19:00 and 05:00 daily were exhibited in Figure 11. No significant interaction was observed between the evaluation days and the treatments, but there was a significant effect among the evaluation days (Table S5; Supplementary data B). In general, the R_{dark} values throughout Cycles 1 (Figure 11a) and 3 (Figure 11b) remained around the mean value of -0.45 μmol.m^{-2}.s^{-1}.

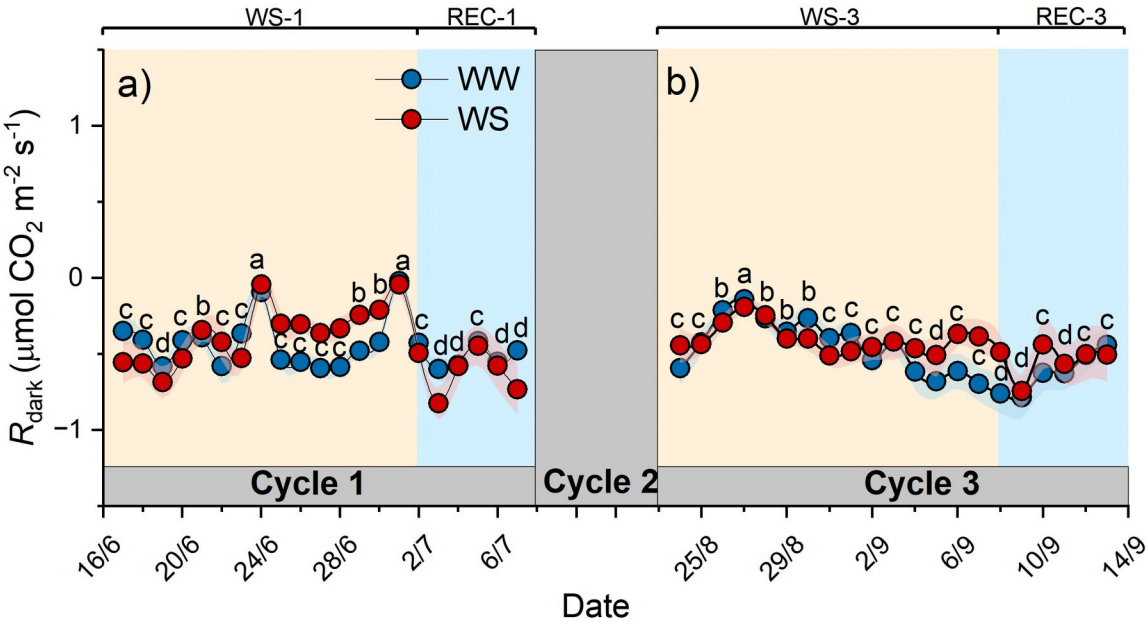

Figure 11: Whole-canopy dark respiration (R_{dark}, μmol m^{-2} s^{-1}) in *C. canephora* clone LB1 subjected to three recurrent cycles of soil drying and rewetting in a greenhouse. a) R_{dark} during Cycle 1 and b) during Cycle 3 of soil drying and rewetting. Each cycle lasted 21 days, with 16 days of drying (WS-1 and WS-3, indicated by the yellow background) and 5 days of soil rewetting (REC-1 and REC-3, indicated by the blue background). In the figures, blue symbols represent the irrigated condition (WW), and red symbols represent the non-irrigated condition (WS). Lowercase letters indicate significant differences over time, regardless of the water condition, and are grouped by the Scott-Knott test (P-value < 0.05). Each symbol represents the mean ± shaded area of eight plants (n = 8).

Daily CO_2 gain and H_2O loss

The responses in A_{daily} and E_{daily}, evaluated in $g.m^{-2}.day^{-1}$ and $L.m^{-2}.day^{-1}$, respectively, were influenced by the interaction between evaluation days and treatments (Table S6; Supplementary data B). During Cycle 1 (Figure 12a), WW exhibited an A_{daily} with an overall mean of 4.91 $g.m^{-2}.day^{-1}$, with significant reductions between the 13th (June 29) and 16th (July 2) days due to cloudy weather (Figure 12a). In WS, A_{daily} maintained a mean of 3.87 $g.m^{-2}.day^{-1}$ until the 6th day (June 22) of stress, after which there was a significant reduction in A_{daily}, with a slight recovery between the 10th and 12th days (from June 26 to June 28), and a reduction of over 85% by the 16th day (July 02) compared to its initial values and those observed in WW. After two days of irrigation in REC-1, A_{daily} values in WS returned to levels close to those observed in WW. In WS-3 (Figure 12b), WW showed an overall mean of 4.16 $g.m^{-2}.day^{-1}$, with low values observed on the 2nd and 3rd evaluation days, due to system malfunction and predominantly rainy weather, respectively. In WS, the initial mean A_{daily} was 4.70 $g.m^{-2}.day^{-1}$ until the 6th day, after which there was a reduction of over 90% between the 12th and 16th days of stress (from September 4 to September 8). Recovery of A_{daily} values ($\overline{x}$ = 3.52 $g.m^{-2}.day^{-1}$) in REC-3 occurred after three days of irrigation.

During Cycle 1 (Figure 12c), WW exhibited an overall mean of 2.55 $L.m^{-2}.day^{-1}$ for E_{daily}, with higher values observed during REC-1. In WS, the initial mean was 2.15 $L.m^{-2}.day^{-1}$ until the 6th day (June 22), after which there was a gradual reduction, reaching a drop of over 85% (compared to initial values) between the 14th and 16th days of stress (from June 30 to July 2). After two days of irrigation in REC-1, WS recovered high E_{daily} values like those observed in WW, with a mean of 2.26 $L.m^{-2}.day^{-1}$. During WS-3 (Figure 12d), WW had an overall mean E_{daily} of 3.42 $L.m^{-2}.day^{-1}$. In WS, the initial mean E_{daily} was 1.99 $L.m^{-2}.day^{-1}$, and from the 9th day of stress, E_{daily} values began to diverge from those observed in WW, indicating a reduction. In WS, E_{daily} decreased by approximately 70% between September 4 and September 8. Recovery of E_{daily} values occurred on the 3rd day of irrigation in REC-3.

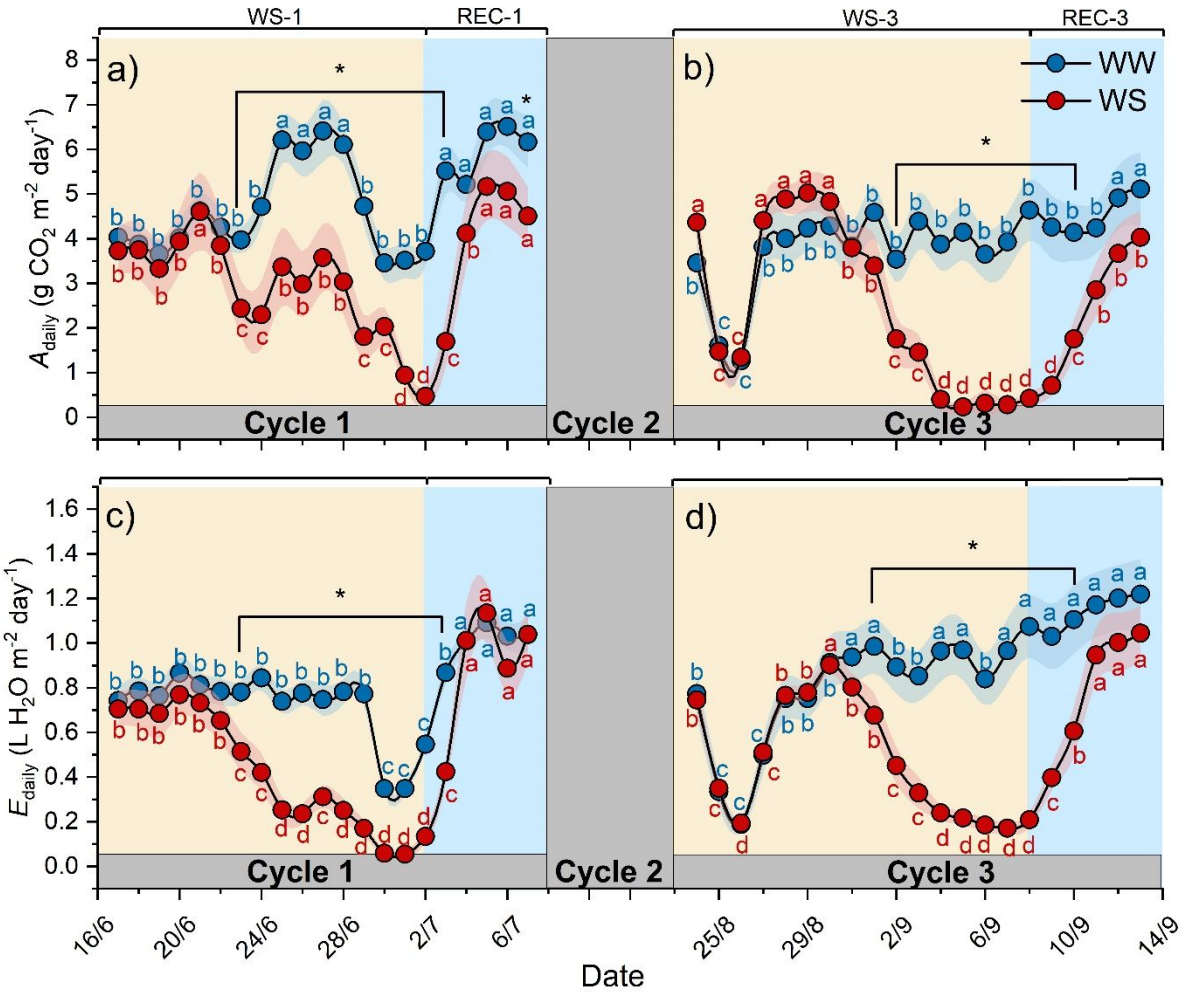

Figure 12: Whole-canopy gas exchange in *C. canephora* clone LB1 subjected to three recurrent cycles of soil drying and rewetting in a greenhouse. a) Daily canopy photosynthetic assimilation (A_{daily}, g CO_2.m^{-2}.day^{-1}) during Cycle 1 and b) during Cycle 3 of soil drying and rewetting. c) Daily canopy transpiration (E_{daily}, L.H_2O.m^{-2}.day^{-1}) during Cycle 1 and d) during Cycle 3 of soil drying and rewetting. Each cycle lasted 21 days, with 16 days of drying (WS-1 and WS-3, indicated by the yellow background) and 5 days of soil rewetting (REC-1 and REC-3, indicated by the blue background). In the figures, blue symbols represent the irrigated condition (WW), and red symbols represent the non-irrigated condition (WS). Lowercase letters indicate significant differences over time for each water condition (blue for WW and red for WS), grouped by the Scott-Knott test (P-value < 0.05). Days marked below the bracket or with an asterisk superscript indicate significant differences between the water conditions for each measurement day, compared using Tukey's test (P-value < 0.05). Each symbol represents the mean ± shaded area of eight plants (n = 8).

The responses in A_{daily} and E_{daily}, evaluated in g.plant^{-1}.day^{-1} and L.plant^{-1}.day^{-1}, respectively, were influenced by the interaction between evaluation days and treatments (Table S6; Supplementary data B). During Cycle 1 (Figure 13a), A_{daily} in WW showed a mean of 15.84 g.plant^{-1}.day^{-1}. In WS, A_{daily} was 11.61 g.plant^{-1}.day^{-1} until the 6th day (June 22), after which there was a gradual reduction until the 16th day (July 2), when it reached a drop of approximately 90% compared to both its initial values and those observed in WW. In WS, even after six days of irrigation in REC-1, A_{daily} values remained about 40% lower than those observed in WW. During WS-3 (Figure 13b), excluding the 2nd and 3rd measurement days in WW, the mean A_{daily} remained around 14.20 g.plant^{-1}.day^{-1}. In WS, the initial mean A_{daily} was 13.39 g.plant^{-1}.day^{-1} until the 8th day of stress (August 31), after which there was a gradual reduction in A_{daily} until it reached a drop of approximately 90% between the 12th and 16th days of stress (from September 4 to September 8). After six days of irrigation in REC-3, A_{daily} in WS remained about 50% lower than in WW.

During Cycle 1 (Figure 13c), in WW, E_{daily} showed an overall mean of 2.55 L.plant^{-1}.day^{-1}. In WS, the initial mean E_{daily} was 2.20 L.plant^{-1}.day^{-1} until the 5th day of stress (June 21), gradually decreasing until it reached a reduction of approximately 90% between the 14th and 16th days of stress (from June 30 to July 2). After two days of irrigation in REC-1, WS recovered E_{daily} to values equal to the beginning of WS-1 ($\bar{x}$ = 2.26 L.plant^{-1}.day^{-1}), but it remained about 30% lower than the values observed in WW. During WS-3 (Figure 13d), in WW, the overall mean E_{daily} was approximately 3.42 L.plant^{-1}.day^{-1}, with a gradual increasing trend throughout the cycle. In WS, the initial mean E_{daily} was 2.28 L.plant^{-1}.day^{-1}, and from the 8th day of stress (August 31), it decreased until it reached a drop of approximately 75% between the 12th and 16th days of stress (from September 4 to September 8). After the 3rd day of irrigation in REC-3, WS recovered mean values of 2.16 L.plant^{-1}.day^{-1}, but these were still about 50% lower than in WW.

By integrating the area under the curve of A_{daily} and E_{daily} [g.plant^{-1}.day^{-1} and L.plant^{-1}.day^{-1}, respectively (Figure 13)] or [kg.ha^{-1}.day^{-1} and L.ha^{-1}.day^{-1} (Figure S4; Supplementary data B)] over the 21 days in Cycle 1, each plant assimilated approximately 316 g (1,580 kg.ha^{-1}) and 170 g (850 kg.ha^{-1}) of CO_2 in WW and WS, respectively, and transpired approximately 51 L (255,000 L.ha^{-1}) and 28 L (140,000 L.ha^{-1}) of water in WW and WS, respectively. In Cycle 3, each plant assimilated

approximately 282 g (1,410 kg.ha^{-1}) and 129 g (645 kg.ha^{-1}) of CO_2 in WW and WS, respectively, and transpired approximately 63 L (315,000 L.ha^{-1}) and 28 L (140,000 L,ha^{-1}) of water in WW and WS, respectively.

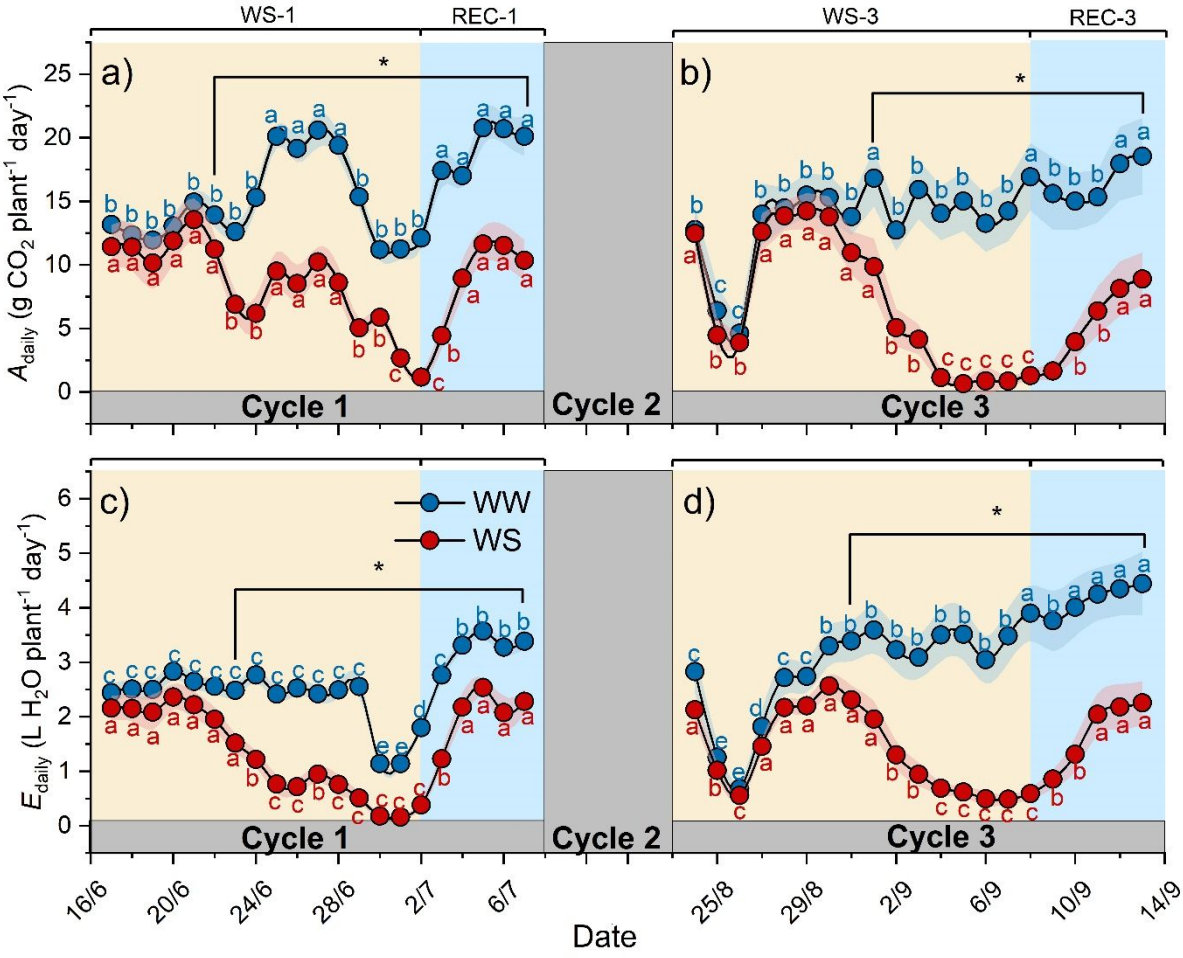

Figure 13: Whole-canopy gas exchange in *C. canephora* clone LB1 subjected to three recurrent cycles of soil drying and rewetting in a greenhouse. a) Daily canopy photosynthetic assimilation (A_{daily}, g CO_2.plant^{-1}.day^{-1}) during Cycle 1 and b) during Cycle 3 of soil drying and rewetting. c) Daily canopy transpiration (E_{daily}, L H_2O.plant^{-1}.day^{-1}) during Cycle 1 and d) during Cycle 3 of soil drying and rewetting. Each Cycle lasted 21 days, with 16 days of drying (WS-1 and WS-3, indicated by the yellow background) and 5 days of soil rewetting (REC-1 and REC-3, indicated by the blue background). In the figures, blue symbols represent the irrigated condition (WW), and red symbols represent the non-irrigated condition (WS). Lowercase letters indicate significant differences over time for each water condition (blue for WW and red for WS), grouped by the Scott-Knott test (P-value < 0.05). Days marked below the bracket or with an asterisk superscript indicate significant differences between the

water conditions for each measurement day, compared using Tukey's test (P-value < 0.05). Each symbol represents the mean ± shaded area of eight plants (n = 8).

The linear regressions plotted between A_{daily} and E_{daily} [water use efficiency, WUE (g CO_2.L H_2O^{-1})] for Cycles 1 (Figure 14a) and 3 (Figure 14b) are shown, as well as the regressions plotted between E_{daily} and A_{daily} [water footprint, WFP (L H_2O. g CO_2^{-1})] for Cycles 1 (Figure 14c) and 3 (Figure 14d). It is observed that in all cases, except for WUE in the WS treatment during Cycle 1 (Figure 14a), the fitting degree of the regression lines was greater than 50% (R^2 > 0.50), and Pearson's correlation coefficient was greater than 0.60 in all cases. For WUE, in Cycle 1, the slopes of the regression lines were 3.36 for WW and 4.14 for WS (Figure 14a); in Cycle 3, the slopes were 3.54 and 6.06 for WW and WS, respectively (Figure 14b). When considering WFP, in Cycle 1, the slopes of the regression lines were 0.17 for WW and 0.14 for WS; in Cycle 3, the slopes were 0.24 and 0.13 for WW and WS, respectively.

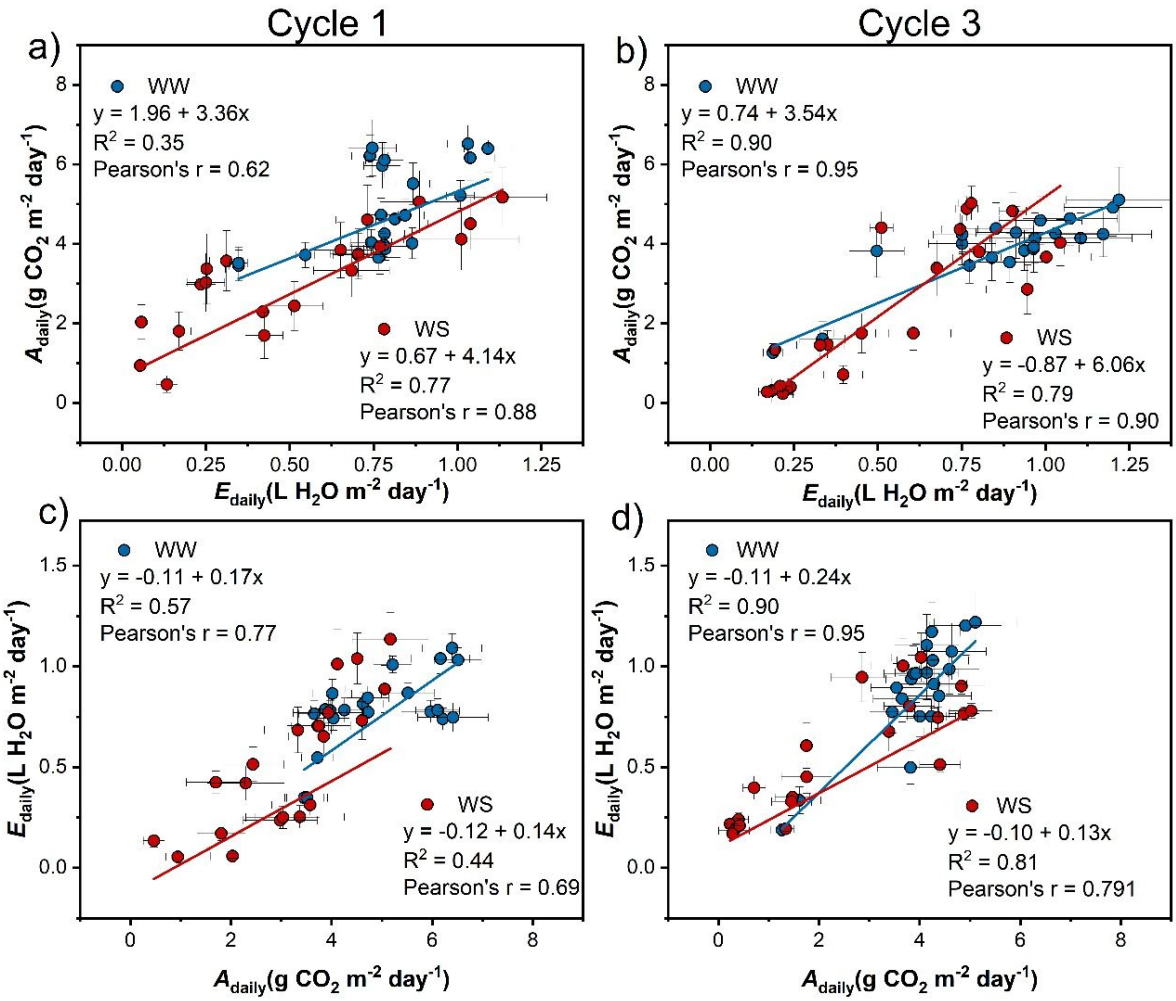

Figure 14: Linear regressions plotted between A_{daily} and E_{daily} (WUE, g CO_2.L H_2O^{-1}) and E_{daily} and A_{daily} (WFP, L H_2O.g CO_2^{-1}) for Cycles 1 and 3 of soil drying and rewetting. In the figures, the equation, the coefficient of determination (R^2), and Pearson's correlation coefficient (r) of the regression lines are shown for the irrigated (WW, in blue) and non-irrigated (WS, in red) conditions, for a) WUE in Cycle 1, b) WUE in Cycle 3, c) WFP in Cycle 1, and d) WFP in Cycle 3. Each symbol represents the mean of eight plants (n = 8), and the horizontal and vertical bars indicate the standard error of the x and y axes, respectively.

The results for biometrics and biomass measured at the end of the experiment are shown in Table 1. It is observed that the variables height, diameter, PBDM, and OBDM were unaffected by the treatments (Table S7; Supplementary data B). However, the number of leaves, leaf area, LDM, and TDM were significantly impacted by the treatments (Table S7; Supplementary data B). In WS, there was a reduction of 41%, 50%, 48%, and 31%, respectively, for these variables.

Table 1: Comparison of means using Tukey's test (P-value < 0.05) for biometric and biomass variables measured at the end of the cultivation of *C. canephora* clone LB1 in a greenhouse under irrigated (WW) and non-irrigated (WS) conditions. Biometric variables: height, diameter, number of leaves, and leaf area. Final biomass variables: leaf dry mass (LDM), plagiotropic branch dry mass (PBDM), orthotropic branch dry mass (OBDM), and total dry mass (TDM).

Treatment	Biometry			
	Height (cm)	Diameter (cm)	Leaf number	Leaf area (m^2)
WW	103.63 ± 3.63 a	20.06 ± 0.47 a	801.75 ± 45.15 a (100%)	4.16 ± 0.26 a (100%)
WS	96.5 ± 3.07 a	20.00 ± 0.55 a	472.5 ± 32.04 b (- 41%)	2.07 ± 0.19 b (- 50%)
Treatment	**Biomass**			
	LDM (g)	PBDM (g)	OBDM (g)	TDM (g)
WW	431.57 ± 26.61 a (100%)	225.87 ± 15.77 a	184.37 ± 12.29 a	841.81 ± 50.00 a (100%)
WS	227.23 ± 21.04 b (- 47%)	199.64 ± 9.07 a	154.22 ± 9.94 a	581.09 ± 28.16 b (- 31%)

Means followed by the same lowercase letter between treatments do not show a significant difference according to Tukey's test at a 5% probability level. The value in parentheses indicates the percentage reduction of WS relative to WW when there was a significant difference.

Discussion

Relations between diurnal trends in micrometeorological variables and whole-canopy gas exchange

Variations in micrometeorological variables across different measurement environments are expected (Figure 2), primarily due to the absorbance/transmittance properties of the greenhouse covering material (Holcman et al., 2015) and the gas exchange measurement chambers (Baker et al., 2014). As observed, a significant portion of the incident PPFD outside the greenhouse was intercepted by the plastic cover (30%), with an additional 15% interception by the measurement chamber. This resulted in an average maximum PPFD of 600 $\mu mol.m^{-2}.s^{-1}$ reaching the plants throughout the experimental period, considering both clear and cloudy days (Figure 2a). Previous studies have reported reductions in PPFD ranging from 13% (Baker et al., 2014) to 19% (Burkart et al., 2007) in open-system measurement chambers. Under the experimental conditions of this study, maximum PPFD values between 500 and 1000 $\mu mol.m^{-2}.s^{-1}$ appeared sufficiently high to achieve light-saturated

photosynthetic rates (*A*c) (Figure 4a). Earlier studies on *C. arabica* and *C. canephora* have shown that *A*c becomes saturated at PPFD levels above 400 $\mu mol.m^{-2}.s^{-1}$ (Rodrigues et al., 2016).

Air temperature across different environments did not exhibit significant differences that would impact whole-canopy gas exchange, as also demonstrated by Rodrigues et al. (2016). This response underscores the importance of maintaining a relatively high airflow rate through the chambers, enabling the plants' transpiration rate to sustain latent heat removal from the chambers (Baker et al., 2014) and maintaining a low ΔT_a (temperature difference between the inside and outside of the chamber; °C) (Peña and Tarara, 2004). Studies have shown that the minimum airflow rate should ideally be 3.2 $m^3.min^{-1}$ (Garcia et al., 1990) and that a gradual increase of 1 $m^3.min^{-1}$ in airflow can reduce the internal chamber temperature by up to 0.4°C (Burkart et al., 2007). Although no significant differences were observed for temperature, variations in relative humidity (RH) (Figure 2c) and vapor pressure deficit (VPD_{air}) (Figure 2d) were noted, primarily due to the plants' transpiration response during the experiment. Water-stressed (WS) chambers exhibited lower RH and, consequently, higher VPD_{air}, due to reduced plant transpiration during periods of higher stress. In well-watered (WW) chambers, higher RH and lower VPD_{air} were observed, driven by the plants' higher transpiration rates during peak demand periods (from 12:00 to 14:00). Similar results were reported in a study on whole-canopy gas exchange in *Quercus ilex* L., where Ψ_{pd} decreased from -0.2 MPa to -1.8 MPa (Sancho-Knapik et al., 2022).

As expected, whole-canopy gas exchange responded strongly to micrometeorological variables, particularly PPFD and air temperature (Figure 4), exhibiting a bell-shaped curve throughout the day (Figure 3). This trend of a stronger correlation between gas exchange and PPFD/air temperature, and a weaker correlation with VPD_{ar}, has also been reported in studies on whole-canopy gas exchange in wheat and sugar beet (Burkart et al., 2007). During the experiment, despite showing the same diurnal trend, lower A_C and E_C values were observed in WS during Cycles 1 and 3, corresponding to days of higher plant stress. The same diurnal trend in A_C and E_C under irrigated conditions was also observed by Rodrigues et al. (2016) in *C. arabica* and *C. canephora*, with *C. canephora* exhibiting maximum E_C values between 1 and 2 $mmol.m^{-2}.s^{-1}$, consistent with the values observed in the current study. However, for A_C, Rodrigues et al. (2016) reported maximum values of

2.5 μmol.m^{-2}.s^{-1} in *C. canephora*, whereas this study recorded A_C values between 5 and 7 μmol.m^{-2}.s^{-1}, aligning with estimates from 3D architectural models of juvenile *C. canephora* clones (Rakocevic et al., 2023).

The declining trend in canopy conductance (g_C) throughout the day, unlike the bell-shaped curve observed for A_C and E_C, is also expected (Tarara and Perez Peña, 2015; Rodrigues et al., 2016; Sancho-Knapik et al., 2022). This occurs because high transpiration rates are observed in the morning, driven primarily by increasing PPFD, even under low VPD_{air}. As the day progresses, transpiration rates tend to increase under high PPFD and VPD_{air}. By late afternoon, the reduction in PPFD decreases the plant's transpiration rate, despite relatively higher VPD_{air} compared to morning values (Sancho-Knapik et al., 2022). Since g_C is strongly coupled to stomatal conductance (g_s) in response to VPD_{air} (Sancho-Knapik et al., 2022), the decline in g_s throughout the day (Suwannarut et al., 2023) and in response to increasing VPD_{air} (Sancho-Knapik et al., 2022) results in reduced g_C and, consequently, lower A_C and E_C. Under irrigated conditions, the coupling of g_C with atmospheric variables, particularly VPD_{air}, tends to be stronger than under non-irrigated conditions (Tarara and Perez Peña, 2015), explaining the reduction of g_C in WS.

Seasonal responses of gas exchange at single-leaf and whole-canopy scales

On average, the leaf gas exchange measurements of well-watered (WW) plants taken in the morning (Figure 5) showed reductions of approximately 20%, 35%, and 5% in net photosynthesis (A_{net}), transpiration (E), and stomatal conductance (g_s), respectively, during Cycle 3 compared to Cycle 1. When measured at midday (Figure 6), reductions of 35% and 20% were observed in A_{net} and g_s, respectively, while E increased by 15%. The use of different leaves in each cycle may explain these differences, particularly due to the lower content of photosynthetic pigments (data not shown) in the leaves used during Cycle 3 measurements. This reduction in pigments is associated with nitrogen accumulation in the leaves, directly impacting their photosynthetic capacity (Netto et al., 2005; Reis et al., 2009). Additionally, minor changes in the growth conditions of these leaves can affect their morphoanatomical structure and, consequently, their gas exchange capacity (Matos et al., 2009). The leaves measured in Cycle 1 grew in an environment with

approximately 15% higher PPFD availability and 12% higher VPD_{air} compared to those used in Cycle 3, which grew inside the measurement chambers.

When examining the leaf gas exchange of water-stressed (WS) plants measured in the morning, a reduction in A_{net} during WS-1 was observed six days after irrigation was suspended, whereas, in WS-3, this reduction occurred only after eight days. This slower decline in A_{net} in WS-3 compared to WS-1 may be related to a slower decrease in soil water potential (Ψ_{mSoil}), due to leaf shedding during preceding stress cycles (Dietze and Matthes, 2014; George-Jaeggli et al., 2017) and, consequently, a delayed sensitivity of plants to water stress (Ferreira et al., 2015). Furthermore, the occurrence of previous water stress cycles may trigger physiological adjustments in *C. canephora* leaves that mitigate the initial impacts of water stress (Menezes-Silva et al., 2017). These adjustments may be linked to a form of stress memory (Guedes et al., 2018), enabling the maintenance of stable photosynthetic rates for longer periods (Demicheli et al., 2023; Wang et al., 2023). However, after sixteen days of water deficit in WS-3, A_{net} experienced a greater reduction compared to WS-1, and the recovery capacity of A_{net} after soil rehydration in REC-1 was higher than in REC-3. These results suggest that, despite the slower decline in A_{net} in WS-3, the severe progression of soil water deficit may cause extensive damage to the photosynthetic capacity of these plants, even when stress memory mechanisms are activated under moderate water deficit conditions (Xu et al., 2010). Additionally, when measured at midday (Figure 6), the intense reduction in A_{net} in WS-3 compared to WS-1 may indicate greater sensitivity of leaf photosynthesis under more critical stress conditions, despite the presence of physiological adjustment mechanisms.

The reduction of E in WS-3 after irrigation suspension in WS plants occurred more slowly when compared to WS-1, and after soil rewetting in REC-1, complete recovery of E was observed in WS plants, but in REC-3, this recovery was less pronounced. These results indicate that during the first cycle of severe water stress, leaves exhibit mechanisms that enable the recovery of transpiration rates after irrigation is resumed. Interestingly, during WS-1 and at midday, WS plants did not fully recover E, even after five days of soil rehydration, whereas in WS-3, this recovery occurred after three days of rehydration. After two successive cycles of severe water stress, leaves grown under these conditions exhibit tolerance mechanisms to mitigate the initial decline in transpiration under moderate stress.

After irrigation is resumed, these leaves demonstrate a greater capacity to recover transpiration rates, particularly during peak demand periods. This ability to recover transpiration after recurrent drought events may indicate improved stomatal control (Thom et al., 2022), which is favorable for plant rehydration. However, the cumulative effects of recurrent water stress must be considered, especially after extreme drought events, as this recovery capacity is directly related to previously stored energy reserves (Ruehr et al., 2019).

As expected, the observed reductions in A_{net} and E, particularly in WS-1 and WS-3 plants under water deficit, are intrinsically related to stomatal closure, as evidenced by the responses of g_s (Figures 5e, 5f, 6e, and 6f). Previous studies have shown that leaf gas exchange in *Coffea* ssp. under moderate water deficit is more limited by stomatal and diffusional factors than by photochemical and biochemical limitations (Semedo et al., 2021; Merga and Beksisa, 2023; Baroni et al., 2024). This response occurs because soil water limitation restricts root water uptake (Silva et al., 2019; Fernandes et al., 2021) and, consequently, the maintenance of leaf turgor and guard cell function, due to reduced leaf water potential (Thioune et al., 2020; Rodrigues et al., 2024). This reduces stomatal aperture, decreasing water loss through the leaves (E) and, particularly, carbon assimilation (A_{net}) (Dubberstein et al., 2020; Baroni et al., 2024). Additionally, the reduction in g_s may result from the synthesis of abscisic acid (ABA) in leaves and roots (Semedo et al., 2021), signaling water stress and inducing stomatal closure to limit water loss (Almeida et al., 2021; Liu et al., 2022). Finally, the reduced capacity for g_s recovery after recurrent drought events may be associated with a more conservative water-use strategy, which can limit the full recovery of A_{net} (Liu et al., 2022).

Although there was a correlation, albeit weak, between leaf-level and whole-canopy gas exchange data (Figure 10), it is evident that leaf-level measurements (A_{net} and E) were overestimated compared to whole-canopy measurements (A_C and E_C). This overestimation typically occurs due to significant light variations within the canopy, branch angle, and differences in leaf age, as very young or senescent leaves contribute to higher respiratory rates (Tarara et al., 2011; Tarara and Perez Peña, 2015; Rodrigues et al., 2016). Therefore, leaf-level gas exchange data should be interpreted cautiously when extrapolated to the whole canopy.

Seasonal responses of whole-canopy gas exchanges

When analyzing whole-canopy gas exchange in response to soil water deficit progression (Figure 7), a decline in $A_{C\text{-}max}$ and $E_{C\text{-}max}$ was observed six days after irrigation suspension in WS-1 and eight days in WS-3. This reduction follows a pattern like that observed in leaf-level gas exchange measurements. However, unlike leaf-level gas exchange, $A_{C\text{-}max}$ showed full recovery after soil rewetting in REC-1 and REC-3. Nonetheless, the recovery of both $A_{C\text{-}max}$ and $E_{C\text{-}max}$ was slower in WS-3. It can be assumed that the greater difficulty in recovering leaf-level gas exchange, particularly A_{net}, compared to whole-canopy gas exchange was primarily due to damage caused by direct solar radiation on the leaves, influenced by their position and exposure within the canopy (DaMatta and Ramalho, 2006; Sanda et al., 2011; Wang and Wen, 2022). Additionally, the continuous use of leaf chambers on already stressed leaves may have increased these photosynthetic limitations. Despite the observed differences in $A_{C\text{-}max}$ and $E_{C\text{-}max}$, R_{dark} did not appear to be affected by water stress, with values like those reported for *C. arabica* (Rodrigues et al., 2016).

In the relation between $A_{C\text{-}max}$ and $E_{C\text{-}max}$ (Figure 8), where the slope of the regression line is associated with WUE, the data showed that in both Cycle 1 and Cycle 3, water stress increased WUE. Under irrigated conditions (WW), WUE values were 1.65 µmol CO_2.mmol H_2O^{-1} and 1.69 µmol CO_2.mmol H_2O^{-1} for Cycles 1 and 3, respectively, which are comparable to those reported by Rodrigues et al. (2016) during spring and summer under irrigated conditions. Under non-irrigated conditions (WS) in Cycle 3, WUE was approximately 20% higher (3.85 µmol CO_2.mmol H_2O^{-1}) than in Cycle 1 (3.12 µmol CO_2.mmol$^{-}H_2O^{1}$). This increase in WUE may indicate physiological (Liu et al., 2010; Zheng et al., 2017), anatomical (Kulkarni et al., 2008), and hydraulic (Gebhardt et al., 2023) adjustments developed by the plants in response to previous stress cycles, aimed at optimizing CO_2 assimilation while minimizing water loss. The increase in WUE among coffee genotypes is strongly associated with stomatal sensitivity, as genotypes with higher stomatal sensitivity regulate water loss more effectively, leading to improved long-term WUE (Pinheiro et al., 2005; DaMatta and Ramalho, 2006).

When correlating the decline in $A_{C\text{-}max}$ and $E_{C\text{-}max}$ with the reduction in Ψ_{mSoil} (Figure 9), the results showed that in WS-3, plants reached lower $A_{C\text{-}max}$ and $E_{C\text{-}max}$ values at higher (less negative) Ψ_{mSoil} levels compared to WS-1. This suggests

increased plant sensitivity following recurrent drought stress cycles. The reduction in transpiration in response to Ψ_{Soil} can result from either a low or high plant-to-root hydraulic conductance ratio, both of which can lead to extensive hydraulic failure (Koehler et al., 2023). The greater the hydraulic resistance of the soil or plant, the higher the risk of hydraulic failure (Koehler et al., 2023). However, stomatal closure and the consequent reduction in g_C can limit water loss through transpiration, alleviating hydraulic tension and promoting greater soil water conservation (Simonneau et al., 2017). Possible explanations for the greater decline in $A_{C\text{-}max}$ and $E_{C\text{-}max}$ during Cycle 3 are as follows: (1) Leaf shedding in response to previous drought stress cycles reduced plant water loss (Figure 13) and soil drying capacity, resulting in the maintenance of Ψ_{mSoil} at higher values; and (2) severe drought stress cycles in coffee plants may trigger a series of hydraulic failures from which plants cannot fully recover, making them more sensitive to future water deficits.

The reduction in $A_{C\text{-}max}$ and $E_{C\text{-}max}$ values consequently led to a decrease in the area under the curve used to calculate A_{daily} and E_{daily} (Figure 12). Therefore, the same pattern of decline and recovery in A_{daily} and E_{daily} ($g.m^{-2}.day^{-1}$ and $L.m^{-2}.day^{-1}$, respectively) was observed in WS-1 and WS-3 when normalized by leaf surface area. However, when A_{daily} and E_{daily} were normalized per plant ($g.plant^{-1}.day^{-1}$ and $L.plant^{-1}.day^{-1}$, respectively) (Figure 13), observations showed that even after soil rewetting in REC-1 and REC-3, the recovery of A_{daily} and E_{daily} was compromised due to the intense reduction in leaf area caused by previous drought stress cycles. This leaf shedding is a typical response of coffee plants under severe water deficit (Venancio et al., 2020; De Souza et al., 2025), leading to a reduction in leaf area and light interception capacity (Alam et al., 2021), which consequently limits carbon assimilation (Schickling et al., 2010) and decreases canopy water loss (Schickling et al., 2010; Jin et al., 2018). Based on these data, it is estimated that over 21 days in Cycle 1, WS plants assimilated approximately 45% less CO_2 while reducing water loss by 44% compared to WW plants. In Cycle 3, WS plants showed a 55% reduction in both CO_2 assimilation and water loss.

Despite the greater reduction in A_{daily} and E_{daily} during Cycle 3, there was an increase in WUE (Figure 14b) and a consequent decrease in WFP (Figure 14d) under these conditions. Additionally, it is important to consider that at the beginning of WS-3, A_{daily} and E_{daily} were similar between both treatments (WW and WS), even though the leaf area in WS was 25% lower compared to WW. Similar results were

reported in grapevines, where a 27% reduction in leaf area did not lead to a decrease in assimilation (Intrieri et al., 1997). Even when a sudden decline in A_C occurs due to reduced leaf area, recovery may take place after a few weeks, either through the growth of new leaves (Thomas et al., 2006) or by increasing light availability within the canopy, which compensates for the effects of reduced leaf area (Han, 2012), thereby optimizing assimilation per unit of leaf area (Petrie et al., 2003). As previously observed, these responses may indicate strategies developed by plants subjected to recurrent cycles of water deficit to optimize carbon gain at the expense of water loss, particularly during the initial stages of drought stress imposition.

As observed, leaf abscission in response to water stress (Venancio et al., 2020; Borgo et al., 2024; De Souza et al., 2025), confirmed by the reduction in leaf number and leaf area (Table 1), had a direct impact on whole-canopy gas exchange. Additionally, it led to a decrease in final biomass, particularly due to the reduction in leaf biomass (Table 1). Leaf shedding in tropical forests is often considered an adaptive strategy under water stress conditions, as the loss of older leaves can minimize the plant's energy costs and prevent hydraulic failure (Wu et al., 2021). Furthermore, the retention of younger leaves may optimize light acquisition and carbon gain (Wu et al., 2021), thereby increasing water use efficiency. However, further studies on *Coffea* spp. genotypes are needed to understand whether the dynamics of leaf abscission in response to water deficits specifically is the result of greater genotype sensitivity or whether it acts as a water conservation strategy for plant survival. Due to the short duration of the experiment, no significant impacts on plant growth were observed. However, evidence indicates that prolonged exposure of these plants to reduced leaf area would impact shoot growth (Rakocevic et al., 2022; 2024; Silva et al., 2022) and, ultimately, plant productivity (DaMatta and Ramalho, 2006).

Conclusions

In this study, it was observed that gas exchange measurements in whole *C. canephora* plants using an open multi-chamber system are strongly coupled with the micrometeorological conditions within the cultivation environment, confirming the hypothesis (3). PPFD and temperature were the variables that were most correlated

with canopy net photosynthetic assimilation (A_C) and canopy transpiration rate (E_C), with E_C also being affected by VPD_{air}.

The gas exchanges at both leaf and canopy levels were significantly impacted by the recurring cycles of soil drying and rewetting. During the third drying cycle (WS-3), photosynthesis (A_{net} and A_C), transpiration (E and E_C), and stomatal conductance (g_s) declined more gradually during the initial soil drying phase. However, after reaching peak stress, these variables were more severely affected in WS-3, compromising their full recovery following the third soil rewetting cycle (REC-3). Furthermore, confirming hypothesis (1), single-leaf gas exchanges (A_{net} and E) always presented higher values than those observed in whole-canopy ($A_{C\text{-}max}$ and $E_{C\text{-}max}$), which confirms that the values measured in single leaves are generally overestimated in relation to whole-canopy. However, despite this difference in values between the two measurement techniques, the reduction and recovery trends of the leaf- and whole-canopy gas exchange were similar, opposing the hypothesis (2).

Whole-canopy gas exchange, when expressed per unit leaf area [$_{A}A_{daily}$ (g $CO_2.m^{-2}.day^{-1}$) and E_{daily} (L $H_2O.m^{-2}.day^{-1}$)], exhibited full recovery even after three cycles of water stress. However, when analyzed on a per-plant basis [A_{daily} (g $CO_2.plant^{-1}.day^{-1}$) and E_{daily} (L $H_2O.plant^{-1}.day^{-1}$)], the initial recovery of these variables was significantly impacted by leaf shedding and a reduction in total leaf area per plant.

The reduction in leaf area due to severe water deficit strongly affects carbon gain, water loss, and biomass accumulation by plants. However, even after two consecutive cycles of water stress and with an approximately 25% reduction in leaf area, *C. canephora* plants subjected to water deficit displayed compensatory adjustments that enabled them to maintain whole-canopy gas exchange rates like those of non-stressed plants.

After three cycles of water stress, *C. canephora* plants exhibited higher water use efficiency (WUE, μmol $CO_2.mmol\ H_2O^{-1}$ and g $CO_2.L\ H_2O^{-1}$) and consequently a lower water footprint (WFP, mmol $H_2O.\mu mol\ CO_2^{-1}$, and L $H_2O.g\ CO_2^{-1}$) compared to those that were never stressed or experienced only a single cycle of water deficit.

Based on the results observed in this work, the gas exchange measurements using a multi-chamber system for the whole canopy allow for a more complex interpretation of the dynamic responses caused by water deficit, especially due to the reduction in the leaf area of coffee plants, confirming the hypothesis (4).

References

Alam, M. S., Lamb, D. W., Warwick, N. W. M. (2021). A Canopy Transpiration Model Based on Scaling Up Stomatal Conductance and Radiation Interception as Affected by Leaf Area Index. *Water*, *13*(3), 252. https://doi.org/10.3390/w13030252

Almeida, W. L., Ávila, R. T., Pérez-Molina, J. P., Barbosa, M. L., Marçal, D. M. S., De Souza, R. P. B., Martino, P. B., Cardoso, A. A., Martins, S. C. V., DaMatta, F. M. (2021). The Interplay Between Irrigation and Fruiting on Branch Growth and Mortality, Gas Exchange and Water Relations of Coffee Trees. *Tree Physiology*, *41*(1), 35–49. https://doi.org/10.1093/treephys/tpaa116

Avila, R. T., Cardoso, A. A., De Almeida, W. L., Costa, L. C., Machado, K. L. G., Barbosa, M. L., De Souza, R. P. B., Oliveira, L. A., Batista, D. S., Martins, S. C. V., Ramalho, J. D. C., DaMatta, F. M. (2020). Coffee Plants Respond to Drought and Elevated [CO_2] Through Changes in Stomatal Function, Plant Hydraulic Conductance, and Aquaporin Expression. *Environmental and Experimental Botany*, *177*, 104148. https://doi.org/10.1016/j.envexpbot.2020.104148

Baker, J. T., Gitz III, D. C., Lascano, R. J. (2014). Field Evaluation of Open System Chambers for Measuring Whole Canopy Gas Exchanges. *Agronomy Journal*, *106*(2), 537–544. https://doi.org/10.2134/agronj2013.0449

Baroni, D. F., De Souza, G. A. R., Bernado, W. D. P., Santos, A. R., Barcellos, L. C. D. S., Barcelos, L. F. T., Correia, L. Z., De Almeida, C. M., Verdin Filho, A. C., Rodrigues, W. P., Ramalho, J. C., Rakočević, M., Campostrini, E. (2024). Stomatal and Non-Stomatal Leaf Responses during Two Sequential Water Stress Cycles in Young *Coffea canephora* Plants. *Stresses*, *4*(3), 575–597. https://doi.org/10.3390/stresses4030037

Bilen, C., El Chami, D., Mereu, V., Trabucco, A., Marras, S., Spano, D. (2022). A Systematic Review on the Impacts of Climate Change on Coffee Agrosystems. *Plants*, *12*(1), 102. https://doi.org/10.3390/plants12010102

Borgo, L., Rabêlo, F. H. S., Marchiori, P. E. R., Guilherme, L. R. G., Guerra-Guimarães, L., Resende, M. L. V. D. (2024). Impact of Drought, Heat, Excess Light, and Salinity on Coffee Production: Strategies for Mitigating Stress Through Plant Breeding and Nutrition. *Agriculture*, *15*(1), 9. https://doi.org/10.3390/agriculture15010009

Bracken, P., Burgess, P. J., Girkin, N. T. (2023). Opportunities for Enhancing the Climate Resilience of Coffee Production Through Improved Crop, Soil and Water Management. *Agroecology and Sustainable Food Systems*, *47*(8), 1125–1157. https://doi.org/10.1080/21683565.2023.2225438

Burkart, S., Manderscheid, R., Weigel, H.-J. (2007). Design and Performance of a Portable Gas Exchange Chamber System for CO_2-and H_2O-Flux Measurements in Crop Canopies. *Environmental and Experimental Botany*, *61*(1), 25–34. https://doi.org/10.1016/j.envexpbot.2007.02.007

Byrareddy, V., Kouadio, L., Mushtaq, S., Kath, J., Stone, R. (2021). Coping With Drought: Lessons Learned From Robusta Coffee Growers in Vietnam. *Climate Services*, *22*, 100229. https://doi.org/10.1016/j.cliser.2021.100229

Campbell, G. S., Norman, J. M. (1998). *An Introduction to Environmental Biophysics*. Springer New York. https://doi.org/10.1007/978-1-4612-1626-1

aaMatta, F. M., Ramalho, J. D. C. (2006). Impacts of Drought and Temperature Stress on Coffee Physiology and Production: A review. *Brazilian Journal of Plant Physiology*, *18*(1), 55–81. https://doi.org/10.1590/S1677-04202006000100006

De Freitas, C. H., Coelho, R. D., De Oliveira Costa, J., Sentelhas, P. C. (2024). A Bitter Cup of Coffee? Assessing the Impact of Climate Change on Arabica

Coffee Production in Brazil. *Science of The Total Environment*, *957*, 177546. https://doi.org/10.1016/j.scitotenv.2024.177546

De Souza, G. A. R., Baroni, D. F., Bernado, W. D. P., Santos, A. R., Barcellos, L. C. D. S., Barcelos, L. F. T., Correia, L. Z., De Almeida, C. M., Verdin Filho, A. C., Rodrigues, W. P., Ramalho, J. C., Rakočević, M., Campostrini, E. (2025). Leaf to Root Morphological and Anatomical Indicators of Drought Resistance in *Coffea canephora* After Two Stress Cycles. *Agriculture*, *15*(6), 574. https://doi.org/10.3390/agriculture15060574

Demicheli, J., Sabljic, I., Beguy, G., Ploschuk, E., Sahrawy, M., Serrato, A. J., Pagano, E. A. (2023). Improving Drought Tolerance in Soybean by Classical Breeding Leads to Physiological Adjustments of Photosynthesis and Stomata Functioning. *Plant Stress*, *10*, 100275. https://doi.org/10.1016/j.stress.2023.100275

Dias, C. G., Martins, F. B., Martins, M. A. (2024). Climate Risks and Vulnerabilities of the Arabica Coffee in Brazil Under Current and Future Climates Considering New CMIP6 Models. *Science of The Total Environment*, *907*, 167753. https://doi.org/10.1016/j.scitotenv.2023.167753

Dietze, M. C., Matthes, J. H. (2014). A General Ecophysiological Framework for Modelling the Impact of Pests and Pathogens on Forest Ecosystems. *Ecology Letters*, *17*(11), 1418–1426. https://doi.org/10.1111/ele.12345

Dubberstein, D., Lidon, F. C., Rodrigues, A. P., Semedo, J. N., Marques, I., Rodrigues, W. P., Gouveia, D., Armengaud, J., Semedo, M. C., Martins, S., Simões-Costa, M. C., Moura, I., Pais, I. P., Scotti-Campos, P., Partelli, F. L., Campostrini, E., Ribeiro-Barros, A. I., DaMatta, F. M., Ramalho, J. C. (2020). Resilient and Sensitive Key Points of the Photosynthetic Machinery of *Coffea* spp. To the Single and Superimposed Exposure to Severe Drought and Heat Stresses. *Frontiers in Plant Science*, *11*, 1049. https://doi.org/10.3389/fpls.2020.01049

Dubberstein, D., Rodrigues, W. P., Semedo, J. N., Rodrigues, A. P., Pais, I. P., Leitão, A. E., Partelli, F. L., Campostrini, E., Reboredo, F., Scotti-Campos, P., Lidon, F. C., Ribeiro-Barros, A. I., DaMatta, F. M., Ramalho, J. C. (2018). Mitigation of the Negative Impact of Warming on the Coffee Crop: The Role of Increased Air [CO_2] and Management Strategies. In *Climate Resilient Agriculture—Strategies and Perspectives*. InTech. https://doi.org/10.5772/intechopen.72374

Ebisa, D. B. (2017). Impacts of Climate Change on Global Coffee Production Industry: Review. *African Journal of Agricultural Research*, *12*(19), 1607–1611. https://doi.org/10.5897/AJAR2017.12147

Fernandes, I., Marques, I., Paulo, O. S., Batista, D., Partelli, F. L., Lidon, F. C., DaMatta, F. M., Ramalho, J. C., Ribeiro-Barros, A. I. (2021). Understanding the Impact of Drought in *Coffea* Genotypes: Transcriptomic Analysis Supports a Common High Resilience to Moderate Water Deficit but a Genotype Dependent Sensitivity to Severe Water Deficit. *Agronomy*, *11*(11), 2255. https://doi.org/10.3390/agronomy11112255

Ferrão, R. G., Fonseca, A. F. A. da, Ferrão, M. A. G., De Muner, L. H. (2017). *Café Conilon*. Instituto Capixaba de Pesquisa Assistência Técnica e Extensão Rural–INCAPER.

Ferraz, T. M., Rodrigues, W. P., Netto, A. T., de Oliveira Reis, F., Peçanha, A. L., de Assis, F. A. M. M., de Sousa, E. F., Glenn, D. M., Campostrini, E. (2016). Comparison Between Single-Leaf and Whole-Canopy Gas Exchange Measurements in Papaya (*Carica papaya* L.) Plants. *Scientia Horticulturae*, *209*, 73–78. https://doi.org/10.1016/j.scienta.2016.06.014

Ferreira, W. N., Lacerda, C. F. D., Costa, R. C. D., Medeiros Filho, S. (2015). Effect of Water Stress on Seedling Growth in Two Species With Different Abundances: The Importance of Stress Resistance Syndrome in Seasonally Dry Tropical Forest. *Acta Botanica Brasilica*, *29*(3), 375–382. https://doi.org/10.1590/0102-33062014abb0045

Garcia, R. L., Norman, J. M., McDermitt, D. K. (1990). Measurements of Canopy Gas Exchange Using an Open Chamber System. *Remote Sensing Reviews*, *5*(1), 141–162. https://doi.org/10.1080/02757259009532126

Gebhardt, T., Hesse, B. D., Hikino, K., Kolovrat, K., Hafner, B. D., Grams, T. E. E., Häberle, K.-H. (2023). Repeated Summer Drought Changes the Radial Xylem Sap Flow Profile in Mature Norway Spruce but Not in European Beech. *Agricultural and Forest Meteorology*, *329*, 109285. https://doi.org/10.1016/j.agrformet.2022.109285

George-Jaeggli, B., Mortlock, M. Y., Borrell, A. K. (2017). Bigger is Not Always Better: Reducing Leaf Area Helps Stay-Green Sorghum Use Soil Water More Slowly. *Environmental and Experimental Botany*, *138*, 119–129. https://doi.org/10.1016/j.envexpbot.2017.03.002

Gil-Gómez, J. A., Florez-Pardo, L. M., Leguizamón-Vargas, Y. C. (2024). Valorization of Coffee By-Products in The Industry, a Vision Towards Circular Economy. *Discover Applied Sciences*, *6*(9), 480. https://doi.org/10.1007/s42452-024-06085-9

Guedes, F. A. D. F., Nobres, P., Rodrigues Ferreira, D. C., Menezes-Silva, P. E., Ribeiro-Alves, M., Correa, R. L., DaMatta, F. M., Alves-Ferreira, M. (2018). Transcriptional Memory Contributes to Drought Tolerance in Coffee (*Coffea canephora*) Plants. *Environmental and Experimental Botany*, *147*, 220–233. https://doi.org/10.1016/j.envexpbot.2017.12.004

Hall, D. O., Scurlock, J., Bolhar-Nordenkampf, H., Leegood, R. C., Long, S. (1993). *Photosynthesis and Production in a Changing Environment: A Field and Laboratory Manual*. Springer Science Business Media.

Han, Q. (2012). Leaf Photosynthetic Responses to Thinning. In *Applied Photosynthesis*. InTech. https://doi.org/10.5772/27455

Holcman, E., Sentelhas, P. C., Mello, S. da C. (2015). Microclimatic Changes Caused by Different Plastic Coverings in Greenhouses Cultivated with Cherry Tomato on Southern Brazil. *Revista Brasileira de meteorologia*, *30*(2), 125–133.

Intrieri, C., Poni, S., Rebucci, B., Magnanini, E. (1997). Effects of Canopy Manipulations on Whole-Vine Photosynthesis: Results From Pot and Field Experiments. *Vitis-Geilweilerhof-*, *36*, 167–174. https://doi.org/10.5073/vitis.1997.36.167-173

Jin, Y., Wang, X., Zhang, Y., Pan, Y., Hu, R. (2018). Extrapolation of Leaf Measurements to Obtain the Whole-Canopy Transpiration of C3 and C4 Xerophytic Shrubs. *Water*, *10*(6), 813. https://doi.org/10.3390/w10060813

Jones, H. G. (1992). *Plants and Microclimate: A Quantitative Approach to Environmental Plant Physiology* (3° ed). Cambridge University Press. https://doi.org/10.1017/CBO9780511845727

Kashyap, S., Agarwala, N., Sunkar, R. (2024). Understanding Plant Stress Memory Traits Can Provide a Way for Sustainable Agriculture. *Plant Science*, *340*, 111954. https://doi.org/10.1016/j.plantsci.2023.111954

Koehler, T., Wankmüller, F. J. P., Sadok, W., Carminati, A. (2023). Transpiration Response to Soil Drying *Versus* Increasing Vapor Pressure Deficit in Crops: Physical and Physiological Mechanisms and Key Plant Traits. *Journal of Experimental Botany*, *74*(16), 4789–4807. https://doi.org/10.1093/jxb/erad221

Leonardos, E. D., Grodzinski, B. (2017). Photosynthesis and Productivity of Vascular Plants in Controlled and Field Environments. In *Comprehensive Biotechnology* (p. 181–195). Elsevier. https://doi.org/10.1016/B978-0-12-809633-8.09199-8

Liu, C.-C., Liu, Y.-G., Guo, K., Zheng, Y.-R., Li, G.-Q., Yu, L.-F., Yang, R. (2010). Influence of Drought Intensity on the Response of Six Woody Karst Species Subjected to Successive Cycles of Drought and Rewatering. *Physiologia Plantarum*, *139*(1), 39–54. https://doi.org/10.1111/j.1399-3054.2009.01341.x

Liu, H., Song, S., Zhang, H., Li, Y., Niu, L., Zhang, J., Wang, W. (2022). Signaling Transduction of ABA, ROS, and Ca^{2+} in Plant Stomatal Closure in Response to Drought. *International Journal of Molecular Sciences*, *23*(23), 14824. https://doi.org/10.3390/ijms232314824

Lorençone, J. A., De Oliveira Aparecido, L. E., Lorençone, P. A., Torsoni, G. B., De Lima, R. F., Da Silva Cabral De Moraes, J. R., De Souza Rolim, G. (2023). Agricultural Zoning of *Coffea arabica* in Brazil for Current and Future Climate Scenarios: Implications for the Coffee Industry. *Environment, Development and Sustainability*, *27*(2), 4143–4166. https://doi.org/10.1007/s10668-023-04066-3

Mannino, G., Kunz, R., Maffei, M. E. (2023). Discrimination Of Green Coffee (*Coffea arabica* and *Coffea canephora*) of Different Geographical Origin Based on Antioxidant Activity, High-Throughput Metabolomics, and DNA RFLP Fingerprinting. *Antioxidants*, *12*(5), 1135. https://doi.org/10.3390/antiox12051135

Martins, S. C. V., Sanglard, M. L., Morais, L. E., Menezes-Silva, P. E., Mauri, R., Avila, R. T., Vital, C. E., Cardoso, A. A., DaMatta, F. M. (2019). How do Coffee Trees Deal with Severe Natural Droughts? An Analysis of Hydraulic, Diffusive and Biochemical Components at the Leaf Level. *Trees*, *33*(6), 1679–1693. https://doi.org/10.1007/s00468-019-01889-4

Marur, C. J., de Faria, R. T. (2007). A Chamber for Measurement of Net Photosynthesis on a Whole Plant. *Acta Scientiarum. Agronomy*, *29*(3), 415–419.

Matos, F. S., Wolfgramm, R., Gonçalves, F. V., Cavatte, P. C., Ventrella, M. C., DaMatta, F. M. (2009). Phenotypic Plasticity in Response to Light in the Coffee Tree. *Environmental and Experimental Botany*, *67*(2), 421–427. https://doi.org/10.1016/j.envexpbot.2009.06.018

Menezes-Silva, P. E., Sanglard, L. M. V. P., Ávila, R. T., Morais, L. E., Martins, S. C. V., Nobres, P., Patreze, C. M., Ferreira, M. A., Araújo, W. L., Fernie, A. R., DaMatta, F. M. (2017). Photosynthetic and Metabolic Acclimation to Repeated Drought Events Play Key Roles in Drought Tolerance in Coffee. *Journal of Experimental Botany*, *68*(15), 4309–4322. https://doi.org/10.1093/jxb/erx211

Merga, D., Beksisa, L. (2023). Mechanisms of Drought Tolerance in Coffee (*Coffea arabica* L.): Implication for Genetic Improvement Program: Review. *American Journal of BioScience*. https://doi.org/10.11648/j.ajbio.20231103.12

Netto, A. T., Campostrini, E., Oliveira, J. G. D., Bressan-Smith, R. E. (2005). Photosynthetic Pigments, Nitrogen, Chlorophyll a Fluorescence and SPAD-502 Readings in Coffee Leaves. *Scientia Horticulturae*, *104*(2), 199–209. https://doi.org/10.1016/j.scienta.2004.08.013

Ngolo, A. O., Fernandes Filho, E. I., Ferreira, W. P. M., Fernandes, R. B. A. (2018). Agroclimatic Zoning for Coffee Crop in Angola. *Pesquisa Agropecuária Tropical*, *48*(1), 19–28. https://doi.org/10.1590/1983-40632018v4850109

Niinemets, Ü. (2016). Leaf Age Dependent Changes in Within-Canopy Variation in Leaf Functional Traits: A Meta-Analysis. *Journal of Plant Research*, *129*(3), 313–338. https://doi.org/10.1007/s10265-016-0815-2

Peña, J. P., Tarara, J. (2004). A Portable Whole Canopy Gas Exchange System for Several Mature Field-Grown Grapevines. *Vitis-Geilweilerhof-*, *43*(1), 7–14. https://doi.org/10.5073/vitis.2004.43.7-14

Petrie, P. R., Trought, M. C. T., Howell, G. S., Buchan, G. D. (2003). The Effect of Leaf Removal and Canopy Height on Whole-Vine Gas Exchange and Fruit Development of *Vitis vinifera* L. Sauvignon Blanc. *Functional Plant Biology*, *30*(6), 711. https://doi.org/10.1071/FP02188

Pinheiro, H. A., DaMatta, F. M., Chaves, A. R. M., Loureiro, M. E., Ducatti, C. (2005). Drought Tolerance is Associated with Rooting Depth and Stomatal Control of

Water Use in Clones of *Coffea canephora*. *Annals of Botany*, *96*(1), 101–108. https://doi.org/10.1093/aob/mci154

Prieto, J. A., Louarn, G., Perez Peña, J., Ojeda, H., Simonneau, T., Lebon, E. (2020). A Functional–Structural Plant Model that Simulates Whole- Canopy Gas Exchange of Grapevine Plants (*Vitis vinifera* L.) Under Different Training Systems. *Annals of Botany*, *126*(4), 647–660. https://doi.org/10.1093/aob/mcz203

Pritzkow, C., Szota, C., Williamson, V., Arndt, S. K. (2021). Previous Drought Exposure Leads to Greater Drought Resistance in Eucalypts Through Changes in Morphology Rather than Physiology. *Tree Physiology*, *41*(7), 1186–1198. https://doi.org/10.1093/treephys/tpaa176

Rakocevic, M., Baroni, D. F., De Souza, G. A. R., Bernado, W. D. P., De Almeida, C. M., Matsunaga, F. T., Rodrigues, W. P., Ramalho, J. C., Campostrini, E. (2023). Correlating *Coffea Canephora* 3D Architecture to Plant Photosynthesis at a Daily Scale and Vegetative Biomass Allocation. *Tree Physiology*, *43*(4), 556–574. https://doi.org/10.1093/treephys/tpac138

Rakocevic, M., Marchiori, P. E. R., Zambrosi, F. C. B., Machado, E. C., Maia, A. D. H. N., Ribeiro, R. V. (2022). High Phosphorus Supply Enhances Leaf Gas Exchange and Growth of Young Arabica Coffee Plants Under Water Deficit. *Experimental Agriculture*, *58*, e30. https://doi.org/10.1017/S0014479722000266

Reis, A. R., Favarin, J. L., Malavolta, E., Júnior, J. L., Moraes, M. F. (2009). Photosynthesis, Chlorophylls, and SPAD Readings in Coffee Leaves in Relation to Nitrogen Supply. *Communications in Soil Science and Plant Analysis*, *40*(9–10), 1512–1528. https://doi.org/10.1080/00103620902820373

Rodrigues, A. P., Pais, I. P., Leitão, A. E., Dubberstein, D., Lidon, F. C., Marques, I., Semedo, J. N., Rakocevic, M., Scotti-Campos, P., Campostrini, E., Rodrigues, W. P., Simões-Costa, M. C., Reboredo, F. H., Partelli, F. L., DaMatta, F. M., Ribeiro-Barros, A. I., Ramalho, J. C. (2024). Uncovering The Wide Protective

Responses in *Coffea* spp. Leaves to Single and Superimposed Exposure of Warming and Severe Water Deficit. *Frontiers in Plant Science*, *14*, 1320552. https://doi.org/10.3389/fpls.2023.1320552

Rodrigues, W. P., Machado Filho, J. A., Da Silva, J. R., De Assis Figueiredo, F. A. M. M., Ferraz, T. M., Ferreira, L. S., Da Silva Bezerra, L. B., De Abreu, D. P., De Paula Bernado, W., Cespom Passos, L., De Sousa, E. F., Glenn, D. M., Ramalho, J. C., Campostrini, E. (2016). Whole-Canopy Gas Exchanges in *Coffea* spp. is Affected by Supra-Optimal Temperature and Light Distribution Within he Canopy: The Insights From an Improved Multi-Chamber System. *Scientia Horticulturae*, *211*, 194–202. https://doi.org/10.1016/j.scienta.2016.08.022

Rowland, L., Ramírez-Valiente, J., Hartley, I. P., Mencuccini, M. (2023). How Woody Plants Adjust Above- and Below-Ground Traits in Response to Sustained Drought. *New Phytologist*, *239*(4), 1173–1189. https://doi.org/10.1111/nph.19000

Ruehr, N. K., Grote, R., Mayr, S., Arneth, A. (2019). Beyond the Extreme: Recovery of Carbon and Water Relations in Woody Plants Following Heat and Drought Stress. *Tree Physiology*, *39*(8), 1285–1299. https://doi.org/10.1093/treephys/tpz032

Salvador, H. P., Berilli, A. P. C. G., Rodrigues, W. P., Mazzafera, P., Partelli, F. L. (2025). A Climate Change Perspective on the Selection, Development, and Management of *Coffea canephora* Genotypes. In *Advances in Botanical Research, 114*, 283–315. Elsevier. https://doi.org/10.1016/bs.abr.2024.04.005

Sancho-Knapik, D., Mendoza-Herrer, Ó., Alonso-Forn, D., Saz, M. Á., Martín-Sánchez, R., Dos Santos Silva, J. V., Ogee, J., Peguero-Pina, J. J., Gil-Pelegrín, E., Ferrio, J. P. (2022). Vapor Pressure Deficit Constrains Transpiration and Photosynthesis in Holm Oak: A Comparison of Three Methods During Summer Drought. *Agricultural and Forest Meteorology*, *327*, 109218. https://doi.org/10.1016/j.agrformet.2022.109218

Sanda, S., Yoshida, K., Kuwano, M., Kawamura, T., Munekage, Y. N., Akashi, K., Yokota, A. (2011). Responses of the Photosynthetic Electron Transport System to Excess Light Energy Caused by Water Deficit in Wild Watermelon. *Physiologia Plantarum*, *142*(3), 247–264. https://doi.org/10.1111/j.1399-3054.2011.01473.x

Sarzynski, T., Vaast, P., Rigal, C., Marraccini, P., Delahaie, B., Georget, F., Nguyen, C. T. Q., Nguyen, H. P., Nguyen, H. T. T., Ngoc, Q. L., Ngan, G. K., Bossolasco, L., Etienne, H. (2024). Contrasted Agronomical and Physiological Responses of Five *Coffea arabica* Genotypes Under Soil Water Deficit in Field Conditions. *Frontiers in Plant Science*, *15*, 1443900. https://doi.org/10.3389/fpls.2024.1443900

Schickling, A., Graf, A., Pieruschka, R., Plückers, C., Geiß, H., Lai, I.-L., Schween, J. H., Erentok, K., Schmidt, M., Wahner, A., Crewell, S., Rascher, U. (2010). The Influence of Leaf Photosynthetic Efficiency and Stomatal Closure on Canopy Carbon Uptake and Evapotranspiration – A Model Study in Wheat and Sugar Beet. *Biogeosciences Discussions*, *7*(5), 7131-7172. https://doi.org/10.5194/bgd-7-7131-2010

Semedo, J. N., Rodrigues, A. P., Lidon, F. C., Pais, I. P., Marques, I., Gouveia, D., Armengaud, J., Silva, M. J., Martins, S., Semedo, M. C., Dubberstein, D., Partelli, F. L., Reboredo, F. H., Scotti-Campos, P., Ribeiro-Barros, A. I., DaMatta, F. M., Ramalho, J. C. (2021). Intrinsic Non-Stomatal Resilience to Drought of the Photosynthetic Apparatus in *Coffea* spp. is Strengthened by Elevated Air [CO_2]. *Tree Physiology*, *41*(5), 708–727. https://doi.org/10.1093/treephys/tpaa158

Siddique, A. B., Parveen, S., Rahman, Md. Z., Rahman, J. (2024). Revisiting Plant Stress Memory: Mechanisms and Contribution to Stress Adaptation. *Physiology and Molecular Biology of Plants*, *30*(2), 349–367. https://doi.org/10.1007/s12298-024-01422-z

Silva, B. M., Oliveira, G. C., Serafim, M. E., Silva, É. A., Guimarães, P. T. G., Melo, L. B. B., Norton, L. D., Curi, N. (2019). Soil Moisture Associated with Least Limiting Water Range, Leaf Water Potential, Initial Growth and Yield of Coffee as Affected by Soil Management System. *Soil and Tillage Research*, *189*, 36–43. https://doi.org/10.1016/j.still.2018.12.016

Simonneau, T., Lebon, E., Coupel-Ledru, A., Marguerit, E., Rossdeutsch, L., Ollat, N. (2017). Adapting Plant Material to Face Water Stress in Vineyards: Which Physiological Targets for an Optimal Control of Plant Water Status? *OENO One*, *51*(2), 167–179. https://doi.org/10.20870/oeno-one.2017.51.2.1870

Suwannarut, W., Vialet-Chabrand, S., Kaiser, E. (2023). Diurnal Decline in Photosynthesis and Stomatal Conductance in Several Tropical Species. *Frontiers in Plant Science*, *14*, 1273802. https://doi.org/10.3389/fpls.2023.1273802

Tarara, J. M., Peña, J. E. P., Keller, M., Schreiner, R. P., Smithyman, R. P. (2011). Net Carbon Exchange in Grapevine Canopies Responds Rapidly to Timing and Extent of Regulated Deficit Irrigation. *Functional Plant Biology*, *38*(5), 386. https://doi.org/10.1071/FP10221

Tarara, J. M., Perez Peña, J. E. (2015). Moderate Water Stress from Regulated Deficit Irrigation Decreases Transpiration Similarly to Net Carbon Exchange in Grapevine Canopies. *Journal of the American Society for Horticultural Science*, *140*(5), 413–426. https://doi.org/10.21273/JASHS.140.5.413

Thioune, E.-H., Strickler, S., Gallagher, T., Charpagne, A., Decombes, P., Osborne, B., McCarthy, J. (2020). Temperature Impacts the Response of *Coffea canephora* to Decreasing Soil Water Availability. *Tropical Plant Biology*, *13*(3), 236–250. https://doi.org/10.1007/s12042-020-09254-3

Thom, J. K., Livesley, S. J., Fletcher, T. D., Farrell, C., Arndt, S. K., Konarska, J., Szota, C. (2022). Selecting Tree Species with High Transpiration and Drought Avoidance to Optimize Runoff Reduction in Passive Irrigation Systems. *Science*

of The Total Environment, *812*, 151466. https://doi.org/10.1016/j.scitotenv.2021.151466

Thomas, D. S., Montagu, K. D., Conroy, J. P. (2006). Effects of Leaf and Branch Removal on Carbon Assimilation and Stem Wood Density of *Eucalyptus grandis* Seedlings. *Trees*, *20*(6), 725–733. https://doi.org/10.1007/s00468-006-0087-x

Valim Da Silva, D., Luiz Naves, V., Alejandra Toro-Herrera, M., Amorim Vieira, D., Das Chagas Mendonça, A. M., Rambal, S., Rodrigues Alves Delfino Barbosa, J. P. (2022). Looking For Adjustments to Severe Drought in Coffee: Lessons of a Rainfall Exclusion Plot in the Southern Brazil. *Coffee Science*, *17*, 1–14. https://doi.org/10.25186/.v17i.2015

Venancio, L. P., Filgueiras, R., Mantovani, E. C., Do Amaral, C. H., Da Cunha, F. F., Dos Santos Silva, F. C., Althoff, D., Dos Santos, R. A., Cavatte, P. C. (2020). Impact of Drought Associated with High Temperatures on *Coffea canephora* Plantations: A Case Study in Espírito Santo State, Brazil. *Scientific Reports*, *10*(1), 19719. https://doi.org/10.1038/s41598-020-76713-y

Wagner, S., Jassogne, L., Price, E., Jones, M., Preziosi, R. (2021). Impact of Climate Change on the Production of *Coffea arabica* at Mt. Kilimanjaro, Tanzania. *Agriculture*, *11*(1), 53. https://doi.org/10.3390/agriculture11010053

Wang, J., Wen, X. (2022). Excess Radiation Exacerbates Drought Stress Impacts on Canopy Conductance Along Aridity Gradients. *Biogeosciences*, *19*(17), 4197–4208. https://doi.org/10.5194/bg-19-4197-2022

Wang, R.H., Chang, J.C., Li, K.T., Lin, T.S., Chang, L.S. (2014). Leaf Age And Light Intensity Affect Gas Exchange Parameters and Photosynthesis Within the Developing Canopy of Field Net-House-Grown Papaya Trees. *Scientia Horticulturae*, *165*, 365–373. https://doi.org/10.1016/j.scienta.2013.11.035

Wang, X., Ge, J., He, M., Li, Q., Cai, J., Zhou, Q., Zhong, Y., Wollenweber, B., Jiang, D. (2023). Enhancing Crop Resilience: Understanding the Role of Drought

Priming in Wheat Stress Response. *Field Crops Research*, *302*, 109083. https://doi.org/10.1016/j.fcr.2023.109083

Wei, A. (2024). China's Coffee Frontier: A Tale of Two Regions and a Global Market. *Finance Economics*, *1*(9). https://doi.org/10.61173/25bcdd02

Wu, J., Su, Y., Chen, X., Liu, L., Yang, X., Gong, F., Zhang, H., Xiong, X., Zhang, D. (2021). Leaf Shedding of Pan-Asian Tropical Evergreen Forests Depends on the Synchrony of Seasonal Variations of Rainfall and Incoming Solar Radiation. *Agricultural and Forest Meteorology*, *311*, 108691. https://doi.org/10.1016/j.agrformet.2021.108691

Xu, Z., Zhou, G., Shimizu, H. (2010). Plant Responses to Drought and Rewatering. *Plant Signaling Behavior*, *5*(6), 649–654. https://doi.org/10.4161/psb.5.6.11398

Zheng, H., Zhang, X., Ma, W., Song, J., Rahman, S. U., Wang, J., Zhang, Y. (2017). Morphological and Physiological Responses to Cyclic Drought in Two Contrasting Genotypes of *Catalpa bungei*. *Environmental and Experimental Botany*, *138*, 77–87. https://doi.org/10.1016/j.envexpbot.2017.02.016

4. CONCLUDING REMARKS

In the context of climate change, recurrent cycles of soil water deficit combined with elevated air temperatures have significantly impacted the physiology and productivity of *C. canephora* cultivations. This study underscores the importance of physiological investigations aimed at understanding the effects of recurrent water deficits on crops.

As demonstrated in the first chapter, different *C. canephora* genotypes exhibit varying degrees of thermal tolerance when subjected to repeated drought cycles. Under irrigated conditions, both clones 'A1' and '3V' displayed sensitivity to supra-optimal temperatures. However, following exposure to recurrent water deficit cycles, clone '3V' exhibited heightened sensitivity of the photosynthetic apparatus to elevated temperatures, whereas clone 'A1' demonstrated greater tolerance. These findings suggest that recurrent water stress can function as a priming agent in certain *C. canephora* clones and that these materials can be selected based on chlorophyll *a* fluorescence emission analysis. A straightforward analysis of the OJIP transient standard curve, combined with key JIP_{Test} variables (φ_{Po}, φ_{Eo}, φ_{Do}, ABS/CS_0, TR_0/CS_0, DI_0/CS_0, RC/CS_0, SFI_{abs}, and PI_{abs}), enables a comprehensive assessment of drought priming-induced thermal tolerance in the photosynthetic apparatus.

In the second chapter, it was observed that recurrent water stress exerts a substantial impact on both single-leaf and whole-canopy gas exchange. Both monitoring approaches proved effective in tracking stress responses progression and subsequent recovery. Notably, whole-canopy gas exchange exhibited greater potential for capturing dynamic processes associated with the progression of water stress, particularly about micrometeorological conditions. Moreover, assessing whole-canopy gas exchange allowed the inference of stress responses both per unit of leaf area and in the whole canopy. These results highlight that *C. canephora* plants employ distinct strategies to cope with water stress at multiple scales, enhancing water-use efficiency and reducing their overall water footprint. These acclimation responses could reflect stress memory mechanisms in coffee plants. However, molecular analyses targeting differentially expressed genes in plants exposed to recurrent drought cycles are necessary to validate the proposed hypothesis and support the findings presented in this study.

REFERENCES

Akhter, Z., Bi, Z., Ali, K., Sun, C., Fiaz, S., Haider, F. U., Bai, J. (2021). In Response to Abiotic Stress, DNA Methylation Confers Epigenetic Changes in Plants. *Plants*, *10*(6), 1096. https://doi.org/10.3390/plants10061096

Almeida, W. L., Ávila, R. T., Pérez-Molina, J. P., Barbosa, M. L., Marçal, D. M. S., De Souza, R. P. B., Martino, P. B., Cardoso, A. A., Martins, S. C. V., DaMatta, F. M. (2021). The Interplay Between Irrigation and Fruiting on Branch Growth and Mortality, Gas Exchange and Water Relations of Coffee Trees. *Tree Physiology*, *41*(1), 35–49. https://doi.org/10.1093/treephys/tpaa116

Araujo, W. L., Dias, P. C., Moraes, G. A. B. K., Celin, E. F., Cunha, R. L., Barros, R. S., DaMatta, F. M. (2008). Limitations to Photosynthesis in Coffee Leaves From Different Canopy Positions. *Plant Physiology and Biochemistry*, *46*(10), 884–890. https://doi.org/10.1016/j.plaphy.2008.05.005

Avila, R. T., Cardoso, A. A., De Almeida, W. L., Costa, L. C., Machado, K. L. G., Barbosa, M. L., De Souza, R. P. B., Oliveira, L. A., Batista, D. S., Martins, S. C. V., Ramalho, J. D. C., DaMatta, F. M. (2020). Coffee Plants Respond to Drought and Elevated [CO_2] Through Changes in Stomatal Function, Plant Hydraulic Conductance, and Aquaporin Expression. *Environmental and Experimental Botany*, *177*, 104148. https://doi.org/10.1016/j.envexpbot.2020.104148

Baker, J. T., Gitz III, D. C., Lascano, R. J. (2014). Field Evaluation of Open System Chambers for Measuring Whole Canopy Gas Exchanges. *Agronomy Journal*, *106*(2), 537–544. https://doi.org/10.2134/agronj2013.0449

Barros, R. S., Da S.e Mota, J. W., Da Matta, F. M., Maestri, M. (1997). Decline of Vegetative Growth in *Coffea arabica* L. in Relation to Leaf Temperature, Water Potential and Stomatal Conductance. *Field Crops Research*, *54*(1), 65–72. https://doi.org/10.1016/S0378-4290(97)00045-2

Bharath, P., Gahir, S., Raghavendra, A. S. (2021). Abscisic Acid-Induced Stomatal Closure: An Important Component of Plant Defense Against Abiotic and Biotic Stress. *Frontiers in Plant Science*, *12*, 615114. https://doi.org/10.3389/fpls.2021.615114

Bragança, S. M., Carvalho, C. H. S. D., Fonseca, A. F. A. D., Ferrão, R. G. (2001). Variedades Clonais de Café Conilon para o Estado do Espírito Santo. *Pesquisa Agropecuária Brasileira*, *36*(5), 765–770. https://doi.org/10.1590/S0100-204X2001000500006

Bunn, C., Läderach, P., Ovalle Rivera, O., Kirschke, D. (2015). A Bitter Cup: Climate Change Profile of Global Production of Arabica and Robusta Coffee. *Climatic Change*, *129*(1–2), 89–101. https://doi.org/10.1007/s10584-014-1306-x

Calvin, K., Dasgupta, D., Krinner, G., Mukherji, A., Thorne, P. W., Trisos, C., Romero, J., Aldunce, P., Barrett, K., Blanco, G., Cheung, W. W. L., Connors, S., Denton, F., Diongue-Niang, A., Dodman, D., Garschagen, M., Geden, O., Hayward, B., Jones, C., … Péan, C. (2023). IPCC, 2023: Climate Change 2023: Synthesis Report. Contribution of Working Groups I, II and III to the Sixth Assessment Report of the Intergovernmental Panel on Climate Change [Core Writing Team, H. Lee and J. Romero (eds.)]. *IPCC, Geneva, Switzerland.* (First). *Intergovernmental Panel on Climate Change* (IPCC). https://doi.org/10.59327/IPCC/AR6-9789291691647

Campos, C. N., Ávila, R. G., De Souza, K. R. D., Azevedo, L. M., Alves, J. D. (2019). Melatonin Reduces Oxidative Stress and Promotes Drought Tolerance in Young *Coffea arabica* L. Plants. *Agricultural Water Management*, *211*, 37–47. https://doi.org/10.1016/j.agwat.2018.09.025

Campuzano-Duque, L. F., Herrera, J. C., Ged, C., Blair, M. W. (2021). Bases for the Establishment of Robusta Coffee (*Coffea canephora*) as a New Crop for Colombia. *Agronomy*, *11*(12), 2550. https://doi.org/10.3390/agronomy11122550

Chacón-Villalobos, Y., Chacón-Sancho, A., Vargas-Chinchilla, M., Cerdà-Subirachs, J. Ma., Hernández-Pérez, R. (2021). Nuevo Bioestimulante de Floración y Maduración en Café (*Coffea arabica* L.). *Agronomía Mesoamericana*, 983–990. https://doi.org/10.15517/am.v32i3.43935

Charng, Y., Mitra, S., Yu, S.-J. (2023). Maintenance of Abiotic Stress Memory in Plants: Lessons Learned From Heat Acclimation. *The Plant Cell*, *35*(1), 187–200. https://doi.org/10.1093/plcell/koac313

DaMatta, F. M. (2018). Coffee Tree Growth and Environmental Acclimation. In *Achieving sustainable cultivation of coffee* (p. 39–66). Burleigh Dodds Science Publishing.

DaMatta, F. M., Ramalho, J. D. C. (2006). Impacts of Drought and Temperature Stress on Coffee Physiology and Production: A Review. *Brazilian Journal of Plant Physiology*, *18*(1), 55–81. https://doi.org/10.1590/S1677-04202006000100006

Davis, A. P., Rakotonasolo, F. (2021). Six New Species of Coffee (*Coffea*) From Northern Madagascar. *Kew Bulletin*, *76*(3), 497–511. https://doi.org/10.1007/s12225-021-09952-5

De Souza, G. A. R., Baroni, D. F., Bernado, W. D. P., Santos, A. R., Barcellos, L. C. D. S., Barcelos, L. F. T., Correia, L. Z., De Almeida, C. M., Verdin Filho, A. C., Rodrigues, W. P., Ramalho, J. C., Rakočević, M., Campostrini, E. (2025). Leaf to Root Morphological and Anatomical Indicators of Drought Resistance in *Coffea canephora* After Two Stress Cycles. *Agriculture*, *15*(6), 574. https://doi.org/10.3390/agriculture15060574

Delrot, S., Medrano, H., Or, E., Bavaresco, L., Grando, S. (2010). *Methodologies and Results in Grapevine Research* (pp. 1-448). New York, NY, USA: Springer.

Dias, P. C., Araujo, W. L., Moraes, G. A. B. K., Barros, R. S., DaMatta, F. M. (2007). Morphological and Physiological Responses of Two Coffee Progenies to Soil

Water Availability. *Journal of Plant Physiology*, *164*(12), 1639–1647. https://doi.org/10.1016/j.jplph.2006.12.004

Dubberstein, D., Lidon, F. C., Rodrigues, A. P., Semedo, J. N., Marques, I., Rodrigues, W. P., Gouveia, D., Armengaud, J., Semedo, M. C., Martins, S., Simões-Costa, M. C., Moura, I., Pais, I. P., Scotti-Campos, P., Partelli, F. L., Campostrini, E., Ribeiro-Barros, A. I., DaMatta, F. M., Ramalho, J. C. (2020). Resilient and Sensitive Key Points of the Photosynthetic Machinery of *Coffea* spp. To the Single and Superimposed Exposure to Severe Drought and Heat Stresses. *Frontiers in Plant Science*, *11*, 1049. https://doi.org/10.3389/fpls.2020.01049

Escalona, J. M., Pou, A., Tortosa, I., Hernández-Montes, E., Tomás, M., Martorell, S., Bota, J., Medrano, H. (2016). Using Whole-Plant Chambers to Estimate Carbon and Water Fluxes in Field-Grown Grapevines. *Theoretical and Experimental Plant Physiology*, *28*(2), 241–254. https://doi.org/10.1007/s40626-016-0073-7

Fahad, S., Bajwa, A. A., Nazir, U., Anjum, S. A., Farooq, A., Zohaib, A., Sadia, S., Nasim, W., Adkins, S., Saud, S., Ihsan, M. Z., Alharby, H., Wu, C., Wang, D., Huang, J. (2017). Crop Production under Drought and Heat Stress: Plant Responses and Management Options. *Frontiers in Plant Science*, *8*, 1147. https://doi.org/10.3389/fpls.2017.01147

Ferrão, R. G., Fonseca, A. F. A. da, Ferrão, M. A. G., De Muner, L. H. (2017). *Café conilon*. Instituto Capixaba de Pesquisa Assistência Técnica e Extensão Rural–INCAPER.

Ferraz, T. M., Rodrigues, W. P., Netto, A. T., de Oliveira Reis, F., Peçanha, A. L., de Assis, F. A. M. M., de Sousa, E. F., Glenn, D. M., Campostrini, E. (2016). Comparison Between Single-Leaf and Whole-Canopy Gas Exchange Measurements in Papaya (*Carica papaya* L.) Plants. *Scientia Horticulturae*, *209*, 73–78. https://doi.org/10.1016/j.scienta.2016.06.014

Ferreira, T., Shuler, J., Guimarães, R., Farah, A. (2019). CHAPTER 1. Introduction to Coffee Plant and Genetics. In *Coffee* (p. 1–25). Royal Society of Chemistry. https://doi.org/10.1039/9781782622437-00001

Fleta-Soriano, E., Munné-Bosch, S. (2016). Stress Memory and the Inevitable Effects of Drought: A Physiological Perspective. *Frontiers in Plant Science*, *7*. https://doi.org/10.3389/fpls.2016.00143

Francesconi, A. H. D., Lakso, A. N., Denning, S. S. (1997). Light and Temperature Effects on Whole-Canopy Net Carbon Dioxide Exchange Rates of Apple Trees. *Acta Horticulturae*, *451*, 287–294. https://doi.org/10.17660/ActaHortic.1997.451.33

Garcia, R. L., Norman, J. M., McDermitt, D. K. (1990). Measurements of Canopy Gas Exchange Using an Open Chamber System. *Remote Sensing Reviews*, *5*(1), 141–162.

Gichimu, B. M., Cheserek, J. (2012). Drought and Heat Tolerance in Coffee: A Review. *International Research Journal of Agricultural Science and Soil Science*, *2*(12), 498–501.

Gomez, L. F., Lopez, J. C., Riano, N. M., Lopez, Y., Montoya, E. C. (2005). Diurnal Changes in Leaf Gas Exchange and Validation of a Mathematical Model for Coffee (*Coffea arabica* L.) Canopy Photosynthesis. *Photosynthetica*, *43*(4), 575–582. https://doi.org/10.1007/s11099-005-0090-2

Guedes, F. A. D. F., Nobres, P., Rodrigues Ferreira, D. C., Menezes-Silva, P. E., Ribeiro-Alves, M., Correa, R. L., DaMatta, F. M., Alves-Ferreira, M. (2018). Transcriptional Memory Contributes to Drought Tolerance in Coffee (*Coffea canephora*) Plants. *Environmental and Experimental Botany*, *147*, 220–233. https://doi.org/10.1016/j.envexpbot.2017.12.004

Haworth, M., Marino, G., Centritto, M. (2018). An Introductory Guide to Gas Exchange Analysis of Photosynthesis and Its Application to Plant Phenotyping

and Precision Irrigation to Enhance Water Use Efficiency. *Journal of Water and Climate Change*, *9*(4), 786–808. https://doi.org/10.2166/wcc.2018.152

ICO. (2025). International Coffee Organization - Coffee Market Report. Available in: https://ico.org/; Accessed on February 02, 2025.

IPCC. (2022). *Global Warming of 1.5°C: IPCC Special Report on Impacts of Global Warming of 1.5°C above Pre-industrial Levels in Context of Strengthening Response to Climate Change, Sustainable Development, and Efforts to Eradicate Poverty* (1º ed). Cambridge University Press. https://doi.org/10.1017/9781009157940

Jacques, C., Salon, C., Barnard, R. L., Vernoud, V., Prudent, M. (2021). Drought Stress Memory at the Plant Cycle Level: A Review. *Plants*, *10*(9), 1873. https://doi.org/10.3390/plants10091873

Jing, Z., Liu, N., Zhang, Z., Hou, X. (2024). Research Progress on Plant Responses to Stress Combinations in the Context of Climate Change. *Plants*, *13*(4), 469. https://doi.org/10.3390/plants13040469

Kambona, C. M., Koua, P. A., Léon, J., Ballvora, A. (2023). Stress Memory and Its Regulation in Plants Experiencing Recurrent Drought Conditions. *Theoretical and Applied Genetics*, *136*(2), 26. https://doi.org/10.1007/s00122-023-04313-1

Katerji, N., Daudet, F. A., Carbonneau, A., Ollat, N. (2015). Etude à L'échelle de La Plante Entière du Fonctionnement Hydrique et Photosynthétique de la Vigne: Comparaison des Systèmes de Conduite Traditionnel et en Lyre. *VITIS - Journal of Grapevine Research*, 197. https://doi.org/10.5073/VITIS.1994.33.197-203

Kath, J., Byrareddy, V. M., Craparo, A., Nguyen-Huy, T., Mushtaq, S., Cao, L., Bossolasco, L. (2020). Not so Robust: Robusta Coffee Production is Highly Sensitive to Temperature. *Global Change Biology*, *26*(6), 3677–3688. https://doi.org/10.1111/gcb.15097

Koutouleas, A., Sarzynski, T., Bordeaux, M., Bosselmann, A. S., Campa, C., Etienne, H., Turreira-García, N., Rigal, C., Vaast, P., Ramalho, J. C., Marraccini, P., Ræbild, A. (2022). Shaded-Coffee: A Nature-Based Strategy for Coffee Production Under Climate Change? A Review. *Frontiers in Sustainable Food Systems*, *6*, 877476. https://doi.org/10.3389/fsufs.2022.877476

Lagiotis, G., Madesis, P., Stavridou, E. (2023). Echoes of a Stressful Past: Abiotic Stress Memory in Crop Plants towards Enhanced Adaptation. *Agriculture*, *13*(11), 2090. https://doi.org/10.3390/agriculture13112090

Liu, H., Song, S., Zhang, H., Li, Y., Niu, L., Zhang, J., Wang, W. (2022). Signaling Transduction of ABA, ROS, and Ca^{2+} in Plant Stomatal Closure in Response to Drought. *International Journal of Molecular Sciences*, *23*(23), 14824. https://doi.org/10.3390/ijms232314824

Long, S. P. (2003). Gas Exchange Measurements, What Can They Tell Us About the Underlying Limitations to Photosynthesis? Procedures and Sources of Error. *Journal of Experimental Botany*, *54*(392), 2393–2401. https://doi.org/10.1093/jxb/erg262

Lorençone, J. A., De Oliveira Aparecido, L. E., Lorençone, P. A., Torsoni, G. B., De Lima, R. F., Da Silva Cabral De Moraes, J. R., De Souza Rolim, G. (2023). Agricultural Zoning of *Coffea arabica* in Brazil for Current and Future Climate Scenarios: Implications for the Coffee Industry. *Environment, Development and Sustainability*, *27*(2), 4143–4166. https://doi.org/10.1007/s10668-023-04066-3

Magrach, A., Ghazoul, J. (2015). Climate and Pest-Driven Geographic Shifts in Global Coffee Production: Implications for Forest Cover, Biodiversity and Carbon Storage. *PLOS ONE*, *10*(7), e0133071. https://doi.org/10.1371/journal.pone.0133071

Martins, S. C. V., Galmés, J., Cavatte, P. C., Pereira, L. F., Ventrella, M. C., DaMatta, F. M. (2014). Understanding the Low Photosynthetic Rates of Sun and Shade

Coffee Leaves: Bridging the Gap on the Relative Roles of Hydraulic, Diffusive and Biochemical Constraints to Photosynthesis. *PLoS ONE*, *9*(4), e95571. https://doi.org/10.1371/journal.pone.0095571

Marur, C. J., de Faria, R. T. (2007). A Chamber for Measurement of Net Photosynthesis on a Whole Plant. *Acta Scientiarum. Agronomy*, *29*(3), 415–419.

Mateus, M. P. D. B., Tavanti, R. F. R., Tavanti, T. R., Santos, E. F., Jalal, A., Reis, A. R. D. (2021). Selenium Biofortification Enhances ROS Scavenge System Increasing Yield of Coffee Plants. *Ecotoxicology and Environmental Safety*, *209*, 111772. https://doi.org/10.1016/j.ecoenv.2020.111772

Mbwambo, S. G., Mourice, S. K., Tarimo, A. J. P. (2022). The Impacts of Current Climate Variability on Coffee Production in the Northern and Southern Highlands of Tanzania. *Journal of Agricultural Science*, *14*(3), 78. https://doi.org/10.5539/jas.v14n3p78

Medrano, H., Pou, A., Tomás, M., Martorell, S., Gulias, J., Flexas, J., Escalona, J. M. (2012). Average Daily Light Interception Determines Leaf Water Use Efficiency Among Different Canopy Locations in Grapevine. *Agricultural Water Management*, *114*, 4–10. https://doi.org/10.1016/j.agwat.2012.06.025

Medrano, H., Tomás, M., Martorell, S., Flexas, J., Hernández, E., Rosselló, J., Pou, A., Escalona, J.-M., Bota, J. (2015). From Leaf to Whole-Plant Water Use Efficiency (WUE) In Complex Canopies: Limitations of Leaf WUE as a Selection Target. *The Crop Journal*, *3*(3), 220–228. https://doi.org/10.1016/j.cj.2015.04.002

Menezes-Silva, P. E., Sanglard, L. M. V. P., Ávila, R. T., Morais, L. E., Martins, S. C. V., Nobres, P., Patreze, C. M., Ferreira, M. A., Araújo, W. L., Fernie, A. R., DaMatta, F. M. (2017). Photosynthetic and Metabolic Acclimation to Repeated Drought Events Play Key Roles in Drought Tolerance in Coffee. *Journal of Experimental Botany*, *68*(15), 4309–4322. https://doi.org/10.1093/jxb/erx211

Miller, D. P., Howell, G. S., Flore, J. A. (1996). A Whole-plant, Open, Gas-exchange System for Measuring Net Photosynthesis of Potted Woody Plants. *HortScience*, *31*(6), 944–946. https://doi.org/10.21273/HORTSCI.31.6.944

Niinemets, Ü. (2007). Photosynthesis and Resource Distribution Through Plant Canopies. *Plant, Cell Environment*, *30*(9), 1052–1071. https://doi.org/10.1111/j.1365-3040.2007.01683.x

Niinemets, Ü., Díaz-Espejo, A., Flexas, J., Galmés, J., Warren, C. R. (2009). Role of Mesophyll Diffusion Conductance in Constraining Potential Photosynthetic Productivity in the Field. *Journal of Experimental Botany*, *60*(8), 2249–2270. https://doi.org/10.1093/jxb/erp036

Pandey, P., Ramegowda, V., Senthil-Kumar, M. (2015). Shared and Unique Responses of Plants to Multiple Individual Stresses and Stress Combinations: Physiological and Molecular Mechanisms. *Frontiers in Plant Science*, *6*. https://doi.org/10.3389/fpls.2015.00723

Pascual, L. S., Segarra-Medina, C., Gómez-Cadenas, A., López-Climent, M. F., Vives-Peris, V., Zandalinas, S. I. (2022). Climate Change-Associated Multifactorial Stress Combination: A Present Challenge for Our Ecosystems. *Journal of Plant Physiology*, *276*, 153764. https://doi.org/10.1016/j.jplph.2022.153764

Peña, J. P., Tarara, J. (2004). A Portable Whole Canopy Gas Exchange System for Several Mature Field-Grown Grapevines. *Vitis*, *43*(1), 7–14. https://doi.org/10.5073/vitis.2004.43.7-14

Pérez-Priego, O., López-Ballesteros, A., Sánchez-Cañete, E. P., Serrano-Ortiz, P., Kutzbach, L., Domingo, F., Eugster, W., Kowalski, A. S. (2015). Analysing Uncertainties in the Calculation of Fluxes Using Whole-Plant Chambers: Random and Systematic Errors. *Plant and Soil*, *393*(1–2), 229–244. https://doi.org/10.1007/s11104-015-2481-x

Pinheiro, H. A., DaMatta, F. M., Chaves, A. R. M., Loureiro, M. E., Ducatti, C. (2005). Drought Tolerance is Associated with Rooting Depth and Stomatal Control of Water Use in Clones of *Coffea canephora*. *Annals of Botany*, *96*(1), 101–108. https://doi.org/10.1093/aob/mci154

Poni, S., Magnanini, E., Rebucci, B. (1997). An Automated Chamber System for Measurements of Whole-vine Gas Exchange. *HortScience*, *32*(1), 64–67. https://doi.org/10.21273/HORTSCI.32.1.64

Poni, S., Merli, M. C., Magnanini, E., Galbignani, M., Bernizzoni, F., Vercesi, A., Gatti, M. (2014). An Improved Multichamber Gas Exchange System for Determining Whole-Canopy Water-Use Efficiency in Grapevine. *American Journal of Enology and Viticulture*, *65*(2), 268–276. https://doi.org/10.5344/ajev.2014.13117

Rakocevic, M., Baroni, D. F., De Souza, G. A. R., Bernado, W. D. P., De Almeida, C. M., Matsunaga, F. T., Rodrigues, W. P., Ramalho, J. C., Campostrini, E. (2023). Correlating *Coffea canephora* 3D Architecture to Plant Photosynthesis at a Daily Scale and Vegetative Biomass Allocation. *Tree Physiology*, *43*(4), 556–574. https://doi.org/10.1093/treephys/tpac138

Rakocevic, M., Costes, E., Campostrini, E., Ramalho, J. C., Ribeiro, R. V. (2024). Drought Responses in *Coffea Arabica* as Affected by Genotype and Phenophase. II – Photosynthesis at Leaf and Plant Scales. *Experimental Agriculture*, *60*, e22. https://doi.org/10.1017/S0014479724000164

Ramírez-Builes, V. H., Küsters, J., De Souza, T. R., Simmes, C. (2020). Calcium Nutrition in Coffee and Its Influence on Growth, Stress Tolerance, Cations Uptake, and Productivity. *Frontiers in Agronomy*, *2*, 590892. https://doi.org/10.3389/fagro.2020.590892

Rejeb, I., Pastor, V., Mauch-Mani, B. (2014). Plant Responses to Simultaneous Biotic and Abiotic Stress: Molecular Mechanisms. *Plants*, *3*(4), 458–475. https://doi.org/10.3390/plants3040458

Richardson, D., Kath, J., Byrareddy, V. M., Monselesan, D. P., Risbey, J. S., Squire, D. T., Tozer, C. R. (2023). Synchronous Climate Hazards Pose an Increasing Challenge to Global Coffee Production. *PLOS Climate*, *2*(3), e0000134. https://doi.org/10.1371/journal.pclm.0000134

Rodrigues, A. P., Pais, I. P., Leitão, A. E., Dubberstein, D., Lidon, F. C., Marques, I., Semedo, J. N., Rakocevic, M., Scotti-Campos, P., Campostrini, E., Rodrigues, W. P., Simões-Costa, M. C., Reboredo, F. H., Partelli, F. L., DaMatta, F. M., Ribeiro-Barros, A. I., Ramalho, J. C. (2024). Uncovering the Wide Protective Responses in *Coffea* spp. Leaves to Single and Superimposed Exposure of Warming and Severe Water Deficit. *Frontiers in Plant Science*, *14*, 1320552. https://doi.org/10.3389/fpls.2023.1320552

Rodrigues, W. P., Machado Filho, J. A., Da Silva, J. R., De Assis Figueiredo, F. A. M. M., Ferraz, T. M., Ferreira, L. S., Da Silva Bezerra, L. B., De Abreu, D. P., De Paula Bernado, W., Cespom Passos, L., De Sousa, E. F., Glenn, D. M., Ramalho, J. C., Campostrini, E. (2016). Whole-Canopy Gas Exchanges in *Coffea* spp. is Affected by Supra-Optimal Temperature and Light Distribution Within the Canopy: The Insights From an Improved Multi-Chamber System. *Scientia Horticulturae*, *211*, 194–202. https://doi.org/10.1016/j.scienta.2016.08.022

Rodrigues, W. P., Martins, M. Q., Fortunato, A. S., Rodrigues, A. P., Semedo, J. N., Simões-Costa, M. C., Pais, I. P., Leitão, A. E., Colwell, F., Goulao, L., Máguas, C., Maia, R., Partelli, F. L., Campostrini, E., Scotti-Campos, P., Ribeiro-Barros, A. I., Lidon, F. C., DaMatta, F. M., Ramalho, J. C. (2016). Long-Term Elevated Air [CO_2] Strengthens Photosynthetic Functioning and Mitigates the Impact of Supra-Optimal Temperatures in Tropical *Coffea arabica* and *C. canephora* species. *Global Change Biology*, *22*(1), 415–431. https://doi.org/10.1111/gcb.13088

Rodrigues, W. P., Silva, J. R., Ferreira, L. S., Filho, J. A. M., Figueiredo, F. A. M. M. A., Ferraz, T. M., Bernado, W. P., Bezerra, L. B. S., De Abreu, D. P., Cespom, L., Ramalho, J. C., Campostrini, E. (2018). Stomatal and Photochemical Limitations of Photosynthesis in Coffee (*Coffea* spp.) Plants Subjected to Elevated Temperatures. *Crop and Pasture Science*, *69*(3), 317. https://doi.org/10.1071/CP17044

Salazar-Tortosa, D., Castro, J., Rubio De Casas, R., Viñegla, B., Sánchez-Cañete, E. P., Villar-Salvador, P. (2018). Gas Exchange at Whole Plant Level Shows That a Less Conservative Water Use is Linked to a Higher Performance in Three Ecologically Distinct Pine Species. *Environmental Research Letters*, *13*(4), 045004. https://doi.org/10.1088/1748-9326/aab18f

Seleiman, M. F., Al-Suhaibani, N., Ali, N., Akmal, M., Alotaibi, M., Refay, Y., Dindaroglu, T., Abdul-Wajid, H. H., Battaglia, M. L. (2021). Drought Stress Impacts on Plants and Different Approaches to Alleviate Its Adverse Effects. *Plants*, *10*(2), 259. https://doi.org/10.3390/plants10020259

Semedo, J. N., Rodrigues, A. P., Lidon, F. C., Pais, I. P., Marques, I., Gouveia, D., Armengaud, J., Silva, M. J., Martins, S., Semedo, M. C., Dubberstein, D., Partelli, F. L., Reboredo, F. H., Scotti-Campos, P., Ribeiro-Barros, A. I., DaMatta, F. M., Ramalho, J. C. (2021). Intrinsic Non-Stomatal Resilience to Drought of the Photosynthetic Apparatus in *Coffea* spp. is Strengthened by Elevated Air [CO_2]. *Tree Physiology*, *41*(5), 708–727. https://doi.org/10.1093/treephys/tpaa158

Semedo, J. N., Rodrigues, W. P., Dubberstein, D., Martins, M. Q., Martins, L. D., Pais, I. P., Rodrigues, A. P., Leitão, A. E., Partelli, F. L., Campostrini, E., Tomaz, M. A., Reboredo, F. H., Scotti-Campos, P., Ribeiro-Barros, A. I., Lidon, F. C., DaMatta, F. M., Ramalho, J. C. (2018). Coffee Responses to Drought, Warming and High [CO_2] in a Context of Future Climate Change Scenarios. Em F. Alves, W. Leal Filho, U. Azeiteiro (Orgs.), *Theory and Practice of Climate*

Adaptation (p. 465–477). Springer International Publishing. https://doi.org/10.1007/978-3-319-72874-2_26

Sharma, M., Kumar, P., Verma, V., Sharma, R., Bhargava, B., Irfan, M. (2022). Understanding Plant Stress Memory Response for Abiotic Stress Resilience: Molecular Insights and Prospects. *Plant Physiology and Biochemistry*, *179*, 10–24. https://doi.org/10.1016/j.plaphy.2022.03.004

Sharma, N., Thakur, M., Suryakumar, P., Mukherjee, P., Raza, A., Prakash, C. S., Anand, A. (2022). 'Breathing Out' under Heat Stress—Respiratory Control of Crop Yield under High Temperature. *Agronomy*, *12*(4), 806. https://doi.org/10.3390/agronomy12040806

Silva, V. A., Prado, F. M., Antunes, W. C., Paiva, R. M. C., Ferrão, M. A. G., Andrade, A. C., Di Mascio, P., Loureiro, M. E., DaMatta, F. M., Almeida, A. M. (2018). Reciprocal Grafting Between Clones with Contrasting Drought Tolerance Suggests a Key Role of Abscisic Acid in Coffee Acclimation to Drought Stress. *Plant Growth Regulation*, *85*(2), 221–229. https://doi.org/10.1007/s10725-018-0385-5

Sseremba, G., Tongoona, P. B., Musoli, P., Eleblu, J. S. Y., Melomey, L. D., Bitalo, D. N., Atwijukire, E., Mulindwa, J., Aryatwijuka, N., Muhumuza, E., Kobusinge, J., Magambo, B., Kagezi, G. H., Danquah, E. Y., Kizito, E. B., Kyalo, G., Iyamulemye, E., Arinaitwe, G. (2023). Viability of Deficit Irrigation Pre-Exposure in Adapting Robusta Coffee to Drought Stress. *Agronomy*, *13*(3), 674. https://doi.org/10.3390/agronomy13030674

Sun, C., Ali, K., Yan, K., Fiaz, S., Dormatey, R., Bi, Z., Bai, J. (2021). Exploration of Epigenetics for Improvement of Drought and Other Stress Resistance in Crops: A Review. *Plants*, *10*(6), 1226. https://doi.org/10.3390/plants10061226

Takahashi, N., Ling, P. P., Frantz, J. M. (2008). Considerations for Accurate Whole Plant Photosynthesis Measurement. *Environmental Control in Biology*, *46*(2), 91-101. https://doi.org/10.13031/2013.23449

Tani, E., Chronopoulou, E. G., Labrou, N. E., Sarri, E., Goufa, M., Vaharidi, X., Tornesaki, A., Psychogiou, M., Bebeli, P. J., Abraham, E. M. (2019). Growth, Physiological, Biochemical, and Transcriptional Responses to Drought Stress in Seedlings of *Medicago sativa* L., *Medicago arborea* L. and Their Hybrid (*Alborea*). *Agronomy*, *9*(1), 38. https://doi.org/10.3390/agronomy9010038

Venancio, L. P., Filgueiras, R., Mantovani, E. C., Do Amaral, C. H., Da Cunha, F. F., Dos Santos Silva, F. C., Althoff, D., Dos Santos, R. A., Cavatte, P. C. (2020). Impact of Drought Associated with High Temperatures on *Coffea canephora* Plantations: A Case Study in Espírito Santo State, Brazil. *Scientific Reports*, *10*(1), 19719. https://doi.org/10.1038/s41598-020-76713-y

Whiting, M. D., Lang, G. A. (2001). Canopy Architecture and Cuvette Flow Patterns Influence Whole-canopy Net CO_2 Exchange and Temperature in Sweet Cherry. *HortScience*, *36*(4), 691–698. https://doi.org/10.21273/HORTSCI.36.4.691

Xu, W.-B., Cao, F., Liu, P., Yan, K., Guo, Q.-H. (2024). The Multifaceted Role of RNA-Based Regulation in Plant Stress Memory. *Frontiers in Plant Science*, *15*, 1387575. https://doi.org/10.3389/fpls.2024.1387575

Yang, X., Lu, M., Wang, Y., Wang, Y., Liu, Z., Chen, S. (2021). Response Mechanism of Plants to Drought Stress. *Horticulturae*, *7*(3), 50. https://doi.org/10.3390/horticulturae7030050

Zahra, N., Hafeez, M. B., Ghaffar, A., Kausar, A., Zeidi, M. A., Siddique, K. H. M., Farooq, M. (2023). Plant Photosynthesis Under Heat Stress: Effects and Management. *Environmental and Experimental Botany*, *206*, 105178. https://doi.org/10.1016/j.envexpbot.2022.105178

Zia, R., Nawaz, M. S., Siddique, M. J., Hakim, S., Imran, A. (2021). Plant Survival Under Drought Stress: Implications, Adaptive Responses, and Integrated Rhizosphere Management Strategy for Stress Mitigation. *Microbiological Research*, *242*, 126626. https://doi.org/10.1016/j.micres.2020.126626

SUPLEMETARY DATA

SUPLEMENTARY DATA A

Table S1: Equations and definitions of JIP_{Test} parameters obtained from chlorophyll *a* fluorescence emission (O-J-I-P) analysis (Strasser et al., 2004; Stirbet and Govindjee, 2011; Goltsev et al., 2016).

Parameter	Name and description
Fluorescence technical parameter	Measured fluorescence and derived from measured data
F_O	minumun fluorescence recorded when all PSII reaction centers are open
F_M	maximum fluorescence emitted when all PSII reaction centers are closed
$F_{50\mu s}$ or $F_{20\mu s}$	minimum fluorescence signal (corresponding to F_O) recorded at 50 µs or 20 µs
$F_{100\mu s}$	fluorescence at t = 100 µs
$F_{300\mu s}$	fluorescence at t = 300 µs
$F_{2ms} = F_J$	fluorescence at t = 2 ms, during the J phase
$F_{30ms} = F_I$	fluorescence measured 30 ms after the onset of illumination (at the I phase)
$V_J = (F_J - F_O)/(F_M - F_O)$	normalized variable fluorescence at the stage J (2 ms after switching on the light)
Quantum Yields or Flux Ratios	Derived from measured data
$\varphi_{Po} = TR_o/ABS = [1 - (F_O/F_M)] = F_V/F_M$	maximum quantum yield of primary photochemical reactions (at t = 0)
$\Psi_{Eo} = ET_o/TR_o = (1 - V_J)$	probability of electron transport beyon Q_A^- to electron transport chain beyond Q_A^- (at t = 0)
$\varphi_{Eo} = ET_o/ABS = [1 - (F_O/F_M)] * \Psi_{Eo} = \varphi_{Po} * \Psi_{Eo}$	quantum efficiency of electron tranfer from Q_A^- (at t = 0)
$\varphi_{Do} = 1 - \varphi_{Po} = (F_O/F_M)$	quantum efficiency of energy dissipation (at t = 0)
$\delta_{Ro} = RE_0/ET_0 = (1 - V_I)/(1 - V_J)$	probability with which the electron on intersystems carriers is able to reduce the terminal electron acceptors on the aceptor side os PSI
$\varphi_{Ro} = \varphi_{Po} * \Psi_{Eo} * \delta_{Ro} = RE_0/ABS = \varphi_{Po} * (1 - V_I)$	quantum yield for the reduction of terminal electron acceptors on the acceptor side of PSI
Phenomenological energy fluxes	by excited cross section (CS)
RC/CS_0	density of reaction centers capable of Q_A reduction
ABS/CS_0	energy absorbed per unit cross section at the onset of measurement (at t = 0)
TR_0/CS_0	energy flux trapped by PSII reaction centers per unit cross section (at t = 0)
ET_0/CS_0	electron flux through PSII per unit cross section (at t = 0)
DI_0/CS_0	thermal dissipation of energy in PSII per unit cross section (at t = 0)
Performance index	Parameters combination
$PI_{abs} = (RC/ABS) * [\varphi_{Po}/(1-\varphi_{Po})] * [\Psi_{Eo}/(1-\Psi_{Eo})]$	performance index. An indicator of PSII functional activity normalized to absorbed energy
Structure-function index	
$SFI_{abs} = (Chl_{RC}/Chl_{tot}) * \varphi_{Po} * \Psi_{Eo}$	provides structural and functional information about the strength of the influence of internal factors promoting of reactions in PSII

Table S2: Summary of ANOVA showing P-values for parameters derived from the JIP_{Test}, for treatments '3V'-WW, '3V'-WS, 'A1'-WW, and 'A1'-WS incubated at different temperatures (35 °C, 40 °C, 45 °C, 50 °C, and 55 °C) for 15 minutes.

Sources of variation	Parameters (*P* - value)								
	F_0	F_M	$F_{50\mu s}$	$F_{100\mu s}$	F_{300ms}	F_{2ms}	F_{30ms}	V_J	V_I
Treatment*Temperature	**<0.0001**	**0.0001**	**<0.0001**	**<0.0001**	**<0.0001**	**<0.0001**	**<0.0001**	0.0829	0.2327
Treatment	**0.0025**	0.9993	**0.0007**	**0.0001**	**<0.0001**	**<0.0001**	**0.0013**	**<0.0001**	0.0749
Temperature	**<0.0001**	**<0.0001**	**<0.0001**	**<0.0001**	**<0.0001**	**0.0345**	**<0.0001**	**0.0048**	0.0165
	φ_{Po}	Ψ_{Eo}	φ_{Eo}	φ_{Do}	δ_{Ro}	φ_{Ro}			
Treatment*Temperature	**<0.0001**	0.0829	**<0.0001**	**<0.0001**	0.6096	**<0.0001**			
Treatment	**0.0066**	**<0.0001**	**<0.0001**	**0.0066**	0.3252	**<0.0001**			
Temperature	**<0.0001**	**0.0048**	**<0.0001**	**<0.0001**	**0.0069**	**<0.0001**			
	ABS/RC	TR_0/RC	ET_0/RC	DI_0/RC		SFI_{abs}	PI_{abs}		
Treatment*Temperature	**<0.0001**	**0.0002**	**0.0066**	**<0.0001**		**<0.0001**	**<0.0001**		
Treatment	**0.0021**	0.0733	0.0804	**0.002**		**<0.0001**	**<0.0001**		
Temperature	**<0.0001**	**<0.0001**	**0.0013**	**<0.0001**		**<0.0001**	**<0.0001**		
	ABS/CS_0	TR_0/CS_0	ET_0/CS_0	DI_0/CS_0	RC/CS_0				
Treatment*Temperature	**<0.0001**	**<0.0001**	**<0.0001**	**<0.0001**	**<0.0001**				
Treatment	**0.0007**	**<0.0001**	**<0.0001**	**0.0007**	**<0.0001**				
Temperature	**<0.0001**	**<0.0001**	**<0.0001**	**<0.0001**	**<0.0001**				

Red values indicate statistical significance for the source of variation to each parameter (P - value < 0.05).

Table S2. Technical parameters of ChlF derived from the analysis of OJIP transients using the JIP_{Test}, for treatments '3V'-WW, '3V'-WS, 'A1'-WW, and 'A1'-WS incubated at different temperatures (35 °C, 40 °C, 45 °C, 50 °C, and 55 °C) for 15 minutes. F_0, initial or minimum fluorescence; F_m, maximum fluorescence; $F_{50\mu s}$, fluorescence signal recorded at 50 µs; $F_{100\mu s}$, fluorescence signal recorded at 100 µs; $F_{300\mu s}$, fluorescence signal recorded at 300 µs; F_{2ms}, fluorescence signal recorded at 2 ms; F_{30ms}, fluorescence signal recorded at 30 ms.

Parameter	Treatment	Temperature					
		35 °C	40 °C	45 °C	50 °C	55 °C	Means
F_O	'3V'-WW	7902.60 aC	8144.80 aC	8355.00 aBC	11600.60 aB	19680.40 bA	11136.68 a
	'3V'-WS	7269.40 aB	7245.60 aB	8813.40 aB	9643.40 aB	23010.60 aA	11196.48 a
	'A1'-WW	8019.40 aC	8261.60 aC	8980.20 aBC	11808.80 aB	15975.20 cA	10609.04 ab
	'A1'-WS	7381.60 aC	7493.00 aC	8168.60 aBC	12583.80 aA	10925.20 dAB	9310.44 b
	Means	7643.25 C	7786.25 C	8579.3 C	11409.15 A	17397.85 B	
F_M	'3V'-WW	33814.20 aA	30445.80 aA	30399.20 aA	25664.40 aB	20834.20 bcC	28231.56
	'3V'-WS	30841.8 0 abA	32015.80 aA	30866.80 aA	24513.80 aB	23190.00 abB	28285.64
	'A1'-WW	29759.40 bA	30270.20 aA	31279.00 aA	24673.00 aB	25288.00 aB	28253.92
	'A1'-WS	32354.80 abA	33183.40 aA	31539.80 aA	25589.60 aB	19011.20 cC	28335.76
	Means	31692.55 A	31478.80 A	31021.20 A	25110.20 B	22080.85 C	
$F_{50\mu s}$	'3V'-WW	8392.60 aC	8738.20 aC	9016..00 aC	12662.20 aB	19739.60 bA	11709.72 a
	'3V'-WS	7639.60 aB	7600.80 aB	9356.80 aB	10266.20 aB	23038.00 aA	11580.28 a
	'A1'-WW	8624.20 aC	8943.80 aC	9855.60 aBC	12781.00 aB	16631.80 cA	11367.28 a
	'A1'-WS	7735.40 aC	7889.00 aBC	8651.60 aBC	13103.00 aA	11141.60 dAB	9704.12 b
	Means	8097.95 C	8292.95 C	9220.00 C	12203.10 B	17637.75 A	
$F_{100\mu s}$	'3V'-WW	8869.20 aC	9325.80 aC	9655.80 aC	13733.60 aB	19842.60 bC	12285.40 a
	'3V'-WS	8010.20 aA	7952.40 aB	9909.60 aB	10908.60 aB	23105.80 aA	11977.32 a
	'A1'-WW	9203.40 aC	9614.60 aC	10711.00 aBC	13806.40 aB	17350.40 bA	12137.16 a
	'A1'-WS	8074.20 aC	8288.00 aBC	9126.40 aBC	13638.40 aA	11369.00 cAB	10099.20 b
	Means	8539.25 C	8795.20 C	9850.70 C	13021.75 B	17916.95 A	
$F_{300\mu s}$	'3V'-WW	10929.40 aB	11792.60 aB	12266.00 abB	17375.80 aA	19981.00 bA	14468.96 ab
	'3V'-WS	9550.60 aC	9412.40 aC	12001.80 abBC	13226.20 bB	23115.40 aA	13461.28 b
	'A1'-WW	11684.80 aC	12299.00 aC	14030.60 aBC	16881.40 aAB	19517.00 bA	14882.56 a
	'A1'-WS	9518.80 aB	9929.40 aB	11015.60 bB	15493.60 abA	12123.80 cB	11616.24 b
	Means	10420.90 D	10858.35 CD	12328.50 C	15744.25 B	18684.30 A	
F_{2ms}	'3V'-WW	20381.20 aA	20201.00 aA	18509.40 abA	19983.40 aA	20400.00 aA	19895.00 a
	'3V'-WS	17284.80 bB	17277.40 aB	17077.80 bB	16375.60 bB	23110.00 aA	18225.12 b
	'A1'-WW	19267.80 abAB	19786.80 aAB	20569.60 aAB	18444.2 0 abB	21867.20 aA	19987.12 a
	'A1'-WS	17228.00 bAB	17445.40 aA	16760.00 bAB	18306.60 abA	14161.40 bB	16780.28 c
	Means	18540.45 AB	18677.65 AB	18229.20 B	18277.45 AB	19884.65 A	
F_{30ms}	'3V'-WW	30056.00 aA	27229.20 aA	21532.20 bB	20751.00 aB	20714.60 aB	24056.60 ab
	'3V'-WS	25876.20 bAB	27034.40 aA	20965.40 bC	15978.00 bD	23090.60 aBC	22588.92 b
	'A1'-WW	26437.60 bA	26599.80 aA	26481.20 aA	20217.80 aB	24022.40 aA	24751.76 a
	'A1'-WS	27114.60 abA	26944.20 aA	23025.20 abB	20812.80 aB	16494.80 bC	22878.32 b
	Means	27371.10 A	26951.90 A	23001.00 B	21080.60 C	19439.90 C	

The estimated mean for each treatment is presented (n = 5). P-value < 0.05 was considered significant. Means followed by the same lowercase letter between treatments, and the same uppercase letter between temperatures, do not differ by Tukey's test at 5%.

SUPLEMENTARY DATA B

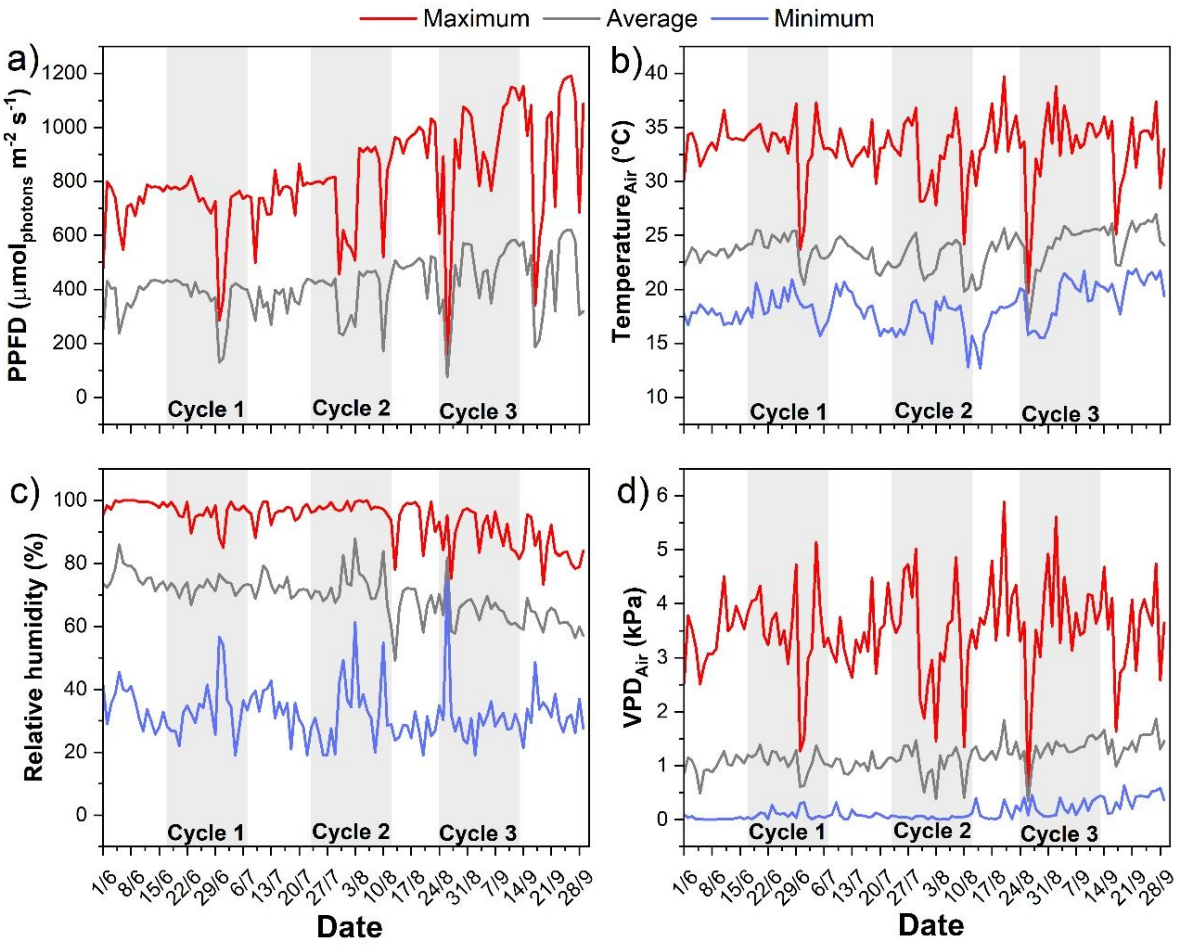

Figure S1: Micrometeorological data inside the greenhouse monitored throughout the experimental period, from June 1, 2024, to June 28, 2024. a) Photosynthetic photon flux density (PPFD, µmol.m^{-2}.s^{-1}); b) air temperature (°C); c) relative humidity (%); and d) vapor pressure deficit (kPa). The red lines indicate the maximum daily values recorded for each variable; the gray lines indicate the daily mean calculated for each variable; and the blue lines indicate the minimum daily values recorded for each variable (except PPFD). The gray backgrounds behind the data indicate the three periods during which *C. canephora* plants were subjected to recurrent cycles of soil drying and rewetting (Cycle 1, from June 17, 2024, to July 7, 2024; Cycle 2, from July 23, 2024 to August 8, 2024; and Cycle 3, from August 24, 2024 to September 13, 2024).

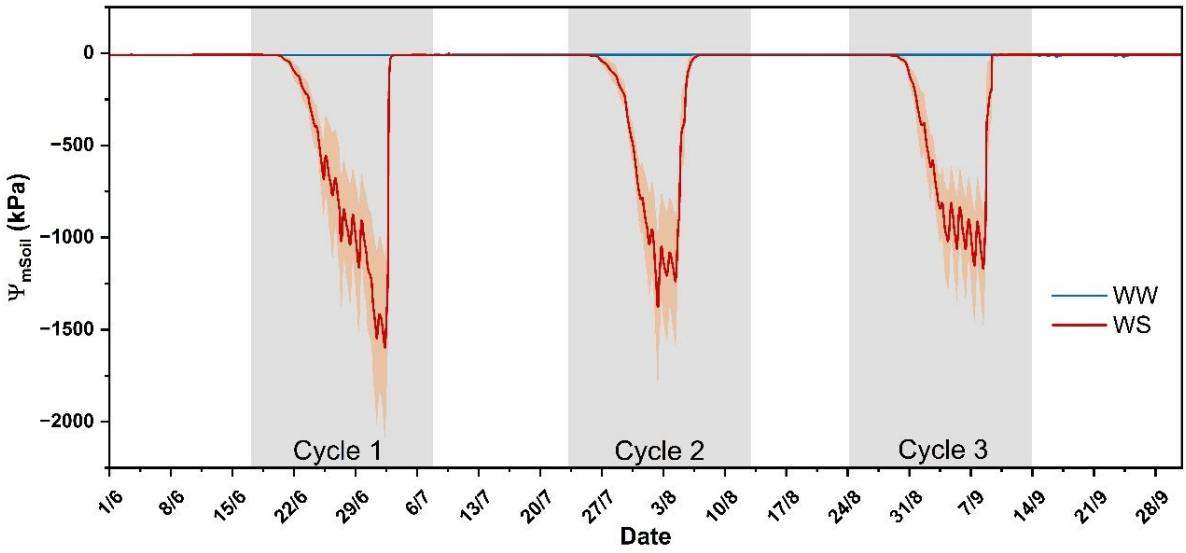

Figure S2: Soil matric potential (Ψ_{mSoil}) recorded throughout the experimental period at 0.3 m below the soil surface for the well-irrigated (WW; blue line) and recurrent water stress (WS; red line) conditions during the cultivation of *C. canephora* clone LB1. The shaded area around the lines indicates the standard error of the mean (n = 5). The gray backgrounds behind the data indicate the three periods during which the plants were subjected to recurrent cycles of soil drying and rewetting (Cycle 1, from June 17, 2024, to July 7, 2024; Cycle 2, from July 23, 2024 to August 8, 2024; and Cycle 3, from August 24, 2024 to September 13, 2024).

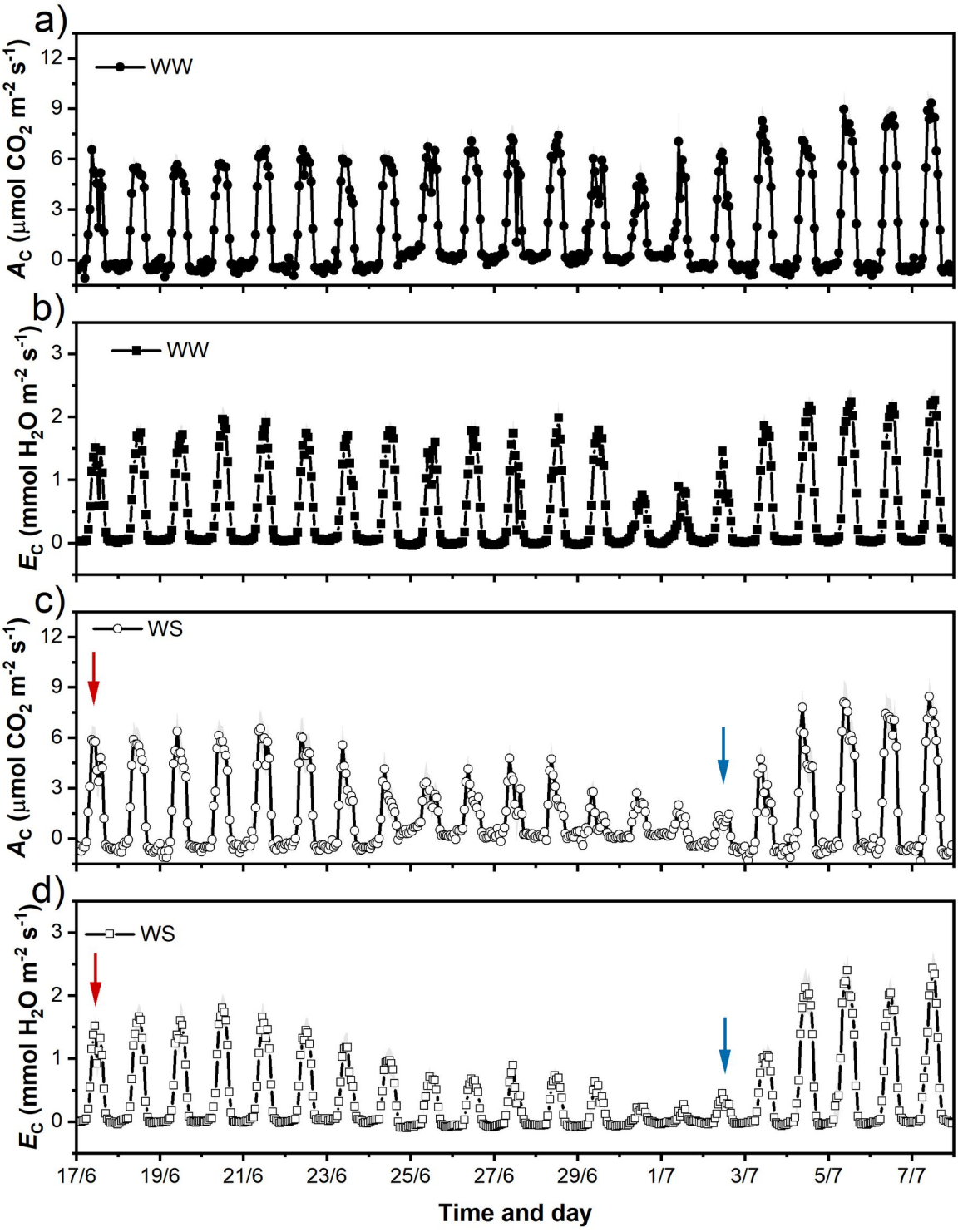

Figure S3: Whole-canopy gas exchange measurements representative data in *C. canephora* clone LB1 during Cycle 1 (WS-1 and REC-1) of soil drying and rewetting. a) A_C = net canopy CO_2 assimilation rate (µmol.m^{-2}.s^{-1}) under irrigated conditions (WW); b) E_C = canopy transpiration rate (mmol.m^{-2}.s^{-1}) under irrigated conditions (WW); c) A_C = net canopy CO_2 assimilation rate (µmol.m^{-2}.s^{-1}) under water stress conditions (WS); d) E_C = canopy transpiration rate (mmol.m^{-2}.s^{-1}) under water stress

conditions (WS). Red arrows indicate the day of irrigation suspension, and blue arrows indicate the day of irrigation resumption. Each point represents the hourly mean of each variable, and the shaded area indicates the standard error (n = 8).

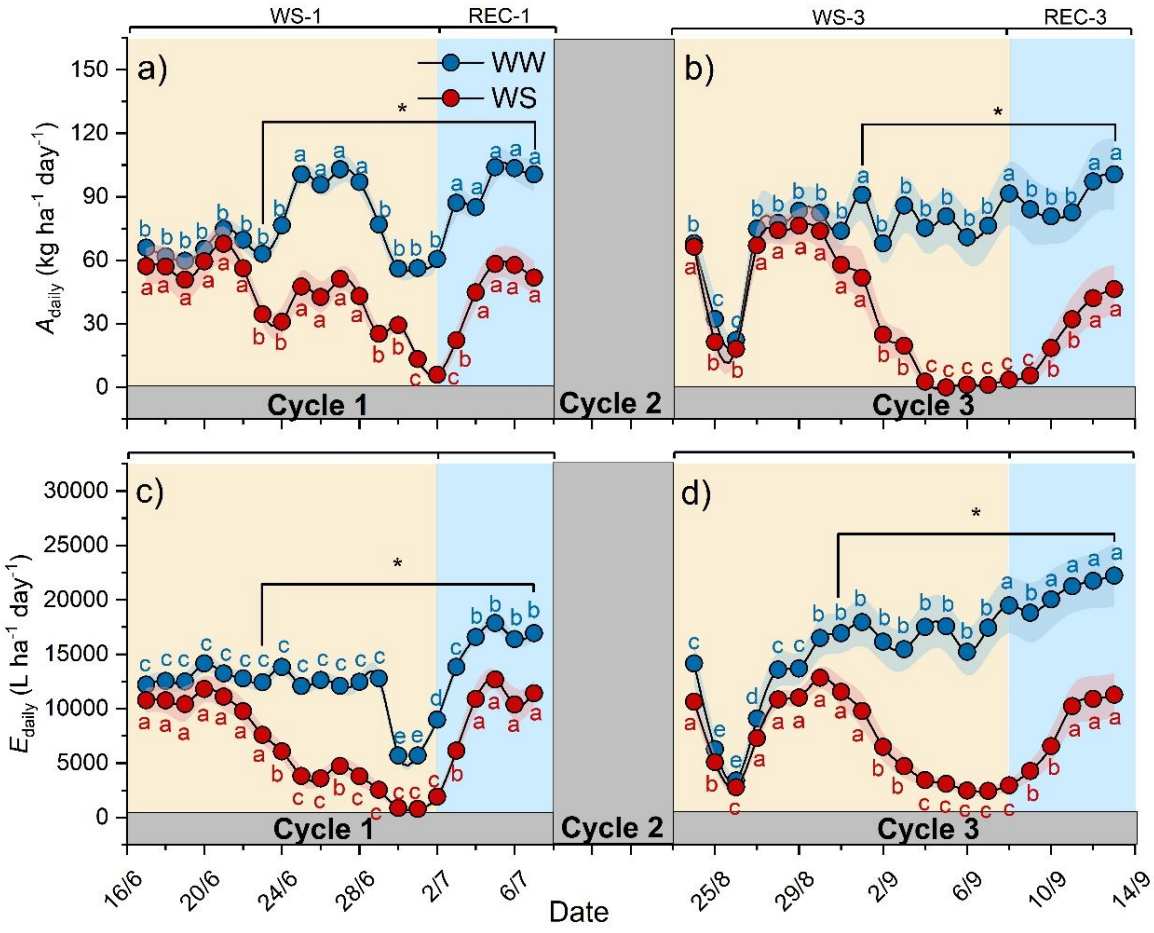

Figure S4: Whole-canopy gas exchange in *C. canephora* clone LB1 subjected to three recurrent cycles of soil drying and rewetting in a greenhouse. a) Daily canopy photosynthetic rate (A_{daily}, kg CO_2.ha^{-1}.day^{-1}) during Cycle 1 and b) during Cycle 3 of soil drying and rewetting. c) Daily canopy transpiration rate (E_{daily}, L H_2O.ha^{-1}.day^{-1}) during Cycle 1 and d) during Cycle 3 of soil drying and rewetting. Each cycle lasted 21 days, with 16 days of drying (WS-1 and WS-3, indicated by the yellow background) and 5 days of soil rewetting (REC-1 and REC-3, indicated by the blue background). In the figures, blue symbols represent the irrigated condition (WW), and red symbols represent the non-irrigated condition (WS). Lowercase letters indicate significant differences over time for each water condition (blue for WW and red for WS), grouped by the Scott-Knott test (P-value < 0.05). Days marked below the bracket or with an asterisk superscript indicate significant differences between the

water conditions for each measurement day, compared using Tukey's test (P-value < 0.05). Each symbol represents the mean ± SE (shaded area) of eight plants (n = 8).

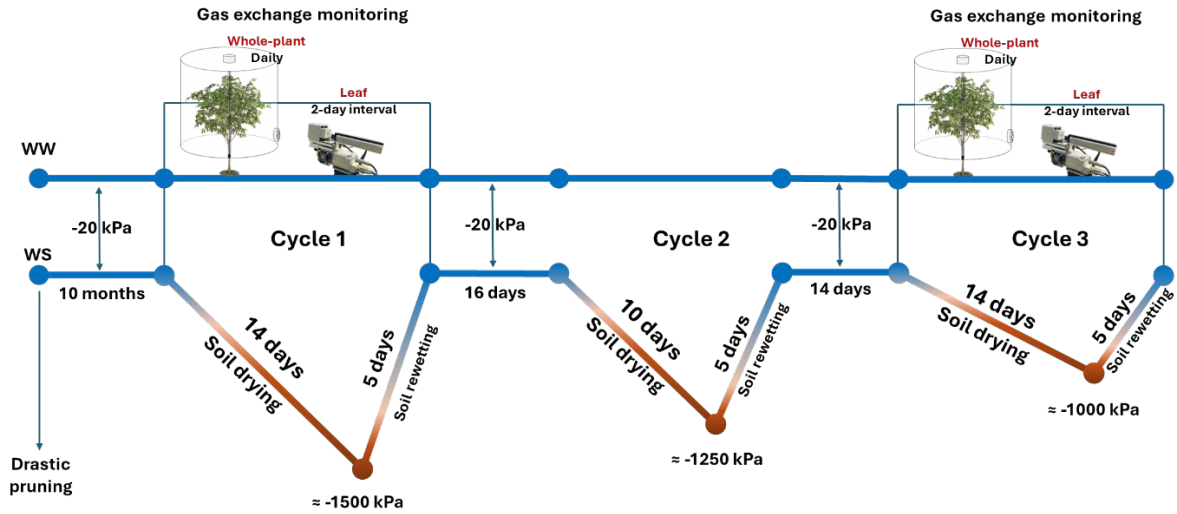

Figure S5: Scheme cultivation, application of drying and rewetting cycles of the soil, and gas exchange measurements in *C. canephora* plants grown in a greenhouse. After drastic pruning, two groups of plants (WW and WS) with two orthotropic axes were cultivated for 10 months under full irrigation. After this period, WS plants were subjected to Cycle 1 of drying (Ψ_{mSoil} ≈ -1500 kPa) and soil rewetting, lasting 14 and 5 days, respectively. After rewetting, the plants were maintained under full irrigation for 16 days and then subjected to Cycle 2 of drying (Ψ_{mSoil} ≈ -1250 kPa) and soil rewetting, lasting 10 and 5 days, respectively. After rewetting, the plants were maintained under full irrigation for 14 days and then subjected to Cycle 3 of drying (Ψ_{mSoil} ≈ -1000 kPa) and soil rewetting, lasting 14 and 5 days, respectively. Gas exchange in eight plants from each group (WW and WS) was monitored daily at the whole-canopy level and every two days at the single-leaf. Measurements were performed only during drying and rewetting Cycles 1 and 3.

Table S1: Estimated leaf area (m^2) for *C. canephora* clone LB1 plants during two cycles of soil drying (WS-1 and WS-3) and rewetting (REC-1 and REC-3) cultivated in a greenhouse.

Variable	Treatment	WS-1	REC-1	WS-3	REC-3
$LA_{estimated}$	WW	3.48 ± 0.14	3.48 ± 0.14	3.74 ± 0.28	3.74 ± 0.28
	WS	3.13 ± 0.19	2.29 ± 0.19	2.83 ± 0.14	2.09 ± 0.17
Fallen leaves	WW	-	-	-	-
	WS	-	0.84 ±0.19	-	0.74 ±0.15

Table S2: Summary of the two-way analysis of variance (ANOVA) for the photosynthetic photon flux density (PPFD, in μmol.m^{-2}.s^{-1}), temperature (°C), relative humidity (%), and air vapor pressure deficit (VPD_{air}, kPa) measured in different environments in a greenhouse for the cultivation and gas exchange measurements of *C. canephora* clone LB1 plants subjected to three recurrent cycles of soil drying and rewetting.

SV	DF	MS			
		PPFD	Temperature	Humidity	VPD_{air}
Hour*Treatment	46	257324.75*	4.87*	134.76*	1.18*
Hour	23	11208217.09*	5323.16*	27205.12*	168.86*
Treatment	2	2975838.57*	12.32*	2059.86*	11.45*
Error	2952	15046.39	10.17	49.95	0.42
CV (%)		59.25	12.23	9.26	57.24

SV: source of variation; DF: degrees of freedom; MS: mean square; CV: coefficient of variation; * Indicates statistical significance at the 5% probability level, according to the F-test.

Table S3: Summary of the two-way analysis of variance (ANOVA) for the variables canopy assimilation (A_C, in μmol.m^{-2}.s^{-1}), canopy transpiration (EC, in mmol.m^{-2}.s^{-1}), and canopy conductance (g_C, in mmol.m^{-2}.s^{-1}) in *C. canephora* clone LB1 plants subjected to three recurrent cycles of soil drying and rewetting in a greenhouse.

SV	DF	MS					
		Cycle 1			Cycle 3		
		A_C	E_C	g_C	A_C	E_C	g_C
Hour*Treatment	23	86.65*	3.13*	10109.97*	67.18*	4.99*	2299.19*
Hour	23	12.32*	108.14*	50811.51*	1315.72*	109.73*	211317.28*
Treatment	1	989.42*	56.51*	226233.97*	747.66*	94.32*	95666.74*
Error	8016	2.62	0.15	1502.15	2.43	0.19	525.72
CV (%)		100.71	91.68	86.93	127.29	96.57	59.43

SV: source of variation; DF: degrees of freedom; MS: mean square; CV: coefficient of variation; * Indicates statistical significance at the 5% probability level, according to the F-test.

Table S4: Summary of the two-way analysis of variance (ANOVA) for the variables leaf net assimilation (A_{net}, in μmol.m^{-2}.s^{-1}), leaf transpiration rate (E, in mmol.m^{-2}.s^{-1}), and leaf stomatal conductance (g_s, in mol.m^{-2}.s^{-1}) in *C. canephora* clone LB1 plants subjected to three recurrent cycles of soil drying and rewetting in a greenhouse.

SV	DF	MS					
		A_{net}	E	g_s	A_{net}	E	g_s
		Morning			Midday		
Day*Treatment	21	37.62*	2.02*	0.01*	42.69*	6.24*	0.01*
Day	21	45.64*	4.81*	0.02*	70.58*	4.61*	0.01*
Treatment	1	977.66*	40.37*	0.31*	1394.83*	197.62	0.19*
Error	308	4.29	0.36	0.002	5.09	1.05	0.001
CV (%)		23.49	30.79	38.92	40.98	47.83	53

SV: source of variation; DF: degrees of freedom; MS: mean square; CV: coefficient of variation; * Indicates statistical significance at the 5% probability level, according to the F-test.

Table S5: Summary of the two-way analysis of variance (ANOVA) for the variables maximum canopy assimilation ($A_{C\text{-}max}$, in μmol.m^{-2}.s^{-1}), maximum canopy transpiration ($E_{C\text{-}max}$, in mmol.m^{-2}.s^{-1}) and dark respiration (R_{dark}, in μmol.m^{-2}.s^{-1}) in *C. canephora* clone LB1 plants subjected to three recurrent cycles of soil drying and rewetting in a greenhouse.

SV	DF	MS		
		$A_{C\text{-}max}$	$E_{C\text{-}max}$	R_{dark}
Day*Treatment	23	18.3*	1.47*	0.09^{ns}
Day	23	37.86*	3.92*	0.35*
Treatment	1	542.72*	73.27*	0.19^{ns}
Error	8016	5.33	0.39	0.07
CV (%)		38.5	39.02	57.7

SV: source of variation; DF: degrees of freedom; MS: mean square; CV: coefficient of variation; * Indicates statistical significance at the 5% probability level, according to the F-test.

Table S6: Summary of the two-way analysis of variance (ANOVA) for the variables Daily CO_2 Assimilation (A_{daily}, in $g.m^{-2}.s^{-1}$, $g.plant^{-1}.s^{-1}$, and $kg.ha^{-1}.s^{-1}$) and Daily Transpiration (E_{daily}, in $L.m^{-2}.s^{-1}$, $L.plant^{-1}.s^{-1}$, and $L.ha^{-1}.s^{-1}$), in *C. canephora* clone LB1 plants subjected to three recurring cycles of soil drying and rewetting in a greenhouse.

SV	DF	MS					
		A_{daily}	E_{daily}	A_{daily}	E_{daily}	A_{daily}	E_{daily}
		$g\ m^{-2}\ day^{-1}$	$L\ m^{-2}\ day^{-1}$	$g\ plant^{-1}\ day^{-1}$	$L\ plant^{-1}\ day^{-1}$	$kg\ ha^{-1}\ day^{-1}$	$L\ ha^{-1}\ day^{-1}$
Day*Treatment	41	9.26*	0.28*	89.28*	3.16*	2231.79*	$7.91x10^{7}$*
Day	41	20.58*	0.94*	152.07*	7.42*	3701.74*	$1.86x10^{8}$*
Treatment	1	426.76*	14.21*	9172.99*	342.01*	229318.35*	$8.55x10^{13}$*
Error	588	2.33	0.06	19.11	0.59	477.74	$1.49x10^{7}$
CV (%)		42.34	36.13	38.6	35.78	38.6	35.78

SV: source of variation; DF: degrees of freedom; MS: mean square; CV: coefficient of variation; * Indicates statistical significance at the 5% probability level, according to the F-test.

Table S7: Summary of the two-way analysis of variance (ANOVA) for the biometric variables: height, diameter, number of leaves, and leaf area; and final biomass variables: leaf dry mass (LDM), plagiotropic branch dry mass (PBDM), orthotropic branch dry mass (OBDM), and total dry mass (TDM).

	SV	DF	MS			
			Height	**Diameter**	**Leaf number**	**Leaf area**
Biometry	**Treatment**	1	203.06	0.01	433622.25*	17.51*
	Error	14	90.81	2.08	12259.54	0.41
	CV (%)		9.52	7.2	17.38	20.47
			LDM*	**PBDM**	**OBDM**	**TDM**
Biomass	**Treatment**	1	167015.26	2750.22	3637.89	271891.85*
	Error	14	4602.72	1323.96	1000.37	13171.48
	CV (%)		20.6	17.1	18.68	16.13

SV: source of variation; DF: degrees of freedom; MS: mean square; CV: coefficient of variation; * Indicates statistical significance at the 5% probability level, according to the F-test.